

600385064

Aug 1985

GREEN RIVER AIR QUALITY MODEL DEVELOPMENT
VALMET - A Valley Air Pollution Model

ATMOSPHERIC SCIENCES RESEARCH LABORATORY
OFFICE OF RESEARCH AND DEVELOPMENT
U.S. ENVIRONMENTAL PROTECTION AGENCY
RESEARCH TRIANGLE PARK, NORTH CAROLINA 27711

GREEN RIVER AIR QUALITY MODEL DEVELOPMENT
VALMET - A Valley Air Pollution Model

by

C. D. Whiteman, and K. J. Allwine
Pacific Northwest Laboratory
Richland, Washington 99352

Interagency Agreement AD89F20970
with the U.S. Department of Energy

Project Officer

Alan H. Huber
Meteorology and Assessment Division
Atmospheric Sciences Research Laboratory
U.S. Environmental Protection Agency
Research Triangle Park, NC 27711

ATMOSPHERIC SCIENCES RESEARCH LABORATORY
OFFICE OF RESEARCH AND DEVELOPMENT
U.S. ENVIRONMENTAL PROTECTION AGENCY
RESEARCH TRIANGLE PARK, NORTH CAROLINA 27711

DISCLAIMER

The research described in this report has been funded wholly or in part by the United States Environmental Protection Agency through Interagency Agreement AD-89-F-2-097-0 to the Pacific Northwest Laboratory. This document has been reviewed in accordance with U.S. Environmental Protection Agency policy and approved for publication. Mention of trade names or commercial products does not constitute endorsement or recommendation for use.

PREFACE

This final report is submitted as part of the Green River Ambient Model Assessment (GRAMA) project conducted at the U.S. Department of Energy's Pacific Northwest Laboratory for the U.S. Environmental Protection Agency. The GRAMA Program has, as its ultimate goal, the development of validated air quality models that can be applied to the complex terrain of the Green River Formation of western Colorado, eastern Utah and southern Wyoming. The Green River Formation is a geologic formation containing large reserves of oil shale, coal, and other natural resources. Development of these resources may lead to a degradation of the air quality of the region. Air quality models are needed immediately for planning and regulatory purposes to assess the magnitude of these regional impacts. This report documents one of the models being developed for this purpose within GRAMA--specifically a model developed to predict worst case air pollutant concentrations caused by elevated continuous point sources of pollution located in deep valley terrain. The model shows promise for use as a planning tool and eventually as a regulatory tool. Further testing and evaluations of the model are needed to gain a measure of confidence in the model's performance.

ABSTRACT

An air quality model is described for predicting air pollution concentrations in deep mountain valleys arising from nocturnal down-valley transport and diffusion of an elevated pollutant plume, and the fumigation of the plume on the valley floor and sidewalls after sunrise. Included is a technical description of the model, a discussion of the model's applications, the required model inputs, sample calculations and model outputs, and a full listing of the FORTRAN computer program.

EXECUTIVE SUMMARY

Pacific Northwest Laboratory has developed an air quality model for application in valleys for the U.S. Environmental Protection Agency (EPA) under their Green River Ambient Model Assessment (GRAMA) program. This program was initiated in response to the need for air quality assessment tools applicable in the Green River Oil Shale Formation region of western Colorado, eastern Utah, and southern Wyoming. This region has the potential for large-scale growth because vast energy resources, especially oil shale, are located in the region.

Following a thorough analysis of meteorological data obtained from deep valleys of western Colorado, a modular air pollution model has been developed to simulate the transport and diffusion of pollutants released from an elevated point source in a well-defined mountain valley during the nighttime and morning transition periods. This initial version of the model, named VALMET, operates on a valley cross section at an arbitrary distance down-valley from a continuous point source. The model has been constructed to include parameterizations of the major physical processes that act to disperse pollution during these time periods.

The nighttime simulation uses a modified Gaussian plume to calculate concentrations on the valley floor and sidewalls. The Gaussian plume model uses Briggs' plume rise equations and Pasquill-Gifford diffusion coefficients, as modified for complex terrain diffusion enhancement. Dilution of the plume due to tributary flows can be handled in the model, and a new method has been incorporated to ensure conservation of plume mass as the plume is transported down the valley axis. The purpose of the nighttime simulation is to provide air pollution concentrations on a cross-valley section at sunrise, as an initial condition for the daytime simulation.

The daytime simulation uses numerical techniques and a valley energy budget to predict how concentrations will vary in time as pollutants from the elevated plume are fumigated onto the valley floor and sidewalls during the post-sunrise temperature inversion breakup period. The effects of CBL growth, temperature inversion subsidence, transport and diffusion in upslope flows, warm air advection above the valley, albedo, sensible heat flux, and other physical processes are incorporated in the model. The daytime simulation is driven by solar radiation and a simplified surface energy budget, taking account of valley topography.

Valley meteorological observations are required in order to obtain the necessary input parameters to the model. The required observations can be obtained using standard meteorological instrumentation, and the costs for

the observations necessary to perform a simple screening analysis are expected to be within the means of a small industrial applicant wanting a permit for operation in a mountain valley. The VALMET model could form the basis for a more comprehensive site-specific model if further meteorological and tracer data were available in a given valley. The model outputs are in a form suitable for regulatory decision making. The model predicts the maximum 1- and 3-hr-average concentrations for locations on the valley floor and sidewalls.

The model shows promise for use as a planning tool and, eventually as a regulatory tool. Further development, testing, and tracer evaluations of the model will be necessary before sufficient confidence can be gained to justify the model's use in a regulatory setting. The priorities for further development and testing have been provided in the body of the report. Testing of the model's sensitivity to input parameters, and an initial evaluation of the model with tracer experiment data are high priority tasks. These tests will, no doubt, result in future modifications to the initial version of the model.

The authors stress that the model's ultimate utility in addressing and providing solutions to potential air pollution problems in mountain valleys will depend on the further evaluation of the model. In order to have confidence in model predictions it is necessary to test the model against actual air pollution data. Several parameters in the model (A_0 , k , σ_y , and σ_z) are, at present, poorly understood for mountain valleys due to a dearth of experimental data and theoretical research. We hope, by pointing out these deficiencies, that attention will be focused on the need for information on both turbulent diffusion and valley energy budget studies. The use of full physics models may help in providing some of the answers necessary to improve the present model.

CONTENTS

| | |
|--|------|
| Preface..... | iii |
| Abstract..... | iv |
| Executive Summary..... | v |
| Figures..... | ix |
| Tables..... | xii |
| Acknowledgments..... | xiii |
| 1. Introduction..... | 1 |
| 2. Background..... | 4 |
| Nocturnal Valley Meteorology..... | 4 |
| Valley Meteorology During the Temperature Inversion Breakup Period..... | 5 |
| 3. Technical Discussion..... | 14 |
| Coordinate System..... | 14 |
| Topographic Cross Section..... | 14 |
| Nocturnal Model..... | 17 |
| Pollutant Source..... | 17 |
| Plume Rise..... | 18 |
| Gaussian Plume Model..... | 21 |
| Dispersion Coefficients..... | 22 |
| Channeling..... | 22 |
| Plume Dilution..... | 24 |
| Reflections..... | 26 |
| Calculation of Steady-State Nighttime Concentrations..... | 31 |
| Daytime Model..... | 32 |
| Extraterrestrial Solar Radiation..... | 33 |
| Parameterization of Sensible Heat Flux..... | 36 |
| Model Grid..... | 36 |
| Thermodynamic Equations for CBL Ascent and Inversion Descent..... | 38 |
| Advection in the Slope Flows..... | 42 |
| Pollution Concentration Calculation Method..... | 44 |
| Exponential Decay of Concentration..... | 47 |
| Maximum 1- and 3-Hour Average Concentrations..... | 48 |
| 4. Overview of Modular VALMET Model..... | 49 |
| Features of the Computer Code..... | 50 |
| Model Inputs..... | 50 |
| Specification of the Model Inputs by the User..... | 53 |
| Valley Characteristics..... | 53 |
| Date..... | 55 |
| Site Location..... | 56 |

| | |
|--|-----|
| Model Characteristics..... | 56 |
| Valley Atmosphere..... | 57 |
| Stack Characteristics..... | 57 |
| Inversion Characteristics..... | 58 |
| Gaussian Plume Parameters..... | 58 |
| Sensible Heat Flux..... | 60 |
| Error Messages..... | 62 |
| 5. Technical Description of Individual Modules..... | 64 |
| VALMET-Main Program..... | 64 |
| INPUT-Input Module..... | 69 |
| JULIAN-Julian Day Module..... | 71 |
| PRISE-Plume Rise Module..... | 72 |
| DILUTE-Plume Dilution Module..... | 74 |
| INGRAT-Valley Plume Reflection Module..... | 75 |
| NORMAL-Normal or Gaussian Curve Integration Module.... | 77 |
| GAUSS-Gaussian Plume Module..... | 78 |
| SOLAR-Extraterrestrial Solar Radiation Module..... | 79 |
| EBDGT-Surface Energy Budget Module..... | 81 |
| DESCNT-Inversion Descent and CBL Growth Module..... | 82 |
| PROFIL-Concentration Profile Module..... | 84 |
| VELOCITY-Upslope Flow Velocity Module..... | 86 |
| BRKUP-Pollutant Mass Budget Module..... | 88 |
| PSTPRC-Post Processor Module..... | 90 |
| 6. Sample Model Runs..... | 92 |
| Simulation Number 1..... | 92 |
| Simulation Number 2..... | 97 |
| 7. Further Work..... | 100 |
| Guidance from the 1982 Experiments..... | 100 |
| Suggested Modifications to the VALMET Model..... | 103 |
| Deposition..... | 103 |
| Emission Above or Below Stable Core..... | 103 |
| Energy Budget..... | 104 |
| Cross Valley Flows..... | 104 |
| Turbulent Erosion of the Valley Inversion by Overlying Flows..... | 104 |
| Effect of Tributary Flows on the Enhancement of Diffusion..... | 105 |
| Diffusion Coefficients..... | 105 |
| Time-Varying Wind Speeds in the Stable Core..... | 105 |
| Temperature Inversion Buildup..... | 105 |
| Differential Heating..... | 105 |
| Stacks Located on Sidewalls..... | 106 |
| References..... | 109 |
| Appendices | |
| A. FORTRAN Listing of VALMET..... | 115 |
| B. FORTRAN Listing of VALMET Output Plotting Program..... | 147 |
| C. Research Paper Entitled "Breakup of Temperature Inversions in Deep Mountain Valleys: Part II. Thermodynamic Model".. | 155 |
| D. Summary of Modifications to VALMET..... | 173 |

FIGURES

| <u>Number</u> | | <u>Page</u> |
|---------------|--|-------------|
| 1 | Three patterns of temperature structure evolution during the inversion breakup period..... | 7 |
| 2 | Typical mid-morning wind structure over and within a deep valley on the western slope of the Rockies, illustrating the five interrelated wind systems identified in field studies..... | 8 |
| 3 | Relationship between temperature structure layers and wind systems..... | 9 |
| 4 | Dual soundings from a valley floor and a valley sidewall illustrating the up-slope flow found within the CBL over the sidewall..... | 9 |
| 5 | Illustration of the hypothesis of inversion destruction. In the center of the diagram cross sections of a valley are shown at times t_1 , t_2 , t_3 , t_4 , and t_D | 10 |
| 6 | Air pollution implications of CBL growth and inversion top descent..... | 12 |
| 7 | Illustration of the nocturnal down-valley transport and dispersion of a pollutant plume..... | 15 |
| 8 | Illustration of the local coordinate system on a cross valley section..... | 16 |
| 9 | Parameters used in the VALMET model to approximate a valley topographic cross section..... | 16 |
| 10 | Illustration of the definitions of secondary topographic variables used in the model..... | 16 |
| 11 | Cross section of pollutant plume and valley topography illustrating the integral method of calculation for plume reflection and diffusion out the top of the valley temperature inversion..... | 28 |

| <u>Number</u> | | <u>Page</u> |
|---------------|---|-------------|
| 12 | VALMET grid configuration on a valley cross section illustrating the nomenclature used in the model..... | 32 |
| 13 | Extraterrestrial solar heat flux as a function of time, showing solar model nomenclature..... | 37 |
| 14 | Cross section of the valley floor and sidewalls illustrating the grid elements whose height corresponds to the CBL heights..... | 38 |
| 15 | Illustration of the effect of topography in controlling the heating rates of the air within a valley temperature inversion versus the air within an inversion over the plains..... | 39 |
| 16 | Diagram showing the changes in CBL and inversion depth at a given time step above a valley floor grid element..... | 43 |
| 17 | Representation of the volumetric element of mass incorporated into the growing CBL above a valley floor grid element at each model time step..... | 43 |
| 18 | Schematic diagram of an individual model grid element illustrating the pollutant mass balance..... | 45 |
| 19 | Flow diagram of VALMET model, showing the modular structure of the model and the physical processes parameterized in the modules..... | 51 |
| 20 | Illustration of the VALMET model input table as it appears on the user's interactive screen..... | 54 |
| 21 | Listing of summary output file generated by Sample Simulation 1..... | 93 |
| 22 | Plots of Sample Simulation 1: (a) nocturnal vertical concentration profile through plume centerline, (b) CBL height (long dashes) and inversion height (short dashes) as a function of time, and (c) nocturnal cross-valley concentration profile through plume centerline..... | 95 |
| 23 | Pollutant concentration versus time for selected grid elements for Sample Simulation 1..... | 96 |
| 24 | Same as Figure 22, for Sample Simulation 2..... | 98 |
| 25 | Same as Figure 23, for Sample Simulation 2..... | 99 |

| <u>Number</u> | | <u>Page</u> |
|---------------|--|-------------|
| 26 | Illustration of differential solar flux on opposing sidewalls for Brush Creek Colorado on August 4, 1982..... | 107 |
| 27 | Brehm's (1981) conceptual model of temperature inversion destruction in Austria's Inn Valley, showing differential CBL growth over the opposite sidewalls and continued down-valley flow in the elevated stable core..... | 108 |

TABLES

| <u>Number</u> | | <u>Page</u> |
|---------------|---|-------------|
| 1 | Values of the Constants I, J, and K, for σ_y as a Function of Downwind Distance, for Six Stability Conditions..... | 23 |
| 2 | Values of the Constants I, J, and K, for σ_z as a Function of Downwind Distance, for Six Stability Conditions..... | 23 |
| 3 | Relationship Between Weather Conditions and Stability Categories..... | 24 |
| 4 | Equation of Time Correction..... | 35 |
| 5 | Default values of VALMET Input Parameters..... | 55 |
| 6 | Limits on the Values of Input Parameters..... | 56 |

ACKNOWLEDGMENTS

The work reported here had its origins in research conducted at the Department of Atmospheric Science at Colorado State University while one of the authors (CDW) was a student there. Dr. Thomas B. McKee's contributions to the work at that time, as a thesis advisor, are greatly appreciated.

The authors' colleagues at PNL contributed suggestions and criticisms as the work progressed that led to significant improvements in the model's design and in the clarity of the text. Drs. Thomas W. Horst and J. Christopher Doran are especially thanked for their help in that regard.

Mr. Alan Huber, the EPA Project Officer, and Mr. Rich Fisher, EPA Region VIII meteorologist, are thanked for their guidance, support, and encouragement of the work. Mr. Fisher tested early versions of the model and provided a number of very useful suggestions from the viewpoint of a model user that resulted in improvements of the model code. The final set of technical revisions to this report was made following suggestions by Mr. Bill Bernardo of EPA's Region VIII office, arising from sensitivity tests he conducted on the model in late 1983. We wish to thank Mr. Bernardo for his help.

SECTION 1

INTRODUCTION

This report documents an air quality model that was developed to predict concentrations of nonreactive pollutants arising from elevated continuous point sources that emit pollutants within well-defined deep mountain valleys. The model, termed VALMET, is intended to simulate the effects on pollutant transport and diffusion of various meteorological processes that are thought to result in worst-case pollutant concentrations. The model is run for situations when pollutants are carried in locally developed circulations within a valley when these circulations are "decoupled" from prevailing circulations above the valley. The primary physical processes included in the model are

Nocturnal Simulation:

- Transport by down-valley drainage flows
- Plume channeling within the valley
- Enhanced horizontal and vertical diffusion due to topography
- Plume reflections off valley floor and sidewalls
- Pollutant diffusion out the top of the valley
- Dilution of the plume due to clean air inflow from tributaries.

Post-Sunrise Simulation During Temperature Inversion Breakup Period:

- Convective boundary layer growth
- Plume subsidence in the valley inversion
- Fumigation into growing convective boundary layers
- Transport and diffusion in upslope flows over the sidewalls.

The model, while including a variety of meteorological processes, is highly parameterized so that it is simple in concept and easy to run. The model is composed of 13 modules, or subroutines, arranged in such a way that an improved understanding of individual valley meteorological phenomena can be easily incorporated in future versions of the model. The modules within the model can be replaced by data if they are available. Thus, the model can be used in one of two modes. It can be used in a "screening" mode to calculate pollutant concentrations within a valley when little site specific data is available, or the model can be "calibrated" with site-specific data so that it can be used as a site-specific model.

The two-dimensional model was developed primarily to predict pollutant concentrations on the valley floor and sidewalls on a valley cross section an arbitrary distance down-valley from a pollutant source during the post-sunrise temperature inversion breakup period. It is necessary, however, to know the air pollution concentration within the valley cross section at sunrise, as an initial condition for the post-sunrise simulation. The model is therefore comprised of two parts--a nighttime part whose purpose is to predict concentrations on the valley cross section at sunrise, and the daytime part which predicts concentrations on the valley floor and sidewalls during the post-sunrise temperature inversion breakup period. The temperature inversion breakup period has been identified by previous investigators [1] as a period when diurnal fumigations [2] can produce high pollutant concentrations in valleys.

The nighttime simulation, which applies during the steady-state period after valley temperature inversions and drainage wind systems have become established, uses a modified valley-following Gaussian plume algorithm to calculate air pollution concentrations for points on the valley floor and sidewalls. A plume rise formulation is used to simulate the initial rise of a pollutant plume at the stack due to momentum and buoyancy of the effluent. Pasquill-Gifford diffusion coefficients are modified to account for enhanced nocturnal diffusion caused by rough terrain. The Gaussian plume is also modified to allow for dilution of the plume during its down-valley transport caused by clean air flowing into the plume from valley tributaries or by converging downslope drainage flows. An integral constraint on pollutant mass is applied to ensure that pollutant mass is conserved during the plume's transport down the valley and within any valley cross section down-valley from the emission source, except for pollution diffusion out the top of the valley.

The daytime simulation uses numerical techniques that simulate the fumigation of the nocturnal plume onto the valley floor and sidewalls as a convective boundary layer grows upwards from the heated valley surfaces and as subsiding motions occur over the valley center after sunrise. The rate of growth of convective boundary layers and subsidence within the valley temperature inversion are simulated using the bulk thermodynamic model of Whiteman and McKee [3]. This model is driven by sensible heat flux, estimated as a fraction of the solar radiation using a highly parameterized surface energy budget. The effects of such factors as snow cover, soil moisture, cloud cover, or surface albedo are not explicitly included in the model but can be incorporated into the model in the future through an expanded energy budget module. The shape of the topographic cross section of the valley is explicitly included in the model through the specification of valley floor width and sidewall inclination angles at the valley cross section of interest. The retarding effect on temperature inversion breakup and pollution dispersion due to warm air advection above the inversion is also included in the model. Fumigated pollutants are transported from the valley cross section in upslope flows that develop within the convective boundary layers over the slopes. Pollutants are diffused through model grid elements during this transport up the slopes in the growing convective

boundary layer. Pollutant concentrations decay exponentially within individual grid elements high on the sidewall as they are dropped from the simulation as the inversion top subsides below them.

The output from the nighttime simulation includes the steady-state pollutant concentration at valley floor and sidewall grid elements on the valley cross section of interest. The fraction of plume mass that has diffused out the top of the valley during the plume's travel is also an output of the model. Since an analytical formula describes the concentrations within a valley cross section, cross valley and vertical profiles of pollutant concentration can be calculated and plotted. The plume centerline concentration is an output of the model.

The primary output of the daytime simulation is the maximum 1- and 3-hr average pollutant concentrations in each of the model grid elements on the valley floor and sidewalls. The time varying 5-min-average concentrations for each of the grid elements between sunrise and the time of inversion destruction is also an output of the model. In addition to these primary outputs, intermediate model outputs come from individual modules in the program. The local standard time of sunrise, the duration of the daylight period, and the solar flux on a horizontal surface at solar noon come from the solar module. The convective boundary layer height and inversion top height as a function of time come from the temperature inversion breakup module.

Twenty-seven input parameters are necessary to drive the model. These input parameters include the date, site location, topographic characteristics of the valley cross section, temperature inversion characteristics at sunrise, emission and stack characteristics, down-valley wind speed(s), atmospheric stability, grid element length, and sensible heat flux parameters. If known, the rate of warm air advection above the valley can be input. The necessary model inputs can be obtained from topographic maps, engineering information on the pollutant source, and one or more seasonal meteorological data collection campaigns in the valley of interest using tethered balloon data collection systems and/or doppler acoustic sounders.

This report is written following U.S. Environmental Protection Agency (EPA) reporting guidelines [4,5] and is organized in the following way. First, meteorological observations taken in a number of deep valleys in western Colorado are summarized in order to provide a brief description of the salient meteorological features that must be included in a realistic air quality model. Second, a technical discussion is given of the mathematical representation of these processes used in VALMET. Third, a brief overview is given of the air quality model's structure. Fourth, the individual modules of the model are described in detail, including the FORTRAN code, inputs, outputs, etc. Fifth, sample runs of the model are presented. Finally, the need for further data and verification studies is indicated and an overall summary of the modeling approach is presented. Appendices include a complete listing of the VALMET source code, a listing of a sample plotting program for depicting model outputs, and a reprint of a scientific paper which describes the theoretical basis of one of the major components of the modeling approach.

SECTION 2

BACKGROUND

The VALMET model is a further development of ideas that were published in research papers and reports over the last 5 years, based on a comprehensive set of valley meteorological field experiments conducted in western Colorado. These earlier papers summarize a case study of temperature inversion buildup [6]; describe the data analysis, hypothesis, and mathematical foundation of the temperature inversion destruction part of the model [3,7-10]; describe the initial idea of an air pollution model framework able to incorporate upslope winds and fumigations arising after sunrise [11]; and present a general summary of Colorado valley meteorology based on data analyses [12]. Progress in the development of VALMET has been described in two progress reports submitted to EPA in 1981 and 1982 [13,14].

The present version of VALMET, as described in this report, must be considered as an initial or preliminary version of the model. This report is written to facilitate the limited distribution of the model to users who will provide comments and suggestions regarding the further development of the model. The present version has not yet undergone a full set of sensitivity tests, has not been fully evaluated with respect to its performance in simulating air pollution concentrations in actual valleys, and contains modules that have not yet been fully developed.

The user is cautioned against applying the air quality model for meteorological or topographical conditions that are contrary to assumptions made in the model. In order for the user to understand fully the assumptions and hypotheses used in the model, it is necessary to summarize briefly the results and hypotheses that arose from the observational program and the work of previous investigators. In this section we present a condensed summary of this material for both the nocturnal and temperature inversion breakup periods, emphasizing the physical mechanisms in the valley that are responsible for the transport and diffusion of pollutants. It is these individual mechanisms that are parameterized in the air pollution model.

NOCTURNAL VALLEY METEOROLOGY

The most universal features of nighttime valley meteorology, reported in valleys all over the globe [15-19, and others], is the drainage of cooled air down the valley sidewalls and valley axes. The initiation of these flows, which is closely related to changes in the temperature structure above valley surfaces, has received inadequate study to date and cannot be adequately parameterized for inclusion in the model. After the short (2 to

4 hr) initiation period, the down-valley flows become well-established through the valley depth, and attain a speed that is characteristic of the valley and is reasonably steady-state. Observations [9,12] show that the strength of the down-valley flows is quite variable from valley to valley, and no model is yet available which can accurately predict their strengths in individual valleys. In Colorado's valleys, however, observations show that windspeeds on a clear undisturbed night in one season are typical of windspeeds on similar nights in other seasons. Observations thus seem to be the best way of specifying down-valley wind system strength.

Down-slope flows on the valley sidewalls become weaker and less organized after the valley inversion develops, since air flowing down the slopes must work against a very stable ambient stratification. Slope flows can more easily become detached from the sidewalls during this period, providing an important stirring mechanism which causes enhanced horizontal diffusion of pollutant plumes within the valley inversion. The effects of terrain roughness and mechanically generated turbulence also play an important role in enhancing dispersion in the down-valley flows.

Pollutant concentrations can be strongly affected by dilution of the plume due to clean air flowing in from valley tributaries. This feature of meteorology, unique to valleys, can make substantial changes in pollutant concentrations, especially where high volume fluxes of clean air are involved, as when a pollutant plume originates in a small tributary and emerges into a major valley.

VALLEY METEOROLOGY DURING THE TEMPERATURE INVERSION BREAKUP PERIOD

Observation in Colorado's deep valleys [9,10] have provided detail on the changes in atmospheric structure during the morning transition period when the nocturnal down-valley flows are reversed to daytime up-valley flows. The transition period is much longer than expected in these deep valleys and the physical processes leading to the transition are expected to be of great importance for air pollution transport and dispersion. In this section, we will summarize the observations of inversion destruction, pointing out typical characteristics of the meteorology of these valleys, and the physical processes that must be included in realistic air pollution models simulating the inversion destruction period.

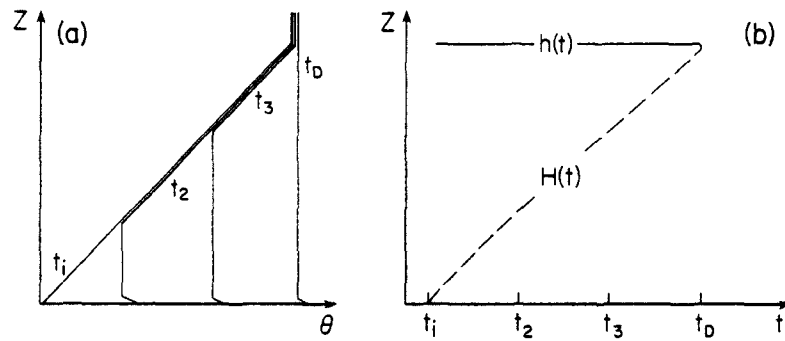
At sunrise nocturnal inversions in most of the valleys were built up to about the level of the surrounding ridgetops. The average depth, based on 21 cases studies, was 604 m. Vertical potential temperature gradients within the inversions averaged $0.0295^{\circ}\text{K m}^{-1}$, but ranged from 0.0187 to $0.0566^{\circ}\text{K m}^{-1}$. The strength and direction of prevailing winds aloft, as determined from the Grand Junction, Colorado, morning rawinsonde sounding, had no demonstrable effect on the characteristics of valley inversions. The valley inversions showed much less variability from day to day and from season to season than inversions over Grand Junction. This suggests that at least for a narrow range of synoptic conditions, valley topography produces more consistent inversions, perhaps by protecting them from winds aloft.

When the along-valley winds were weak, the valley vertical potential temperature profiles frequently were hyperbolic, especially near the ground. In most valleys where along-valley winds were of at least moderate strength, the inversion profiles were nearly linear with height.

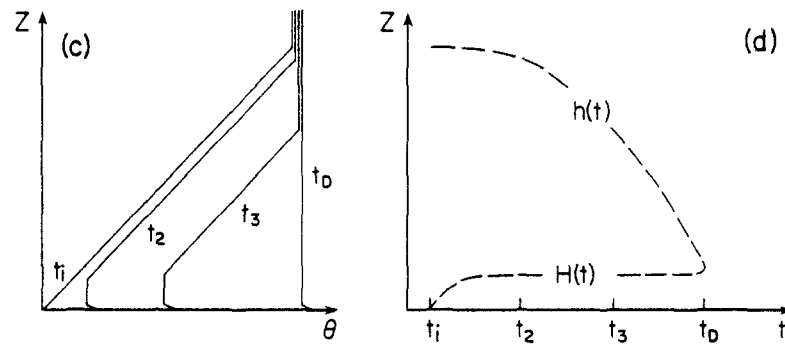
Temperature inversions in all of the valleys investigated were destroyed after sunrise following one of three patterns of temperature structure evolution (Figure 1). The first pattern, observed in the widest valley studied, approximates inversion destruction over flat terrain, in which the nocturnal inversion is destroyed after sunrise by the upward growth from the ground of a warming convective boundary layer (CBL). The second pattern, observed in snow covered valleys, differs significantly from the first. Here the growth of the CBL, which begins after sunrise, is arrested once the CBL has attained a depth of 25 to 50 m. The inversion is then destroyed as the top of the nocturnal inversion descends into the valley. Successive profiles of the valley atmosphere show a warming consistent with a simple subsidence of the previous profiles. The third pattern of temperature structure evolution was observed in all the valleys when snow cover was not present and describes the majority of case studies observed in field experiments. Following this pattern, inversions are destroyed by two processes: the continuous upward growth from the valley floor of a warming CBL and the continuous descent of the top of the nocturnal temperature inversion. Warming of the elevated inversion layer above the CBL is consistent with a simple subsidence of the previous profiles. In the Colorado valleys studied, the time required to break an inversion and establish a neutral atmosphere within the valley was typically 3-1/2 to 5 hr after sunrise. Temperature structure evolution during clear, undisturbed weather was surprisingly uniform from day to day and season to season. Thus, in future work, one may be fairly confident of observing typical inversion breakup during short field studies in undisturbed weather.

The common element of all three patterns of temperature structure evolution is the development of a CBL over the valley floor after it is illuminated by direct sunlight. Observations taken from the sidewall of one valley also show the development of a CBL after direct sunlight illuminates the sidewall. Due to the shading effects of surrounding topography, the different valley surfaces can be illuminated at significantly different times, thus affecting the initiation of CBL growth. The temperature structure of the sidewall CBL is similar to that of the CBL over the valley floor, but winds blow up the sidewall CBL at speeds of up to 3 m sec^{-1} .

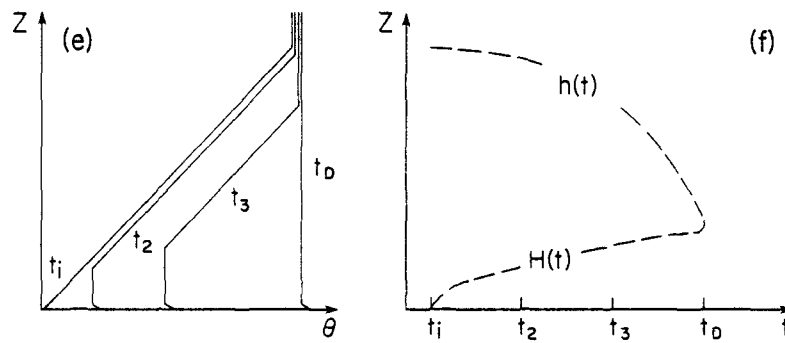
Five different temperature structure layers have been observed during the inversion destruction period. Above the valley floor CBL and the sidewall CBL just mentioned is the stable core of the potential temperature inversion. A neutral stability layer above the stable core appears to be part of a large-scale convective boundary layer that forms over the western slope of the Rocky Mountains. Above this layer is the free atmosphere.



Pattern 1. Growth of CBL.



Pattern 2. Descent of inversion top and arrested growth of CBL.



Pattern 3. Descent of inversion top and continuous growth of CBL.

Figure 1. Three patterns of temperature structure evolution during the inversion breakup period. Potential temperature profiles are on the left, and time-height analyses of CBL height (H) and inversion top height (h) are on the right.

Each of the five temperature structure layers, identified primarily by their potential temperature structure, can also be identified by the winds that prevail within them (see Figures 2, 3 and 4). During inversion destruction, the CBLs over the valley floor and sidewalls contain winds which blow up the floor of the valley and up the slopes. The CBL, or

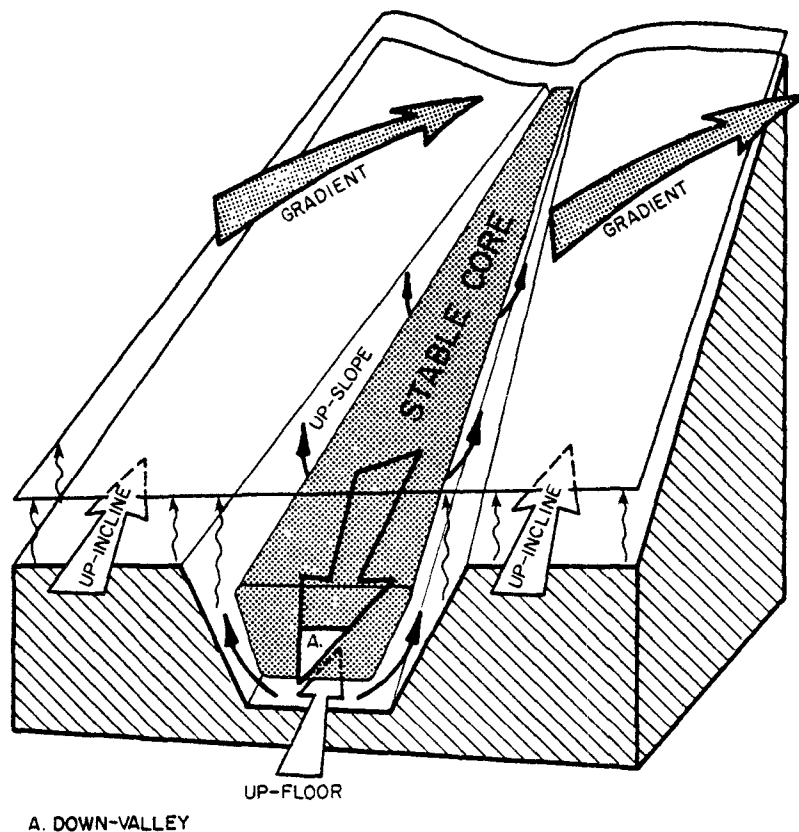


Figure 2. Typical mid-morning wind structure over and within a deep valley on the western slope of the Rockies, illustrating the five interrelated wind systems identified in field studies.

neutral layer, above the valley inversion has winds which blow up the inclined Western Slope of the Rocky Mountains during the day. Winds in the stable core typically continue to blow down-valley after sunrise until the stable core is nearly destroyed. Winds in the stable free atmosphere may blow from any direction with speeds determined by synoptic-scale pressure gradients. Despite variability in the strength and timing of reversal of the winds, the temperature structure evolved uniformly from day to day in individual valleys.

On the basis of the wind and temperature observations summarized above, an hypothesis (Figure 5) has been developed to explain the temperature structure evolution. Since energy is required to change the temperature structure, and the changes begin at sunrise, it is reasonable to hypothesize that solar radiation is the driving force. A fraction of the solar radiation, received on the valley floor and sidewalls, is converted to the sensible heat flux that provides energy to the valley atmosphere. Sensible heat flux from a surface, as over flat terrain, causes a convective boundary

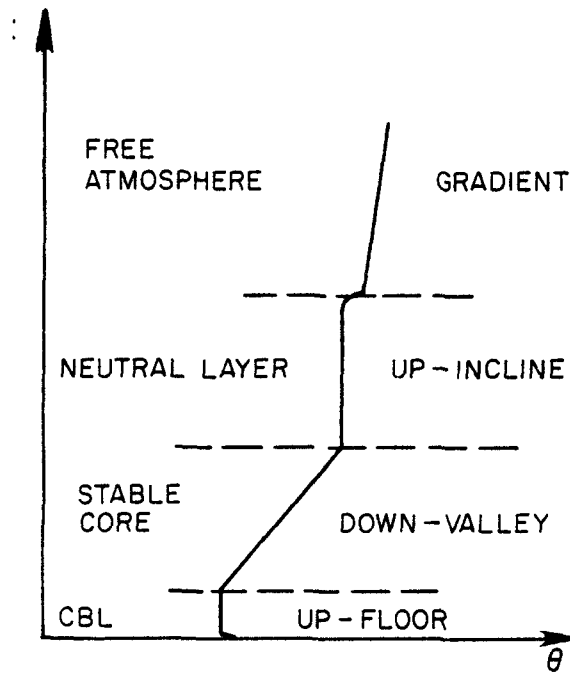


Figure 3. Relationship between temperature structure layers and wind systems. The temperature profile is a typical mid-morning sounding from the floor of a deep valley.

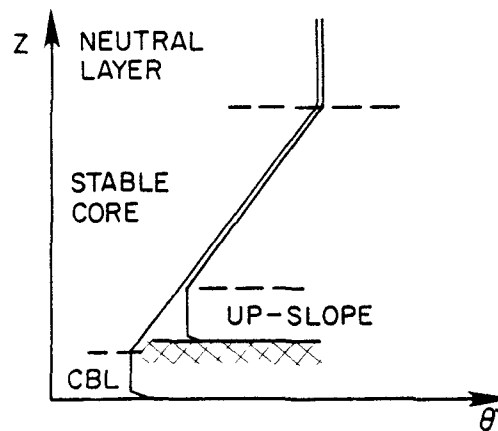


Figure 4. Dual soundings from a valley floor and a valley sidewall illustrating the up-slope flow found within the CBL over the sidewall.

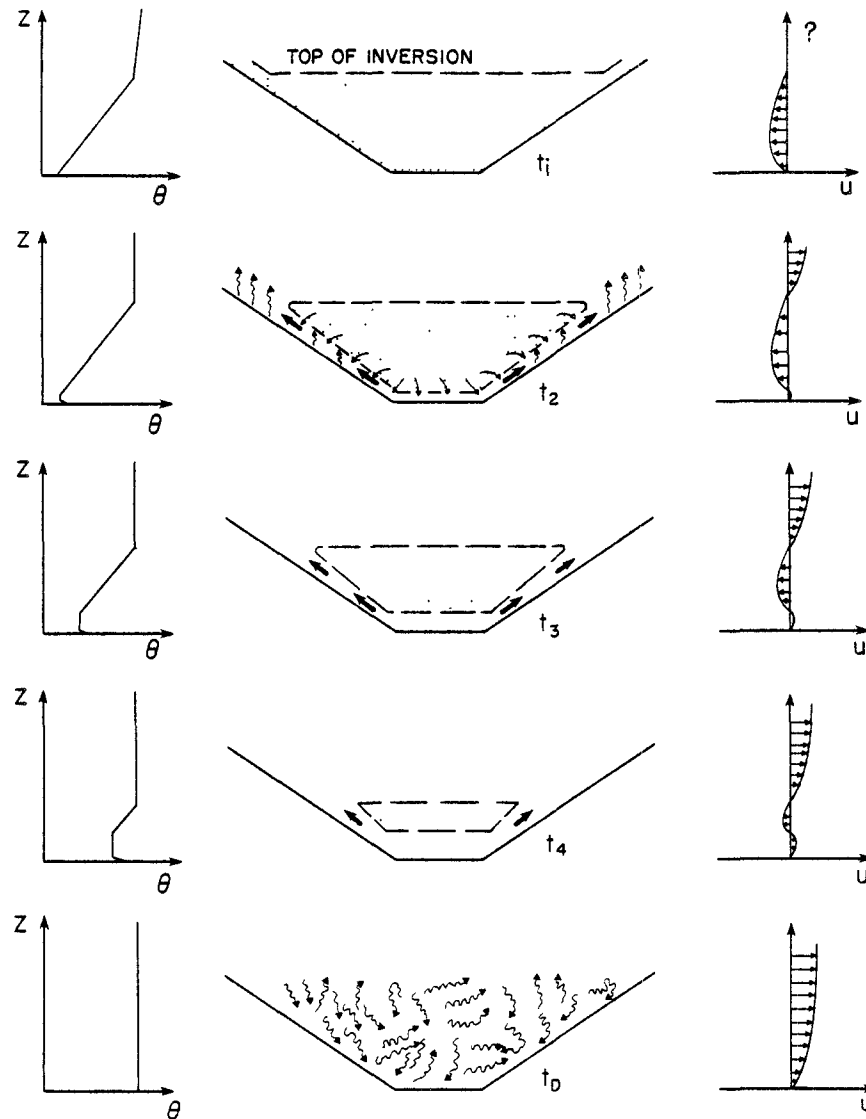


Figure 5. Illustration of the hypothesis of inversion destruction. In the center of the diagram cross sections of a valley are shown at times t_1 , t_2 , t_3 , t_4 , and t_0 . On the left are corresponding potential temperature profiles as taken from the valley center. On the right are corresponding up-valley wind components as a function of height. At sunrise, t_1 , an inversion is present in the valley. At t_2 , a time after sunlight has illuminated the valley floor and slopes, a growing CBL is present over the valley surfaces. Mass and heat are entrained into the CBLs from the stable core above and carried up the sidewalls in the upslope flows. This results in a sinking of the stable core and growth of the CBLs (t_3 and t_4) until the inversion is broken (t_0) and a turbulent well-mixed neutral atmosphere prevails through the valley depth. Down-valley winds continue to blow in the stable core during the inversion breakup period. Winds in the CBL below, and in the region above the stable core often blow up-valley during this same period.

layer to develop over the surface. Mass and heat are entrained into the CBL from the stable core above. Mass entrained into the valley floor and side-wall CBLs, however, is carried from the valley in the upslope flows that develop in the convective boundary layers over the sidewalls. This removal of mass from the base and sides of the stable core causes the elevated inversion to sink deeper into the valley and to warm adiabatically due to subsidence, and decreases the rate of growth of the CBLs. Following this hypothesis, the rate of warming depends directly on the rate of energy input into the valley atmosphere. This energy may be used to deepen the CBLs or to move mass up the sidewalls, allowing the stable core to sink. From this hypothesis a thermodynamic model of temperature inversion destruction has been developed [3]. This model forms the basis for parameterizations of inversion breakup in the VALMET model.

The valley inversion destruction mechanism has important implications for the dispersion of valley air pollution. These implications can be investigated by assuming that the nocturnal inversion at sunrise contains pollutants emitted from a continuous elevated source within the valley. During the night such pollutants would be carried down the valley in the along-valley wind system, undergoing both vertical and horizontal dispersion. The horizontal dispersion in these flows is known to be much greater than over flat terrain [20]. After sunrise a convective boundary layer forms over the valley floor and sidewalls (Figure 6a). The subsequent disposition of pollutants in the stable core will be affected by two competing processes--the sinking of the stable core and the growth of the CBL. The air pollution implications of the two processes can be considered by studying a valley cross section down-valley from the source at a later time. The three inversion breakup patterns discussed above have the following air pollution implications [8]:

1. Pattern 1 - Growth of convective boundary layer (Figure 6b): Pure growth of a CBL will result in fumigation [2] of pollutants at the valley floor as the CBL grows upward into the polluted stable core. This process is favored when the slope flows are ineffective in removing mass from a valley, and thus will occur in very wide or shallow valleys.
2. Pattern 2 - Sinking of stable core (Figure 6c): Failure of the CBL to grow once it has formed over the valley floor and sidewalls results in inversion destruction by sinking of the stable core. Thus, the pollutants sink into the top of a shallow mixed layer, producing high concentrations at the ground. The pollutant plume, once entrained into the CBL, is advected up the sidewalls and dispersed into the neutral layer aloft. This process is favored for narrow-to-wide valleys when sensible heat flux is weak.
3. Pattern 3 - Combination (Figure 6d): A combination of CBL growth and stable core descent results in the sinking of pollutants into the top of a growing mixed layer. Pollution concentrations should be intermediate between the previous two cases. This pattern is the most common one in Colorado mountain valleys.

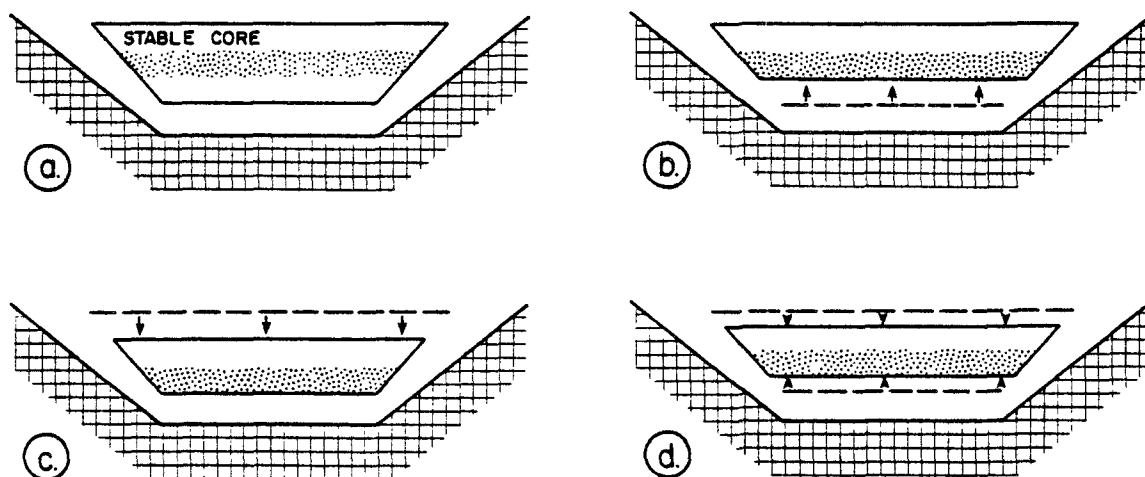


Figure 6. Air pollution implications of CBL growth and inversion top descent.

Another process, that of cross-valley advection of the pollutant plume due to differential heating of the valley sidewalls, may be important in determining the cross-valley position of maximum pollutant concentration. Unfortunately, relatively little observational evidence is presently available on cross-valley advection or the effects of cross valley advection on pollutant dispersion.

Observations in snow-free valleys of Colorado show that inversions are typically destroyed within 3-1/2 to 5 hr after sunrise, regardless of season. Thus, high pollutant concentrations at the ground may be expected following sunrise in polluted Colorado valleys. But inversions are typically broken every day and, once the inversion is destroyed, good mixing will prevail in an up-valley flow regime that is coupled to flows above the valley.

Moist surface conditions or high albedo due to snow cover may change the surface energy budget components so that sensible heat flux is reduced. In these conditions inversion destruction will be delayed or an inversion may persist all day. In Colorado's snow-covered Yampa Valley on February 23, 1978, the CBL failed to grow deeper than 35 m and the observations were characterized by a slow descent of the stable core. The inversion failed to break during this day, although the top of the stable core descended to within 150 m of the ground.

To summarize, the primary factors affecting a valley pollutant plume after sunrise are

- continued transport of the pollutant plume down the valley in the stable core
- sinking motions in the stable core as inversion destruction progresses after sunrise, bringing the plume closer to the valley floor

- fumigation of the plume into convective boundary layers growing over the valley floor and sidewalls
- transport and diffusion of pollution in upslope flows that develop over the sidewalls.

These processes continue from sunrise until the valley temperature inversion is destroyed and the valley atmosphere becomes coupled with the overlying circulations. The amount of time required for temperature inversion destruction in Colorado Mountain Valleys is typically 3-1/2 to 5 hr, but it depends on many factors including the depth and strength of the initial temperature inversion, the incoming solar energy, the sensible heat flux, the pattern of inversion destruction followed, etc.

SECTION 3

TECHNICAL DISCUSSION

In this section we present a technical discussion of the VALMET valley air pollution model. We begin with a short discussion of the coordinate system and the means used in the model to incorporate topography. Discussions of the mathematical equations used in both the nighttime and daytime portions of the model then follow along with a statement of any assumptions used in the model development. Unless otherwise noted, numerical values of the parameters in the equations are assumed to be in the MKS (meter-kilogram-second) system of units, except for pollutant concentrations expressed in micrograms per cubic meter.

COORDINATE SYSTEM

VALMET is a two-dimensional, air pollution transport and diffusion model in which pollutant concentrations are determined on a valley cross section located an arbitrary distance down-valley from a pollutant source. The distance x is measured following the axis of the valley down the centerline of the valley floor (Figure 7). The local coordinate system utilized on the valley cross section is shown in Figure 8. The x -coordinate system specifies the distance of the cross section down-valley from the pollutant source, as measured on the valley floor centerline following any turns in the valley. The y -coordinate system has its origin at the valley floor centerline, is orthogonal to the x -axis, and increases to the right when viewed from the mouth of the valley. The z -coordinate system is a vertical coordinate system with origin at the valley floor centerline.

TOPOGRAPHIC CROSS SECTION

For a particular valley cross section, the model assumes that the valley topography can be simply represented by a horizontal valley floor of width, w , and two inclined sidewalls of inclination angle α_1 and α_2 , as shown in Figure 9, below.

To simulate a real valley, the modeler must approximate the topography of any cross section of interest using a topographic map, from which w , α_1 , and α_2 are estimated. Given the simplified valley cross section and the local coordinate system, one may calculate several secondary topographic parameters that will be used in the model. For example, using definitions shown in Figure 10, the area of the cross section of a valley containing a temperature inversion of depth h is

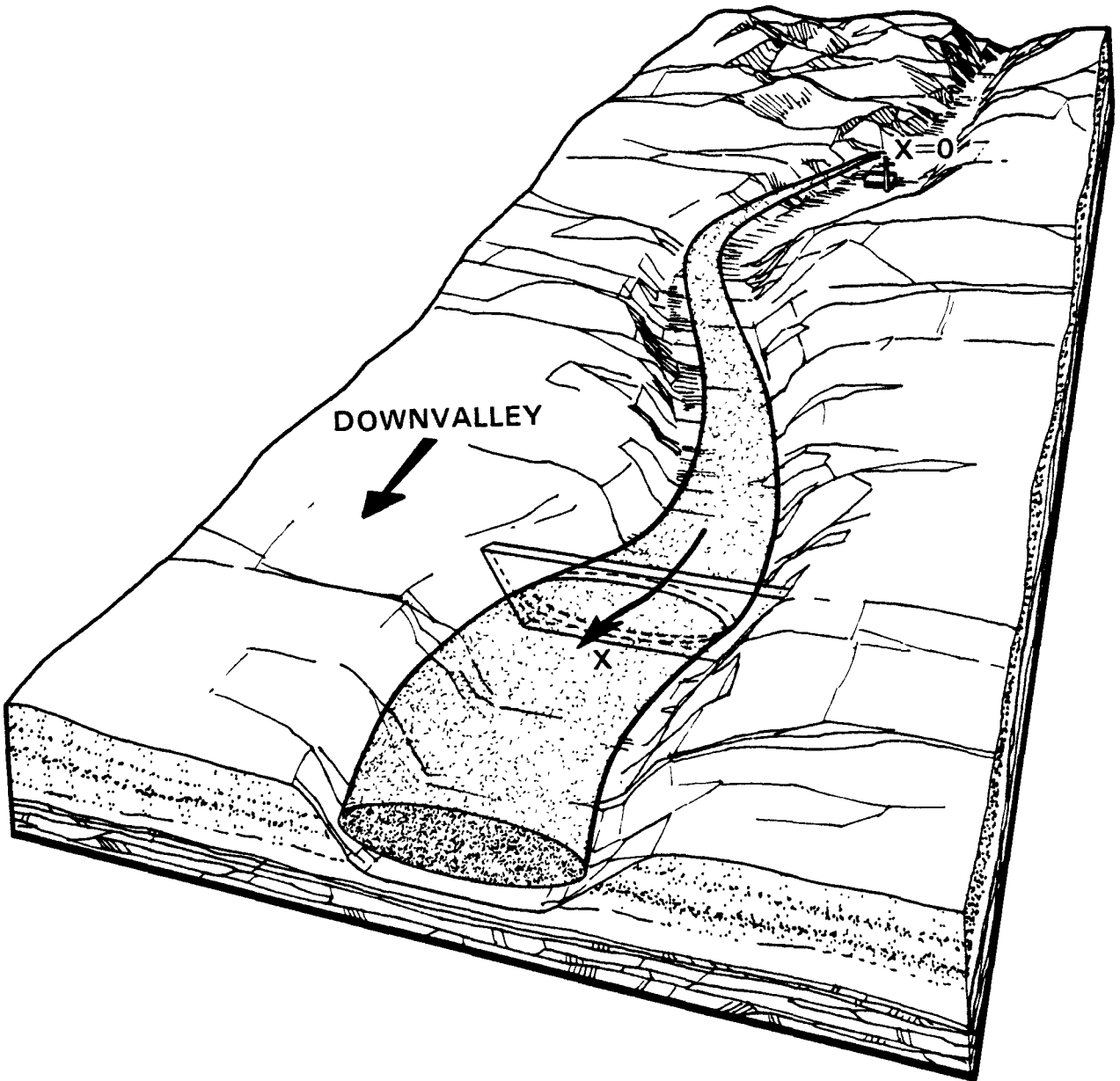


Figure 7. Illustration of the nocturnal down-valley transport and dispersion of a pollutant plume. The terrain following coordinate system, with cross valley section an arbitrary down-valley distance x , is illustrated.

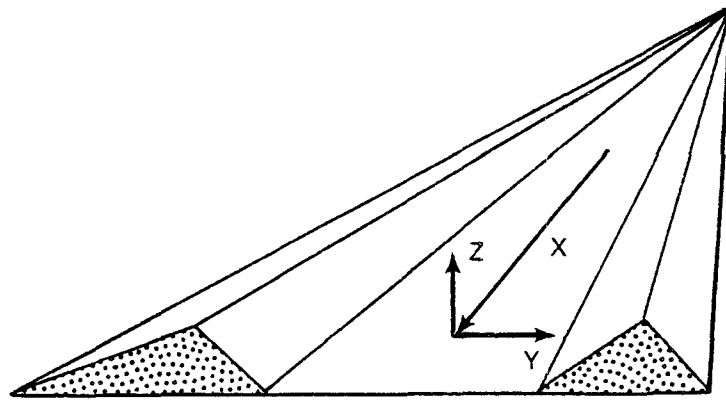


Figure 8. Illustration of the local coordinate system on a cross valley section.

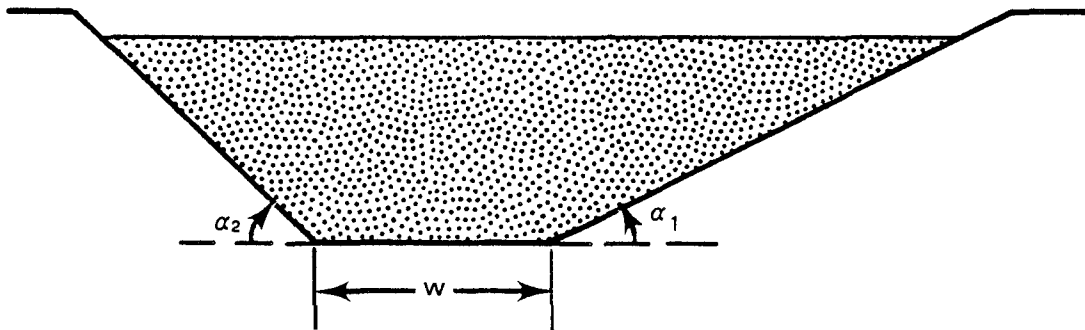


Figure 9. Parameters used in the VALMET model to approximate a valley topographic cross section. The three parameters include the valley width and the two sidewall inclination angles.

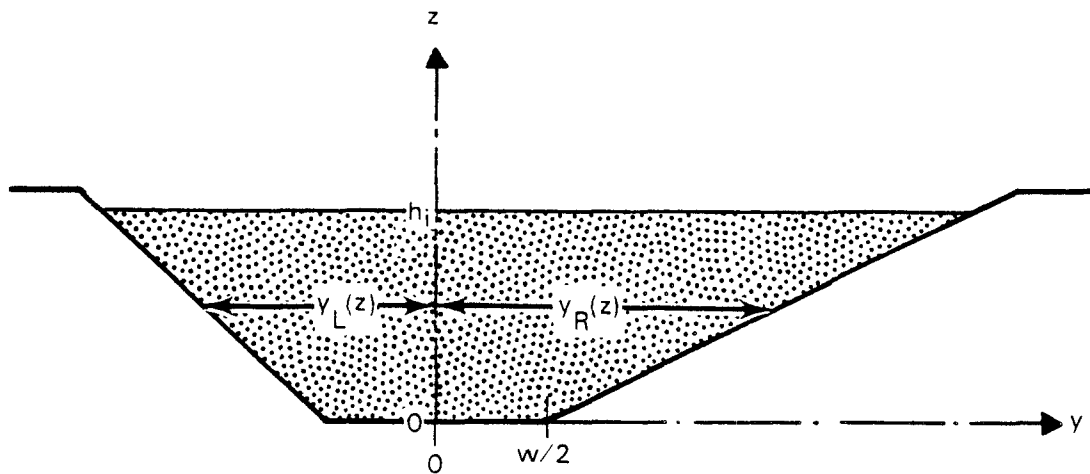


Figure 10. Illustration of the definitions of secondary topographic variables used in the model.

$$A = h w + \frac{h^2}{2} (\cot \alpha_1 + \cot \alpha_2) \quad (1)$$

The y-distance to the left and right sidewalls from the vertical coordinate axis is

$$y_L(z) = -(\frac{w}{2} + z \cot \alpha_2) \quad (2)$$

and

$$y_R(z) = \frac{w}{2} + z \cot \alpha_1 . \quad (3)$$

The topographic cross section may be considered to have a thickness of unity. In this case the area A_T of the top of the inversion ($z = h$) is

$$A_T = y_R(h) - y_L(h) = w + h(\cot \alpha_1 + \cot \alpha_2) . \quad (4)$$

NOCTURNAL MODEL

Pollutant Source

The model begins with an elevated pollutant source on the valley floor at the topographic cross section where $x=0$. The pollutant source may be located anywhere on the valley floor. The y-position of the source is specified relative to the coordinate origin. For example, the y-coordinate of a pollutant source on the valley floor 200 m off the valley floor centerline would be specified as $y_0=+200$ m if the source were in the positive y direction from the centerline, or as $y_0=-200$ m if in the negative direction. The present version of the model cannot handle sources on the valley sidewalls. The source is assumed to emit a continuous elevated pollutant plume into a nocturnal valley temperature inversion of depth $h=h_i$. This pollutant plume is approximated in the model by a modified Gaussian plume algorithm. The potential temperature gradient within the inversion is $\gamma=\partial\theta/\partial z$, and the down-valley wind speed at plume carrying height is u_s . Wind speed is assumed not to vary with height. The model, being run for worst-case dispersion under nocturnal temperature inversion conditions, would be run for Pasquill-Gifford stability categories D, E or F. In later sections, further details of the Gaussian plume formulation will be given along with details concerning dispersion coefficients.

Plume Rise

Plume rise is treated in the model according to formulas described by Briggs [21-24] and used in the MPTER model [25].

The "2/3 law" of plume rise is used for all stability categories up to a certain downwind distance x_f to calculate the plume rise using the equation

$$\Delta h = \frac{1.6 F^{1/3} x^{2/3}}{u_s} \quad (5)$$

where F is the plume's buoyancy flux, x is the downwind distance (m), and u_s is the wind speed at stack height (m/s). The parameter F is calculated as

$$F = g V_e R^2 \left(\frac{T_s - T}{T_s} \right) \quad (6)$$

where g is the acceleration due to gravity (9.8 ms^{-2}), V_e is the exit velocity of gases emitted from the stack (m/s), R is the stack inside radius (m), and T_s and T are the exit and ambient temperatures ($^{\circ}\text{K}$), respectively. The ultimate rise Δh_f and the downwind distance x_f beyond which it applies are calculated as shown below.

Unstable or Neutral Atmospheric Conditions--Calculations of x_f and Δh_f depend on whether the plume rise is "buoyancy-dominated" or "momentum-dominated." This is determined by a crossover temperature difference, calculated as

$$\begin{aligned} (\Delta T)_c &= 0.0297 T_s V_e^{1/3} / (2R)^{2/3} && \text{for } F < 55 \\ \text{or } (\Delta T)_c &= 0.00575 T_s V_e^{2/3} / (2R)^{1/3} && \text{for } F \geq 55. \end{aligned} \quad (7)$$

The actual temperature difference $\Delta T = T_s - T$ is compared to the crossover temperature difference $(\Delta T)_c$ and if $\Delta T \leq (\Delta T)_c$ then the plume rise is momentum-dominated. If $\Delta T > (\Delta T)_c$ then the plume is buoyancy-dominated.

Momentum-Dominated Plume Rise--For a momentum-dominated plume rise the distance to final rise is zero, such that

$$x_f = 0. \quad (8)$$

The final plume rise is given by

$$\Delta h_f = 6RV_e/u_s. \quad (9)$$

Buoyancy-Dominated Plume Rise--For a buoyancy-dominated plume rise the downwind distance of final plume rise is $x_f = 3.5 x^*$, where x^* is the distance at which atmospheric turbulence begins to dominate entrainment, given by

$$x^* = \begin{cases} 14 F^{5/8} & \text{when } F < 55 \text{ m}^4 \text{ sec}^{-3} \\ 34 F^{2/5} & \text{when } F \geq 55 \text{ m}^4 \text{ sec}^{-3} \end{cases}. \quad (10)$$

The final plume rise under these conditions is

$$\Delta h_f = \frac{1.6 F^{1/3} (3.5 x^*)^{2/3}}{u_s}. \quad (11)$$

Stable Atmospheric Conditions--Calculations of x_f and Δh_f , as for unstable conditions, requires a determination of whether the plume rise is buoyancy-dominated or momentum-dominated. This is determined by a crossover temperature difference, calculated as

$$(\Delta T)_c = 0.01958 T V_e s^{1/2} \quad (12)$$

where s is a stability parameter given by

$$s = \frac{g \frac{\partial \theta}{\partial z}}{T}, \quad (13)$$

and $\partial\theta/\partial z$ is the vertical gradient of potential temperature within the valley temperature inversion at sunrise. The actual temperature difference $\Delta T = T_s - T$ is compared to the crossover temperature difference and if $\Delta T < (\Delta T)_c$ the plume rise is momentum-dominated. If $\Delta T > (\Delta T)_c$ the plume rise is buoyancy-dominated.

Momentum-Dominated Plume Rise--For a momentum dominated plume rise the distance to final rise is zero, such that

$$x_f = 0. \quad (14)$$

The final plume rise is given by

$$\Delta h_f = 1.5 \left[\frac{v_e^2 R^2 T}{T_s u_s} \right]^{1/3} s^{-1/6}. \quad (15)$$

Equation (9) for unstable-neutral plume rise is also evaluated and the smaller of the two plume rise calculations is used as the final plume rise.

Buoyancy-Dominated Plume Rise--When the plume rise is buoyancy-dominated, the distance to final rise depends on wind speed at stack height. The actual wind speed is compared to a certain critical wind speed, u_c , and the distance to final rise is calculated using one of two formulas depending on whether the actual wind speed is greater than or less than the critical speed.

The critical wind speed is calculated as follows:

$$u_c = 0.2746 f^{1/4} s^{1/8} \quad (16)$$

The distance to final rise is given by

$$x_f = \left(\frac{4u_s}{1.6} \right)^{3/2} F^{-1/8} s^{-9/16} \quad \text{for } u_s \leq u_c$$

$$\text{or } x_f = \left(\frac{2.6}{1.6} \right)^{3/2} u_s s^{-1/2} \quad \text{for } u_s > u_c. \quad (17)$$

The final plume rise is given by

$$\Delta h_f = \frac{1.6 F^{1/3} x_f^{2/3}}{u_s} . \quad (18)$$

Gaussian Plume Model

Steady-state nocturnal pollutant concentrations within a valley cross section are determined by means of a Gaussian plume model which is modified to account for channeling and reflections off the sidewalls within the valley, dilution due to clean air volume flux convergence within the valley, and diffusion of pollutants out the top of the valley inversion.

We begin with the basic Gaussian plume equations having no reflection terms:

$$x_G(x,y,z;\xi;y_0) = \frac{10^9 Q}{2\pi \sigma_y \sigma_z u_s} G_1(y) G_2(z) \quad (19)$$

where

$$G_1(y) = \exp \left[-\frac{1}{2} \left(\frac{y-y_0}{\sigma_y} \right)^2 \right] \quad (20)$$

$$G_2(z) = \exp \left[-\frac{1}{2} \left(\frac{z-\xi}{\sigma_z} \right)^2 \right] \quad (21)$$

and where $x_G = (x,y,z;\xi;y_0)$ is the pollutant concentration at a receptor located at point $P(x,y,z)$ due to a plume with centerline height ξ and offset distance from the valley floor centerline y_0 . The factor 10^9 is the conversion factor from kilograms to micrograms. σ_y and σ_z are the dispersion coefficients, Q is the source strength and u_s is the transporting down-valley wind speed at the stack. The pollutant stack is constrained to be on the valley floor, so that

$$|y_0| \leq \frac{w}{2} . \quad (22)$$

Dispersion Coefficients

Nocturnal dispersion coefficients σ_y and σ_z for the Gaussian plume equations are determined from the empirically derived Pasquill-Gifford curves [26,27], as developed from atmospheric tracer experiments conducted over homogeneous terrain. The empirical Pasquill-Gifford curves relate the values of σ_y and σ_z to downwind distance and stability category. A numerical approximation to the curves has been provided by McMullen [28] and is given as:

$$\sigma = \exp [I + J (\ln x) + K (\ln x)^2] \quad (23)$$

where

σ = standard deviation of the concentration in the horizontal (σ_y) or vertical (σ_z) in meters,

x = downwind distance (km), and

I, J, K = empirical constants for a given stability condition for σ_y and σ_z .

Tables 1 and 2 provide McMullen's [28] values of the constants I , J , and K for determination of σ_y and σ_z , respectively. Table 3 is provided to determine the proper stability category from meteorological observations.

The above method of determining σ_y and σ_z is appropriate for homogeneous terrain. Previous work [20,29-31] shows that dispersion is enhanced in valleys over that experienced over homogeneous terrain where the original empirical Pasquill-Gifford dispersion coefficients were determined. This enhancement is particularly marked for stable conditions [20]. Enhanced dispersion in valleys is due to a number of physical mechanisms that have, to date, been inadequately studied or characterized. In the VALMET model we have taken the approach, which we do not consider entirely satisfactory, of calculating valley dispersion coefficients from the original empirical Pasquill-Gifford curves [26] by simply adjusting the stability categories. From existing data it appears that the enhancement of the horizontal dispersion can be approximated by dropping the stability two categories (e.g., F becomes D). The vertical enhancement of dispersion is approximated by dropping the stability one category (e.g., F becomes E). The use of these simple adjustments to the stability categories should be considered a stopgap measure. Further work will be required to evaluate its appropriateness and seek more appropriate means of handling nocturnal dispersion in deep valley terrain.

Channeling

Calculations with the Gaussian plume model are made assuming the Gaussian plume follows the valley axis, despite meanders in the valley's course. The model user must therefore use a topographic map to determine the down-valley distance of a given cross section.

TABLE 1. VALUES OF THE CONSTANTS I, J, AND K, FOR σ_y AS A FUNCTION OF DOWNWIND DISTANCE, FOR SIX STABILITY CONDITIONS [28]

| Stability Condition* | I | J | K |
|----------------------|-------|--------|---------|
| A | 5.357 | 0.8828 | -0.0076 |
| B | 5.058 | 0.9024 | -0.0096 |
| C | 4.651 | 0.9181 | -0.0076 |
| D | 4.230 | 0.9222 | -0.0087 |
| E | 3.922 | 0.9222 | -0.0064 |
| F | 3.533 | 0.9181 | -0.0070 |

*As defined in Table 3.

TABLE 2. VALUES OF THE CONSTANTS I, J, AND K, FOR σ_z AS A FUNCTION OF DOWNWIND DISTANCE, FOR SIX STABILITY CONDITIONS [28]

| Stability Condition* | I | J | K |
|----------------------|-------|--------|---------|
| A | 6.035 | 2.1097 | 0.2007 |
| B | 4.694 | 1.0629 | 0.0136 |
| C | 4.110 | 0.9201 | -0.0020 |
| D | 3.414 | 0.7371 | -0.0316 |
| E | 3.057 | 0.6794 | -0.0450 |
| F | 2.621 | 0.6564 | -0.0540 |

*As defined in Table 3.

TABLE 3. RELATIONSHIP BETWEEN WEATHER CONDITIONS AND STABILITY CATEGORIES [26]

| Surface Wind Speed (at 10 m), m sec ⁻¹ | Day | | | Night | |
|---|--------------------------|----------|--------|----------------------------|-------|
| | Incoming Solar Radiation | | | Thinly Overcast or >4/8 | <3/8 |
| | Strong | Moderate | Slight | Low Cloud | Cloud |
| <2 | A | A-B | B | | |
| 2-3 | A-B | B | C | E | F |
| 3-5 | B | B-C | C | D | E |
| 5-6 | C | C-D | D | D | D |
| 6 | C | D | D | D | D |

The neutral class, D, should be assumed for overcast conditions during day or night.

Plume Dilution

An important factor affecting plume concentrations is the dilution of the plume during its travel down a valley due to tributary flows that bring clean air into the plume. This process could be extremely important in decreasing plume concentrations, especially when the volume of diluent air is large relative to the plume volume, as when a pollutant's source is within a small tributary to a larger valley. Other processes occur in valleys that can affect plume dilution, including converging downslope drainage flows and entrainment of clean air into a valley from above. Any process capable of producing volume flux divergence between two vertical valley cross sections is capable of diluting a plume. At present, the physical understanding of these processes is insufficient to incorporate them explicitly into an air pollution model. The extent to which volume flux divergence is a feature of a particular valley's meteorology can be determined, however, by wind observations.

The approach used in the present version of the model is to modify the Gaussian plume equation in a simple way that makes an initial correction for the dilution of a pollutant plume during its down-valley travel. The correction is applied only when data are available to show that a plume would actually be diluted in the valley being modeled. The correction is applied to the plume transporting wind speed at the pollution source cross section to obtain a modified or virtual wind speed u_v . The virtual wind speed is a function of the ratio of the volume fluxes across the source and receptor cross sections, such that

$$u_v = \left[\frac{u_c A_c}{u_s A_s} \right] u_s \quad (24)$$

where u_c is the measured plume-transporting wind speed at the receptor cross section and A_c and A_s are the cross sectional areas at the receptor and source cross sections, respectively. The value of u_v calculated using this equation is simply substituted for u_s in the denominator of the Gaussian plume equation to calculate pollutant concentrations at the receptor cross section. To avoid physically unrealistic results (i.e., plume concentrations increasing with transport distance) u_v must always be equal to or greater than u_s . This is accomplished by specifying

$$\frac{u_c A_c}{u_s A_s} > 1 \quad (25)$$

Using this plume dilution approach, pollutant concentrations at the receptor cross section are calculated using the equation

$$x_v = \frac{u_s}{u_v} x_G \quad (26)$$

The plume dilution method described above is an initial approach that will need improvement as the physics of the dilution process are more fully understood. The advantages of the method are that it should produce more realistic concentrations than when plume dilution is not considered, and the method can be supported by simple measurements. The above method suffers from several drawbacks, however. First, the separate effects of individual physical processes that can lead to dilution are not clearly separated using the current method. Second, the dilution method does not consider the effects on plume dilution of the enhanced lateral and vertical mixing where tributary flows merge into a main valley or of the drift of a plume center-line towards one sidewall caused by incoming tributary flows. Third, the method does not consider stratification effects that may arise in merging flows of different temperature. Finally, dilution air is assumed in the model to be clean with respect to the pollutant species. The dilution method seems appropriate, however, as an initial means of handling plume dilution until a better understanding is obtained for the individual dilution (and dispersion) processes. The wind observations necessary to use the dilution method could be obtained from a doppler acoustic sounder or special pibal and/or tethered sonde campaigns. A user should use data to show that the plume would be diluted due to volume flux divergence.

Reflections

Dispersion of pollutants during the plume's nocturnal transport down the valley will result in a spreading of the plume in both the vertical and horizontal, resulting in the plume's eventual contact with the valley surfaces (valley floor and sidewalls). Additional spreading of the plume, using the basic Gaussian equations, would give the physically unrealistic result of appreciable concentrations occurring "beyond" the valley sidewalls or "below" the valley floor. Concentrations calculated for receptors within the valley cross section would be too low and the total pollutant mass of the plume would not be conserved within the valley. Several methods have been proposed to remedy this situation [26,32]. The valley may, for example, be treated as a channel having vertical sidewalls. Then, single or multiple reflections of the plume from the sidewalls can be simulated by the method of "image plumes", in exact analogy to the way that reflections off an elevated inversion surface are now handled in many Gaussian models [26]. Other similar means of handling such plume reflections have been tried by the authors giving consideration to the inclined sidewalls of real valleys, but all such methods thus far investigated have suffered from drawbacks of one type or another. The most satisfactory solution came from a consideration of pollutant mass conservation within the plume, to be discussed in the following paragraphs.

The Gaussian plume equations are a solution to the classical diffusion equation obtained by means of a number of restrictive assumptions (steady-state motion, $\partial u/\partial z=0$, etc.) and application of certain boundary conditions. Among the boundary conditions is an expression of plume mass conservation, given by

$$Q = \int_{-\infty}^{\infty} \int_{-\infty}^{\infty} u_v x_v dy dz \text{ for } z > 0. \quad (27)$$

This integral constraint, which applies to the basic mathematical form of the Gaussian equation [Equation (9)], has a simple physical meaning. Suppose that a source emits a pollutant at the rate Q of 1 kg/s into a horizontal wind of 1 m/s. This will result in a kilogram of pollutant mass being carried in a meter of transported air. Following the Gaussian plume equation this kilogram of pollutant is simply distributed in the 1-m slice of air following a bi-normal distribution. The total plume mass within the 1-m slice, however, does not change. It is 1 kg regardless of whether the kilogram is relatively concentrated into a tightly confined plume or widely dispersed about the plume center. Thus, when one integrates the pollutant concentration over the volume of the slice from $y=-\infty$ to $y=+\infty$ and from $z=-\infty$ to $z=+\infty$, and u_v is constant, we obtain

$$\frac{Q}{u_v} = \int_{-\infty}^{\infty} \int_{-\infty}^{\infty} \chi_v \, dy \, dz = \frac{1 \text{ kg}}{m} . \quad (28)$$

In terms of a worst-case model of pollutant dispersal in a valley, one must consider ways of preserving or conserving the total pollutant mass so that this relation still holds.

The total amount of pollutant mass in a unit cross section perpendicular to the plume path is determined by Q and u_v , but the distribution of pollutant mass about the plume centerline is determined by the bi-normal probability density function. The characteristics of this function are such that

$$\int_{-\infty}^{\infty} \int_{-\infty}^{\infty} \frac{1}{\sqrt{2\pi} \sigma_y} \exp \left(-\frac{Y^2}{2} \right) \cdot \frac{1}{\sqrt{2\pi} \sigma_z} \exp \left(-\frac{H^2}{2} \right) dY dH \quad (29)$$

where

$$Y = \frac{y-y_0}{\sigma_y} \text{ and } H = \frac{z-\zeta}{\sigma_z} .$$

A valley cross section can be superimposed on the theoretical plume cross section (Figure 11) and, through integrations, one can determine the fraction of total plume mass within the cross section within the valley and below the inversion top, as well as the mass that has diffused above the inversion top and the mass that has diffused beyond the valley sidewalls and valley floor. For example, the fraction of the total mass in the cross section that is within the valley cross section below the inversion top h_i is

$$f_1 = \int_0^{H_i} \int_{Y_L}^{Y_R} \frac{1}{\sqrt{2\pi} \sigma_y} \exp \left(-\frac{Y^2}{2} \right) \cdot \frac{1}{\sqrt{2\pi} \sigma_z} \exp \left(-\frac{H^2}{2} \right) dY dH \quad (30)$$

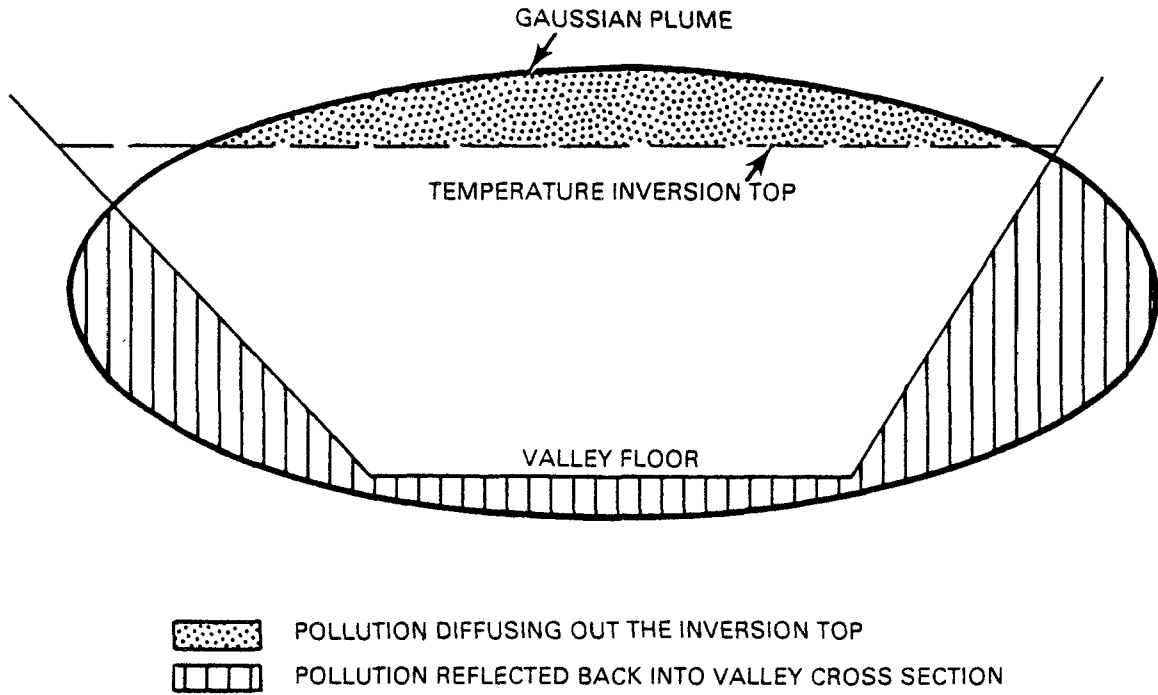


Figure 11. Cross section of pollutant plume and valley topography illustrating the integral method of calculation for plume reflection and diffusion out the top of the valley temperature inversion.

where

$$H_i = \frac{h_i - \zeta}{\sigma_z}, \quad Y_R = \frac{y_r - y_0}{\sigma_y} \text{ and } Y_L = \frac{y_L - y_0}{\sigma_y}.$$

The fraction of plume mass that has diffused out the top of the inversion is

$$f_2 = \int_{H_i}^{\infty} \int_{-\infty}^{\infty} \frac{1}{\sqrt{2\pi} \sigma_y} \exp\left(-\frac{Y^2}{2}\right) \cdot \frac{1}{\sqrt{2\pi} \sigma_z} \exp\left(-\frac{H^2}{2}\right) dY dH. \quad (31)$$

The fraction of plume mass which has diffused "beyond" the valley sidewalls (below the inversion top) and "below" the valley floor is

$$f_3 = 1 - f_1 - f_2. \quad (32)$$

In our simple model of plume reflection we must find a means of folding the mass fraction f_3 back into the valley cross section so that pollutant mass will be conserved within the valley. Although the pollutant mass could be distributed into the valley cross section any number of ways, we choose the simple expedient of mixing it uniformly within the valley unit cross section volume, so that concentrations within the cross section include an offset concentration and are given by

$$\chi(x,y,z;f;y_0) = (\chi_v + \chi_{\text{off}}) \frac{p_0}{p} \frac{T}{T_0} \quad (33)$$

where the factor $p_0 T/p T_0$ adjusts the concentrations to standard atmospheric conditions, with $p_0 = 1013 \text{ mb}$, $T_0 = 293.16^\circ\text{K}$ and T and P are the ambient temperature ($^\circ\text{K}$) and pressure (mb). The offset concentration is given as follows:

$$\chi_{\text{off}} = f_3 \frac{10^9 Q}{U_v A_c} \quad (34)$$

Equation (33) applies within the spatial domain where

- i) $x > 0$,
- ii) $y_L(z) \leq y \leq y_R(z)$, and
- iii) $0 \leq z \leq h_i$.

By mixing the lost mass uniformly we are assured that, in the limit of long travel distances x , plume concentrations within the valley cross section will approach uniformity.

The above method provides a simplified means of allowing some plume mass to escape upwards out of a valley during its down-valley transport, as well as providing for "reflections" of the plume from sidewalls and the valley floor. An objection to the volumetric mixing of the reflected plume mass through the entire cross-sectional volume seems necessary, however. This mixing of reflected plume mass through the whole valley cross section will result in an underestimate of concentrations near the sidewalls and valley floor. The amount of underestimation is not easily calculated due to a lack of understanding of the physics of the reflection processes at the boundaries during nighttime conditions. The effects of deposition on valley surfaces may reduce ambient air concentrations near the valley surfaces, however, and will tend to counteract these errors. Further work is deemed necessary to evaluate both the effects of deposition and the presence of concentration underestimates on the valley surfaces.

The integrations in Equations (30) and (31) are accomplished numerically in VALMET using a polynomial equation given by Abramowitz and Stegun [33] attributed to Hastings [34]. The Gaussian or Normal probability density function is given by

$$Z(x) = \frac{1}{\sqrt{2\pi}} \exp \left(-\frac{x^2}{2} \right) . \quad (35)$$

where variable x is the standard deviation.

The area under the Gaussian function from $-\infty$ to x is given by

$$P(x) = \frac{1}{\sqrt{2\pi}} \int_{-\infty}^x \exp \left(-\frac{t^2}{2} \right) dt = \int_{-\infty}^x Z(t) dt . \quad (36)$$

Using these definitions, we note that $Z(-x) = Z(x)$ and $P(-x) = 1-P(x)$.

Following Hastings [34] we may approximate $P(x)$, for $0 \leq x \leq \infty$, by the polynomial equation

$$P(x) = 1 - Z(x) [b_1 t + b_2 t^2 + b_3 t^3 + b_4 t^4 + b_5 t^5] + \varepsilon(x) \quad (37)$$

where

$$t = \frac{1}{1 + 0.2316419 x} ,$$

$$|\varepsilon(x)| < 7.5 \times 10^{-8} ,$$

and

$$\begin{aligned} b_1 &= 0.319381530 \\ b_2 &= -0.356563782 \\ b_3 &= 1.781477937 \\ b_4 &= -1.821255978 \\ b_5 &= 1.330274429 . \end{aligned}$$

The method for the numerical integration is illustrated below for Equation (30).

$$f_1 \approx \sum_{i=1}^n \left\{ P\left(\frac{y_R(z_i)-y_0}{\sigma_y}\right) + P\left(\frac{y_L(z_i)-y_0}{\sigma_y}\right) - 1 \right\} \cdot \left\{ \frac{1}{\sqrt{2\pi} \sigma_z} \exp \left[-\frac{1}{2} \left(\frac{z_i - \xi}{\sigma_z} \right)^2 \right] \right\} \Delta z \quad (38)$$

where

$n = h/\Delta z$
and $z_i = i\Delta z$.

The numerical integration for f_2 is accomplished in an analogous manner from Equation (31). The approximation is made in VALMET using ± 5 standard deviations as the limits of integration for y as this makes the calculations tractable and produces no appreciable error in the results.

Calculation of Steady-State Nighttime Concentrations

Calculation of nighttime pollutant concentrations at receptor point $P(x,y,z)$ can be made in a straightforward way with Equation (27) assuming steady-state conditions. The receptor must be located within a valley cross section, so that Equation (33) can be applied for

- i) any x
- ii) $0 \leq z \leq h_i$, and
- iii) $y_L(z) \leq y \leq y_R(z)$.

In practice nighttime calculations are performed for a limited number of points on the valley surfaces (floor and sidewalls), choosing points that correspond to locations where daytime pollutant concentrations will be calculated. The fixed daytime grid configuration is shown below in Figure 12. Since the model is run on a half-valley cross section, the cross section sidewall angle α is chosen to be the average of the observed sidewall angles α_1 and α_2 . Points for which nighttime pollutant concentrations are calculated are shown on the figure with x 's.

If the grid element numbers are given by $n = 1, 2, \dots, N_{BOX}$, locations at points $P(y,z)$ on the valley floor are at

$$y = \frac{BOXLEN}{2} + (n - 1) BOXLEN \quad \text{and} \quad z = 0$$

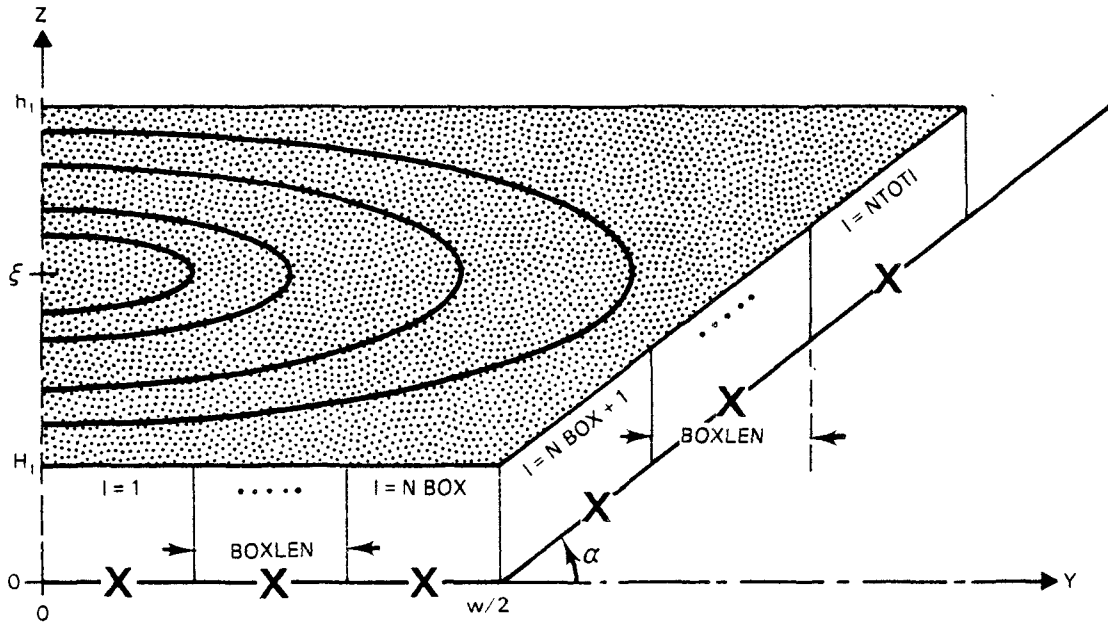


Figure 12. VALMET grid configuration on a valley cross section illustrating the nomenclature used in the model. The cross section is representative of the model configuration at sunrise, when the initial CBL-height (H_i), inversion top-height (h_i) and plume centerline height (ξ) are as shown. The x's on the figure illustrate the locations where nocturnal pollutant concentrations are determined.

Calculation points on the valley sidewalls ($n = NBOX + 1, NBOX + 2, \dots, NTOTI$) are at points $P(y,z)$ where

$$y = \frac{w}{2} + z \cot \alpha ,$$

$$z = \frac{BOXLEN \tan \alpha}{2} + (n - NBOX - 1) BOXLEN \tan \alpha ,$$

$$\text{and } \alpha = \frac{\alpha_1 + \alpha_2}{2} .$$

DAYTIME MODEL

The daytime portion of VALMET begins with solar radiation calculations, a parameterization of the surface energy budget, and estimation of the time variation of sensible heat flux which destroys the temperature inversion after sunrise. The valley energy budget model of Whiteman and McKee [3] is invoked to simulate CBL growth and inversion descent. The nighttime

Gaussian plume on a valley cross section is used as the initial condition from which the numerical model proceeds to calculate concentrations in grid elements fixed to the valley floor and sidewalls. The depth of these vertically growing grid elements is identified with the CBL height. Calculations are made of concentrations within the grid elements taking account of fumigation of the Gaussian plume into the elements and upslope advection from grid element to grid element. Pollutants are mixed uniformly within each grid element, roughly simulating atmospheric diffusion processes in the convective (actually, advective) boundary layer.

Extraterrestrial Solar Radiation

Solar radiation on a plane surface above the earth's atmosphere can be calculated using basic principles of spherical trigonometry. The basic formula for solar flux on a horizontal surface is

$$Q_{Sh} = S_0 \left(\frac{\bar{d}}{d} \right)^2 \cos Z \quad (39)$$

where S_0 is the solar constant (1367 Wm^{-2}), defined as the solar flux on a plane surface perpendicular to the sun's rays at the mean earth-sun distance, d . The factor (\bar{d}/d^2) modifies the solar constant to account for the fact that the earth-sun distance, d , varies during the year as the earth travels in an elliptical orbit about the sun. The cosine term accounts for the projection of solar flux onto the horizontal plane. This term is clearly a function of earth-sun geometry, depending on the time of day, day of year, and latitude of the surface. Z is the angle between the normal to the surface and the direction to the sun, known as the zenith angle. From spherical trigonometry [35,36] this is given as

$$\cos Z = \sin \phi \sin \delta + \cos \phi \cos \delta \cos \ell \quad (40)$$

where

ϕ = latitude

δ = sun's declination

ℓ = sun's hour angle (i.e., an angular measure of time reckoned from solar noon where 15° represents one hour). For example, 30° represents 2 hours after solar noon and -30° represents 2 hours before solar noon.

In these equations both the declination and the factor (\bar{d}/d^2) are a function of the day of year (D , from 1 to 365). McCullough [37] gives some approximate analytical formulas that allow the calculation of these terms, utilizing the longitude of the earth (λ) in its orbit around the sun as reckoned from the earth-sun radius vector at vernal equinox ($D = D_0$). The formulas are

$$\delta = \sin^{-1} (\sin \epsilon \sin \lambda) \quad , \quad (41)$$

$$\lambda = (D - D_0) + 2e(\sin \omega D - \sin \omega D_0), \quad (42)$$

and

$$\left(\frac{\bar{d}}{d}\right)^2 = (1 - e \cos \omega D)^{-2} \quad (43)$$

where

$$\begin{aligned} \epsilon &= 23^\circ 26' = \text{maximum solar declination,} \\ \omega &= 2\pi/365, \\ D_0 &= 80 = \text{day of vernal equinox, and} \\ e &= 0.0167 = \text{eccentricity of earth's orbit.} \end{aligned}$$

Using these equations, the extraterrestrial solar flux on an arbitrarily oriented plane surface can be calculated as a function of hour angle, λ . Input to the equations must include the latitude and the day of year for which calculations are desired.

The equations are used to calculate the solar flux at any time from the hour angle of sunrise, λ_{SR} , to the hour angle of sunset, λ_{SS} . For a horizontal plane, the times of sunrise and sunset are generally specified in terms of half-day length, R , calculated from Equation (40) for $\cos Z = 0$, or

$$R = \cos^{-1} (-\tan \phi \tan \delta) . \quad (44)$$

Then

$$\lambda_{SR} = -R \quad \text{and} \quad \lambda_{SS} = R . \quad (45)$$

Calculations using the above set of equations are made in terms of hour angle and are thus referenced to the time of solar noon at a particular site. To convert the hour angles to local standard time it is necessary to determine the local standard time of solar noon, and to adjust all the times accordingly. This is accomplished by making two corrections to the time of solar noon (12h 00m 00s) in the local solar time coordinate system [38]. Then the standard time of solar noon is given by

$$\begin{aligned} t_{NOON} &= 12\text{h } 00\text{m } 00\text{s} + \begin{array}{c} \text{Equation of} \\ \text{time correction} \end{array} + \begin{array}{c} \text{Longitude} \\ \text{correction} \end{array} \\ &= 12\text{h } 00\text{m } 00\text{s} + C_{ET} + C_L \end{aligned} \quad (46)$$

First, the equation of time correction is applied by adding the appropriate number of minutes and seconds from Table 4. Second, a longitude correction accounting for the difference in geographical longitude between the site and the reference meridian of its time zone is applied. The correction is +4 minutes for each degree of longitude west of the meridian. For example,

TABLE 4. EQUATION OF TIME CORRECTION

| D* | C _{ET} ** | | D | C _{ET} | | D | C _{ET} | | D | C _{ET} | | D | C _{ET} | |
|----|--------------------|-----|-----|-----------------|-----|-----|-----------------|-----|-----|-----------------|-----|-----|-----------------|-----|
| 1 | 3m | 12s | 91 | 4m | 08s | 181 | 3m | 21s | 271 | -9m | 06s | 361 | 0m | 47s |
| 16 | 9 | 32 | 106 | -0 | 01 | 196 | 5 | 46 | 286 | -13 | 33 | | | |
| 31 | 13 | 24 | 121 | -2 | 51 | 211 | 6 | 21 | 301 | -16 | 06 | | | |
| 46 | 14 | 16 | 136 | -3 | 44 | 226 | 4 | 44 | 316 | -15 | 53 | | | |
| 61 | 12 | 23 | 151 | -2 | 33 | 241 | 1 | 07 | 331 | -12 | 34 | | | |
| 76 | 8 | 39 | 166 | 0 | 10 | 256 | -3 | 50 | 346 | -6 | 34 | | | |

* D = day of year

** C_{ET} = equation of time correction (minutes and seconds).

the reference meridian of the Mountain Time Zone is 105°W longitude. For a site at 106°W longitude, the correction is $C_L = 4(106-105) = +4$ minutes.

The above equations can be used to determine extraterrestrial solar flux at any site on a given day for any given time (i.e., hour angle). Calculations using these equations for a latitude of 40°N and longitude of 109°W show that the solar flux Q_{Sh} as a function of time on a given day closely follows a sine curve. This simple analytical form proves so accurate at the latitudes and longitudes of interest and is so easy to calculate that it is used in the model instead of the full formulation. The sine approximation is given by

$$Q_{Sh} = A_1 \sin \frac{\pi}{\tau} (t - t_{SR}) \quad (47)$$

where

A_1 = solar flux at solar noon
 τ = length of daylight period
 t_{SR} = time of sunrise, and
 t = time.

One can calculate A_1 by evaluating Equation (40) with $\lambda = 0$, such that

$$A_1 = S_0 \left(\frac{d}{d_0} \right)^2 (\sin \phi \sin \delta + \cos \phi \cos \delta) \quad (48)$$

The length of the daylight period is given by

$$\tau = 2R = 2 \cos^{-1} (-\tan \phi \tan \delta) \quad (49)$$

The time of sunrise is evaluated in local standard time using

$$t_{SR} = t_{NOON} + \lambda_{SR} \left(\frac{180}{15\pi} \right) . \quad (50)$$

If the model equations are used far from the latitudes of the central Rocky Mountains, the model user should verify that the sine approximation is a valid representation of solar flux, by comparing its calculations with the full analytical equations.

Parameterization of Sensible Heat Flux

The sensible heat flux which constitutes the basic driving term of the daytime portion of the model is parameterized from the extraterrestrial solar flux using the formula

$$F = A_0 [A_1 \sin \frac{\pi}{\tau} (t - t_{SR})] = A_0 Q_{Sh} \quad (51)$$

where A_0 is a fraction between 0 and 1. This formula should be recognized as a crude parameterization for sensible heat flux, simply stating that the sensible heat flux is a constant fraction of the time-dependent extraterrestrial solar flux, as illustrated below in Figure 13.

A_0 depends on a great many factors which are not yet included explicitly in the model. In general, A_0 should be a time-varying function dependent on the

- transmissivity of the earth's atmosphere,
- cloud cover,
- surface albedo,
- soil moisture,
- surface cover or vegetation,
- longwave radiation budget, and
- other factors.

A future version of VALMET should include some of these factors explicitly, at least the ones which may affect worst-case pollutant concentration, using as a basis the extensive work already conducted on these topics by other investigators.

Model Grid

The daytime portion of VALMET uses a numerical technique to simulate time varying pollutant concentrations in grid elements that are fixed to the valley floor and sidewalls. Calculations are made for individual time steps during the temperature inversion breakup period beginning at sunrise and using the nocturnal steady-state concentrations within the valley cross section as an initial condition.

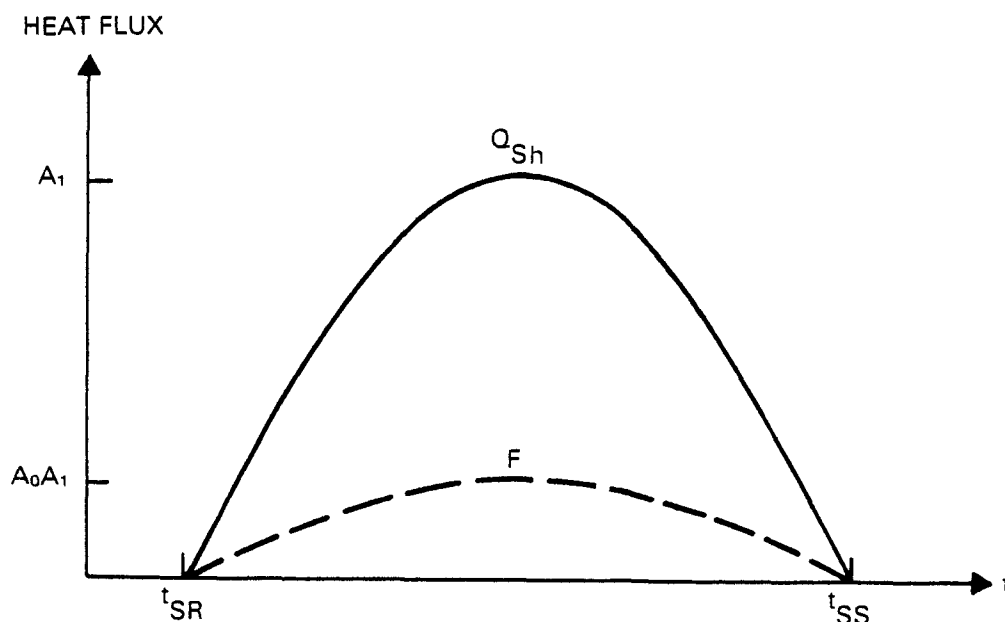


Figure 13. Extraterrestrial solar heat flux as a function of time, showing solar model nomenclature. The figure illustrates how the sensible heat flux F is parameterized as a fraction A_0 of the extraterrestrial solar heat flux on a horizontal surface above the site. The times of sunrise and sunset are shown. The daylength τ is defined in the model as the time difference between sunrise and sunset.

The geometry of the valley cross section, illustrating the numerical grid, is shown in Figure 14. Calculations in the model are performed on a half-valley cross section.

Grid elements are arranged from the valley center across the valley floor and up the sidewall, with grid element height representing the height of the CBL, assumed not to vary from grid element to grid element. At sunrise the model is initiated with a 25 m CBL height, and an inversion top height that is obtained from observations in the modeled valley. These initial heights change after sunrise as sensible heat flux drives the destruction of the valley inversion. Specifically the height of the CBL, $H(t)$, increases and the height of the inversion top, $h(t)$, decreases. The simulation is accomplished by treating the Gaussian plume within the cross section as being "frozen" within the inversion. After sunrise, concentrations within individual grid elements change as the grid elements grow upwards into the frozen plume, as the inversion sinks causing pollutants to sink into the tops of the grid elements, and as upslope flow develops within the CBL. These upslope flows develop as air parcels are heated by sensible heat flux over the sidewalls and rise up the slope. The speed of the slope flows is calculated under a continuity of mass constraint within the cross section below the (sinking) inversion top. That is, sinking of the top of the inversion with time implies that mass is removed from the cross section below the inversion top level. In the

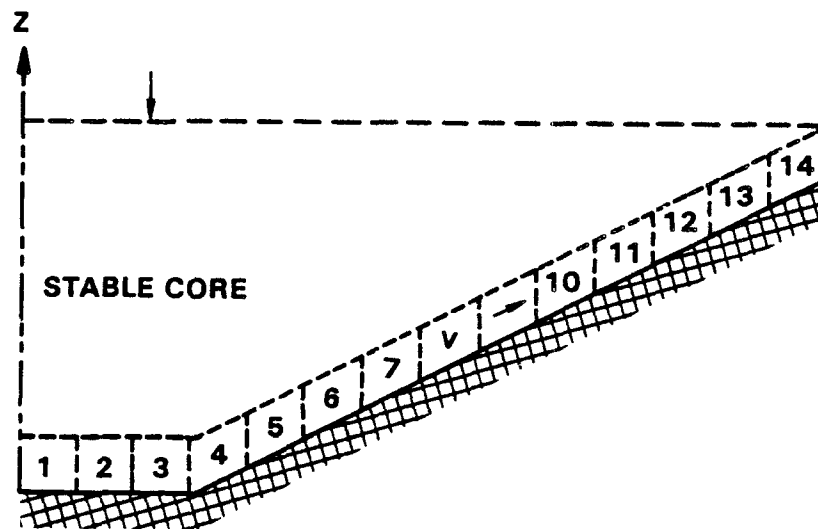


Figure 14. Cross section of the valley floor and sidewalls illustrating the grid elements whose height corresponds to the CBL heights. The rate of sinking of the top of the inversion (arrow) is related to the upslope transport of mass (other arrow) by the equation of mass continuity.

model, the assumption is made that the upslope flows carry the mass required to allow the inversion to sink at the rate predicted from Whiteman and McKee's [3] bulk thermodynamic model. This model is driven by sensible heat flux considering the thermodynamic energy budget of the valley cross section.

One of the assumptions in the model is that the top of the valley inversion at sunrise extends horizontally across the valley cross section. This assumption is supported by data from an observational program conducted in Colorado mountain valleys [9]. In that study several experiments were conducted by dual tethersondes located on a cross valley section. These observations showed that the inversion top was nearly horizontal. This is not unexpected, since hydrostatic forces should produce settling of cold air masses in topographic depressions or valleys and would result in horizontal isentropes in the absence of major cross valley inflows. This effect would be more pronounced for strong inversions where the hydrostatic forces would be stronger. Gravity waves are known to propagate frequently on the upper boundary of such inversion layers and are frequently noted in acoustic sounder records. These waves are generally of small amplitude and should not greatly affect the validity of the assumption of horizontal homogeneity.

Thermodynamic Equations for CBL Ascent and Inversion Descent

For details of Whiteman and McKee's thermodynamic model of temperature inversion breakup in mountain valleys the reader is referred to the original article (Appendix C). Here a brief explanation is given.

One can view a valley temperature inversion as a pool of cold air trapped within a valley. This pool has an energy deficit relative to the air above the valley, and the temperature inversion can be destroyed only by warming the pool to the same potential temperature as the air above the valley. The amount of energy required to warm the pool can be calculated from the First Law of Thermodynamics knowing the depth of the pool, the vertical temperature gradient within the pool (assumed constant) and the cross valley dimensions of the pool, by means of a volumetric integration through the valley cross section. This energy deficit is overcome by sensible heat flux, which can be estimated as a fraction of the downward solar radiation coming across the area of the top of the valley temperature inversion. Conversion from solar energy to sensible heat occurs at the ground. Downwards solar heat flux across the inversion top will be intercepted on a valley surface below the inversion top and will be available as sensible heat flux to warm the inversion airmass.

The topography of the valley strongly affects the course of the inversion destruction by determining which of the patterns of inversion destruction will be followed and by controlling the overall rate of heating of the valley atmosphere. This control on the rate of heating can be explained by Figure 15. Consider, for example, a valley that is completely filled by a temperature inversion. Solar energy coming downwards across the top of the valley inversion will be converted to sensible heat flux at valley surfaces and will be used to heat the inversion volume. The ratio of the area at the inversion top through which this radiation comes to the inversion volume governs the rate of warming of the valley atmosphere and, consequently, the time required to destroy the inversion. Given an equally strong and deep inversion over the plains, the valley inversion will be destroyed more rapidly since the same energy input goes to heat a smaller volume of air in the mountain valley. The thermodynamic model includes this important factor, which arises from the volumetric integration in the derivation of the model equations.

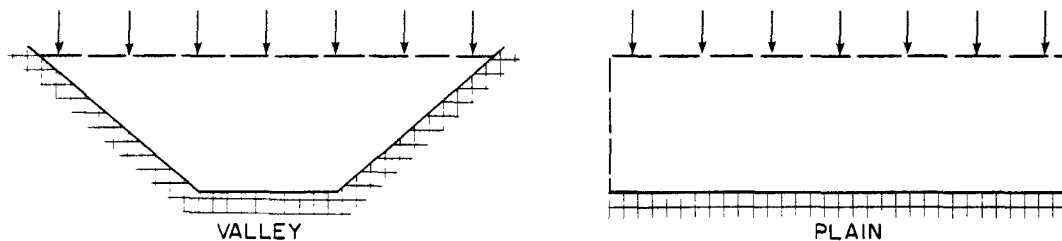


Figure 15. Illustration of the effect of topography in controlling the heating rates of the air within a valley temperature inversion versus the air within an inversion over the plains. The same incoming energy heats a smaller volume of air in the valley case.

Whiteman and McKee's model is a "bulk" thermodynamic model in that it does not differentiate between sensible heat flux over different valley surfaces, dealing only with a bulk heat flux. The heat flux which drives the valley inversion destruction is partitioned or distributed in a fundamentally different way from that for an inversion over homogeneous terrain. There the

sensible heat flux destroys the inversion by driving an upward growth from the ground of a convective boundary layer, which warms the inversion air mass from below until the temperature deficit is overcome and the inversion is destroyed. In contrast, in a valley the upward heat flux over valley surfaces develops a convective boundary layer but also, due to sensible heat flux convergence over the slopes, causes warmed air parcels to flow up the slopes in an upslope flow that develops within the convective boundary layer. These upslope flows remove mass from the base of the temperature inversion in the shallow slope flows, and through mass continuity, results in a general subsiding motion over the valley center. The atmospheric energy budget approach used by Whiteman and McKee is capable of partitioning energy between these two different processes to produce inversion destruction solely by CBL growth, solely by inversion descent (assuming a non-growing CBL is present initially in a simulation), or by a combination of the two processes. The partitioning is controlled by a single parameter, k , defined as the fraction of sensible heat flux going to CBL growth. The remaining fraction, $1-k$, is assumed to be responsible for mass transport up the CBL which results in inversion descent. The proper partitioning of energy (i.e., the most appropriate value of k) in a particular valley can be determined by fitting the thermodynamic model to observations in a particular valley. This was done for a Colorado valley by Whiteman and McKee [9], although they cautioned that the value of k will depend on other factors besides valley geometry, including the magnitude of sensible heat flux.

Further research on the functional value of k is suggested as a high priority in this modeling approach, although the model is functional using the curve fitting approach to determining k .

The thermodynamic model is composed of two coupled equations. The first equation is a prediction equation for CBL height where, in accordance with the bulk nature of the model, the CBL depth H is assumed not to differ over the valley floor and sidewalls. The first equation is

$$H_{j+1} = H_j + \Delta H_j \quad (52)$$

where j is a time step index and

$$\Delta H_j = \frac{\theta}{T} \frac{k}{\rho C_p} \frac{w + H_j C}{w + \frac{H_j C}{2}} \frac{A_0 A_1}{\gamma H_j} \left[\sin \frac{\pi}{\tau} (t - t_i) \right] \Delta t . \quad (53)$$

Note that a non-zero initial CBL height is necessary to make this prognostic numerical equation tractable. In the model, this requirement is met by using an initial CBL height at sunrise of 25 m. The second equation, describing the inversion top height h is

$$h_{j+1} = h_j + \Delta h_j \quad (54)$$

where

$$\Delta h_j = - \frac{\theta}{T} \frac{1}{\rho c_p} \frac{[w+h_j C - k(w+H_j C)] A_0 A_1 \sin \frac{\pi}{\tau} (t-t_i) - \rho c_p \frac{T}{\theta} \frac{\beta}{2} (h_i - h_j) (w + \frac{h_i + h_j}{2} C)}{h_j \gamma (w + \frac{h_j}{2} C) - \frac{\beta}{2} (t-t_i) (w+h_j C)} \Delta t, \quad (55)$$

$$\frac{\theta}{T} = \left(\frac{1000}{p} \right) .286,$$

p = atmospheric pressure,

c_p = specific heat of air at constant pressure,

$$C = \cot \alpha_1 + \cot \alpha_2,$$

$$H_0 \equiv H_i \neq 0,$$

$$h_0 = h_i,$$

$$t = (j+1) \Delta t + t_i, \text{ and}$$

$$j = 0, 1, 2, 3, \dots, n.$$

The terms in the numerator and denominator of Equation (54) involving the warming coefficient for the air above the inversion, $\beta (^{\circ}\text{Ks}^{-1})$, allow the model to incorporate the retarding effect on temperature inversion breakup caused by warm air advection above the valley temperature inversion. Extra energy is required to destroy the valley temperature inversion if this warming occurs during the temperature inversion breakup period since the inversion cannot be broken until the entire valley atmosphere is warmed to the temperature of the air above the valley.

The numerical simulation using these coupled equations proceeds with discrete time steps and is completed when the inversion is destroyed at the first time step n at which the CBL height becomes greater than the inversion top height, such that

$$H_n \geq h_n. \quad (56)$$

In the limit of an infinitely wide valley (i.e., a plain) and $k=1$ (i.e., all sensible heat flux going into CBL growth) the equations reduce to a single equation describing CBL growth over homogeneous terrain. In the limit as k goes to 0, the equations describe inversion destruction where the CBL fails to

grow after attaining an initial height, and inversion destruction occurs due to sinking of the inversion and adiabatic warming of the valley atmosphere. Whiteman and McKee [3] have shown that this approximates inversion destruction in snow covered valleys. Values of k between 0 and 1 allow the coupled equations to describe intermediate methods of inversion breakup in which the sensible heat flux is partitioned between CBL growth and inversion sinking. A typical inversion destruction in the fall in the Eagle Valley of Colorado was simulated well using a value of $k=0.14$. The appropriate value of k for other valleys would be selected based on careful analysis of valley atmospheric data, as discussed further in Section 4.

Sinking of the inversion layer will result in a sinking of the frozen plume within the inversion. The pollution mass can be calculated by considering the vertical Gaussian pollution profile above each of the grid elements. As shown by Equations (52) and (53) for $k \neq 0$ the CBL depth (and hence grid element height) increases with each time step. This CBL growth entrains pollutant mass from the inversion's stable core into the top of each grid element. These two processes, sinking of the frozen plume into the top of each grid element and growth of the grid element upwards into the frozen plume, combine to determine the amount of pollutant mass introduced into each grid element during each time step.

As illustrated in Figure 16 for a grid element on the valley floor, these two processes result in a volume of air of depth $\Delta H_j + \Delta h_j$ and length $y_1 - y_2$ being entrained into the growing grid element during time step j . The average pollutant concentration in this air volume can be calculated from the Gaussian plume equation [Equation (33)] by averaging the pollutant concentrations at the centerpoints of the four sides of this volumetric element (Figure 17). A z -coordinate transformation is useful in these calculations so that one may think of the coordinate origin on the valley floor rising into the fixed plume, rather than the frozen plume sinking towards the valley floor.

Advection in the Slope Flows

Conservation of total air mass on the two-dimensional valley cross section of interest implies that there must be a relationship between the sinking of the inversion top and removal of mass from below the inversion top due to upslope transport of mass in the convective boundary layer over the slope. Thus, at the level of the inversion top, a slow subsidence of the broad stable core must be balanced by stronger upward motions through this level due to flow up the narrower sidewall CBLs.

The continuity equation for air of constant density on the two-dimensional cross section may be written as

$$\frac{\partial v}{\partial y} = - \frac{\partial w}{\partial z} . \quad (57)$$

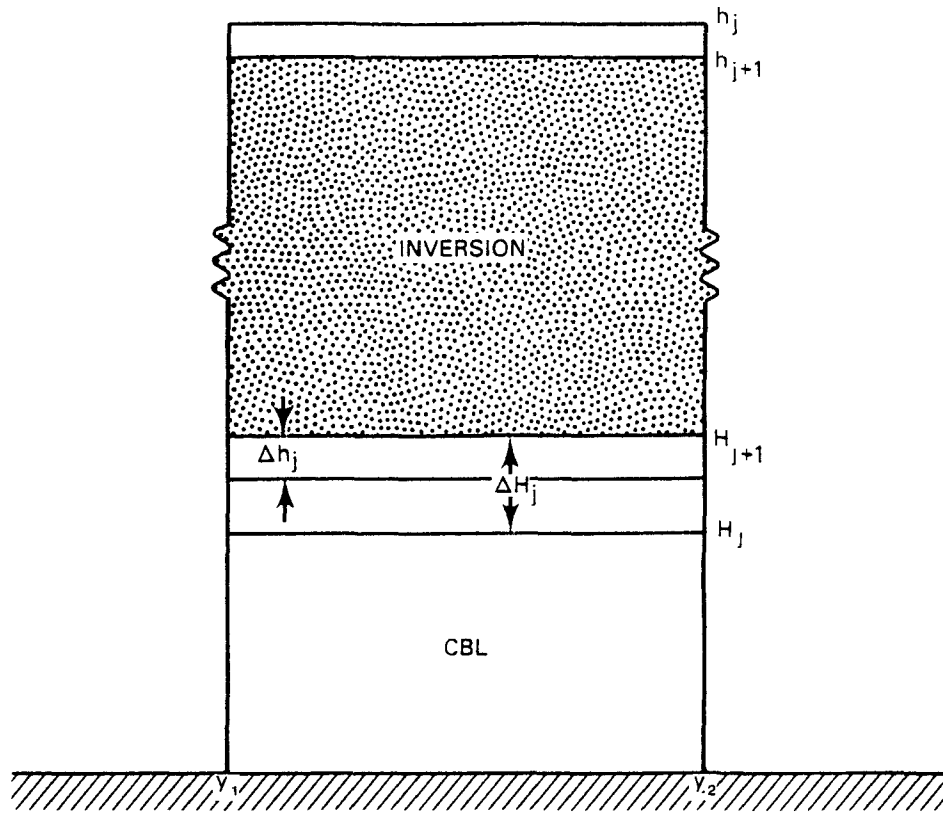


Figure 16. Diagram showing the changes in CBL and inversion depth at a given time step above a valley floor grid element. The amount of air volume incorporated into the growing CBL at each time step is seen to be represented by $(y_2 - y_1) \cdot (\Delta h_j + \Delta H_j)$ cubic meters.

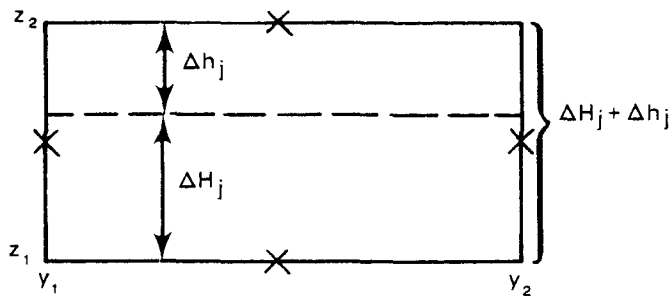


Figure 17. Representation of the volumetric element of mass incorporated into the growing CBL above a valley floor grid element at each model time step. The x's in the figure represent the positions where pollutant calculations are performed at each time step to estimate the average pollutant concentration carried within the volumetric element during the time step.

This equation may be used to calculate wind velocities at the boundaries or septa of the grid elements in the slope flow layer. For the first grid element on the valley floor, we assume that the wind velocity on the left septum at the valley center is zero (i.e., there is no mass transferred across the valley center within the CBL). At a given time step a certain amount of mass sinks into the grid element of length L and depth D . Integrating,

$$\int_0^D \int_0^L \frac{\partial v}{\partial y} dy dz = - \int_0^D \int_0^L \frac{\partial w}{\partial z} dy dz \quad (58)$$

or

$$\overline{V_L - V_0} = \frac{L}{D} \bar{w}_L . \quad (59)$$

Thus, an inversion sinking at the rate of .01 m/s into the top of a 100-m-long grid element of depth 50 m will produce a wind speed increase from the left septum of the grid element to the right septum of the grid element of

$$\overline{V_L - V_0} = \left(\frac{100}{50}\right) .01 = .02 \text{ m/s} . \quad (60)$$

The velocity, v , normal to a given septum of any grid element can thus be determined by summing the velocity changes calculated across each grid element beginning at the valley center and ending at the septum of interest.

Pollution Concentration Calculation Method

Pollution concentration calculations are made for each time step for each grid element following the general outlines of a numerical method described by Whiteman and McKee [11]. Following this method, calculations at each time step are performed sequentially for all of the grid elements, beginning with the grid element at the valley center and progressing up the valley sidewall. Calculations within each grid element (Figure 18) are made under a pollutant mass conservation assumption. The pollutant mass sinking into the top of each growing grid element is calculated using the method described above. Similarly, the advection of pollutant mass into and out of each grid element is accomplished using the velocity calculations at grid element septa as determined using a total air mass conservation constraint as described above. The concentration $C_{n,t}$ of pollutant in grid element n at the end of the t -th time step of length Δt is given by a simple pollutant mass balance:

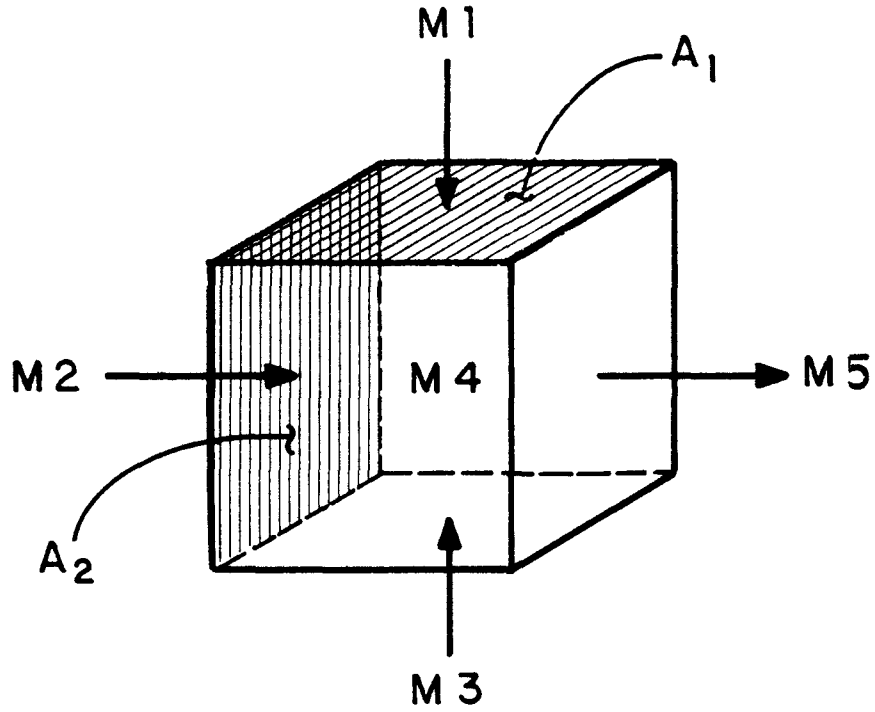


Figure 18. Schematic diagram of an individual model grid element illustrating the pollutant mass balance.

$$C_{n,t} = \frac{M_{\text{initial}} + M_{\text{in}} - M_{\text{out}}}{V_n} \quad (61)$$

$$\sim \frac{M1_{n,t} + M2_{n,t} + M3_{n,t} + M4_{n,t} - M5_{n,t}}{V_n}$$

where

V_n is the volume of the nth grid element

$M1_n$ is the mass of pollutant coming into the growing grid element n during time step Δt

$M2_n$ is the mass of pollutant advected into box n from the adjacent upstream grid element (n-1) during time step Δt

$M3_n$ is the net mass of pollutant introduced into grid element n during time step Δt from pollutant sources and sinks within the grid element

$M4_n$ is the initial mass of pollutant in grid element n at the beginning of time step Δt

$M5_n$ is the mass of pollutant advected out of grid element n into the adjacent downstream grid element (n+1) at the end of time step Δt after complete mixing of masses M1 through M4 has taken place within the grid element.

The separate terms are calculated as follows:

$$M1_{n,t} = \bar{x}_n A_1 (\Delta h_j + \Delta H_j) \quad (62)$$

where \bar{x}_n is the average pollutant concentration within the volume element $(\Delta h_j + \Delta H_j)$ that is incorporated into the grid element n at time step t (or, following our previous nomenclature, j). A_1 , the area of the grid element top (Figure 18), should not be confused with the A_1 used previously in Equation (40).

$$M2_{n,t} = C_{n-1,t} A_2 v_1 \Delta t \quad (63)$$

where

A_2 = area of box septum

v_1 = wind velocity component into grid element normal to box septum.

$$M3_{n,t} = (Q - S) A_1 \Delta t \quad (64)$$

where

Q = pollutant emission rate $[ML^{-2} T^{-1}]$

S = pollutant removal rate $[ML^{-2} T^{-1}]$.

$$M4_{n,t} = C_{n,t-1} V_n \quad (65)$$

$$M5_{n,t} = \left[\frac{M1_{n,t} + M2_{n,t} + M3_{n,t} + M4_{n,t}}{V_n} \right] A_2 v_2 \Delta t \quad (66)$$

where

v_2 = wind velocity component out of box normal to box septum.

Exponential Decay of Concentration

Calculation of concentrations in individual grid elements follows the procedure outlined. A modification of this procedure is necessary, however, for individual grid elements on the sidewalls when the top of the inversion sinks below the level of the grid element, as the depth of the CBL suddenly increases when this occurs. Concentrations would then be expected to decrease rapidly. This is handled in the model by simply allowing the last concentration calculated in the grid element to decay exponentially with time after the inversion top descends below the grid element. In view of the lack of observational evidence, the time constant of the exponential decay is chosen arbitrarily so that the concentration decreases by 2% at each 10-s time step, such that

$$C_{n,t} = .98^{\Delta t/10} C_{n,t-1} \quad (67)$$

As with any numerical model, one must be cognizant of the possibility of numerical instabilities affecting model results. The criteria for maintaining stability [39,40] constrains the model user to maintain a certain relationship between the model time step and the grid element length, depending on the upslope wind speed encountered in the simulation. This relationship is

$$v_{\max} \Delta t \leq y_2 - y_1 \quad (68)$$

Thus, the maximum upslope wind speed simulated in the model, when multiplied by the time step length must be less than the grid element length in order to maintain computational stability. In the VALMET model, the user may choose $(y_2 - y_1)$ but has no control over Δt and v_{\max} . Calculations are made automatically within VALMET to ensure computational stability. Since the maximum upslope wind velocities should never exceed 10 m/s, we may ensure computational stability by setting

$$\Delta t = \frac{y_2 - y_1}{10} \quad (69)$$

Thus, for example, a time step of 10 s is sufficiently small to ensure computational stability in a model simulation with 100 m grid elements.

Following the numerical method outlined above, concentration may be calculated for every time step for every grid element. Rather than storing each of these concentrations, which would take a great deal of computer

memory, 5-min-average concentrations are stored. This greatly reduces computer storage requirements. The 5-min-average concentrations constitute one of the main outputs of the model.

Maximum 1- and 3-Hour-Average Concentrations

Another output of the model is the maximum 1- and 3-hr-average concentrations and their times of occurrence in each of the grid elements. These calculations are made from the basic 5-min-average concentration array for each grid element by means of a moving average method. Initial tests have been conducted to confirm that the maximum 1- and 3-hr-average concentrations calculated from the 5-min-average array do not differ significantly from concentrations calculated from a 10-s-average concentration array.

SECTION 4

OVERVIEW OF MODULAR VALMET MODEL

The initial valley air quality model called VALMET has been designed and constructed based on hypotheses presented in Section 2 that arose from an observational study of Colorado valley meteorology. The model uses the technical approach and equations outlined in Section 3.

The VALMET model can be used to simulate the transport and diffusion of pollutants released from an elevated source in a well-defined mountain valley during the nighttime and morning transition periods. The model operates on a valley cross section an arbitrary distance down-valley from an air pollution source and has been constructed to include parameterizations of the major physical processes that act to disperse pollution during these time periods.

Before a modeler attempts to use VALMET to simulate dispersion in a particular valley, he should critically review Sections 1 through 3 of this report. Since the modeling approach is phenomenological, and individual physical processes affecting pollutant dispersion are parameterized, the modeler should be wary of applying the model to a meteorological or topographical situation where model assumptions are invalidated or physical processes parameterized in the model are clearly not occurring. The modeler should carefully review existing meteorological data for the valley of interest to see whether the model applies.

Even if the model's assumptions seem valid, the present state of the art in such modeling results in the use of rather arbitrarily specified parameters within the model. Further work is necessary to refine our estimates of the values of these parameters (e.g., k , σ_y , and σ_z). This work would benefit from comparisons of model results with actual diffusion trials in real valleys. In view of our rather tentative understanding of valley meteorology, the model has been constructed in a modular fashion. This modularization of the code is a major design feature of the model and should allow the code to be modified easily as we learn more about the meteorology of valleys and find better parameterizations for individual physical processes. The modules have been designed, where possible, so that the analytical or numerical calculations in the modules can be replaced by observational data, when available, with minimal modifications in the computer code structure. For example, if acoustic sounder data are available to measure CBL height and inversion top height, these data can replace the analytical scheme for predicting these heights.

The modular structure of the model is illustrated in Figure 19, where the modules are named and the functions of the modules are indicated. In this section we give the model user an overview of the VALMET model, explaining its structure and its input requirements. A full technical description of the modules, including variable name definitions and module inputs and outputs is given in Section 5 for the interested computer programmer. In Section 6 the model outputs are illustrated for two sample simulations. The full VALMET code is given in Appendix A. A brief historical summary of modifications to the code is given in Appendix D.

FEATURES OF THE COMPUTER CODE

The VALMET model is coded following a FORTRAN 77 standard [41] and should be useable without modification on any computer system having an up-to-date FORTRAN compiler. The model is documented internally through the liberal use of comment statements. These comments explain the purpose of sections of code or individual FORTRAN statements, or serve as variable name definition tables.

Several special features or protocols are included in the code. The dimensions of arrays in the code are generally set using PARAMETER statements. Thus, if the user finds that the array sizes are too small for the length of the simulation or too large to fit in a smaller computer he may easily change the dimensions by modifying PARAMETER statements in the main program and in selected subroutines. COMMON blocks are fully utilized in the code to reduce the memory requirements of the operating program. Most of the parameters passed to the subroutines are generally passed through the subroutine argument lists. Arrays, however, are usually passed through COMMON blocks.

The model was developed on a VAX/VMS 11/780 computer. After compilation, a single model run generally takes 1 minute of central processor time on the VAX, loads in 95,000 bytes (25K words) of core, and costs approximately \$1.00. Costs of optional plotting will vary from installation to installation.

MODEL INPUTS

The VALMET program runs in an interactive mode in which the user controls program execution from a remote interactive terminal. The user enters model inputs by following directions given to the user on the terminal screen.

As with any model, model performance will be a function of the suitability of the input data entered by the user. Where worst-case values of the input parameters are estimated on the basis of few data, the user should consider the model results to be a screening analysis only. On the other hand, an industrial installation having a great deal of pollutant concentration and meteorological data could use the model as a site-specific model by making specific modifications to the model to include observed plume dilution, dispersion coefficients, etc. This would require considerable field experimentation and data analysis.

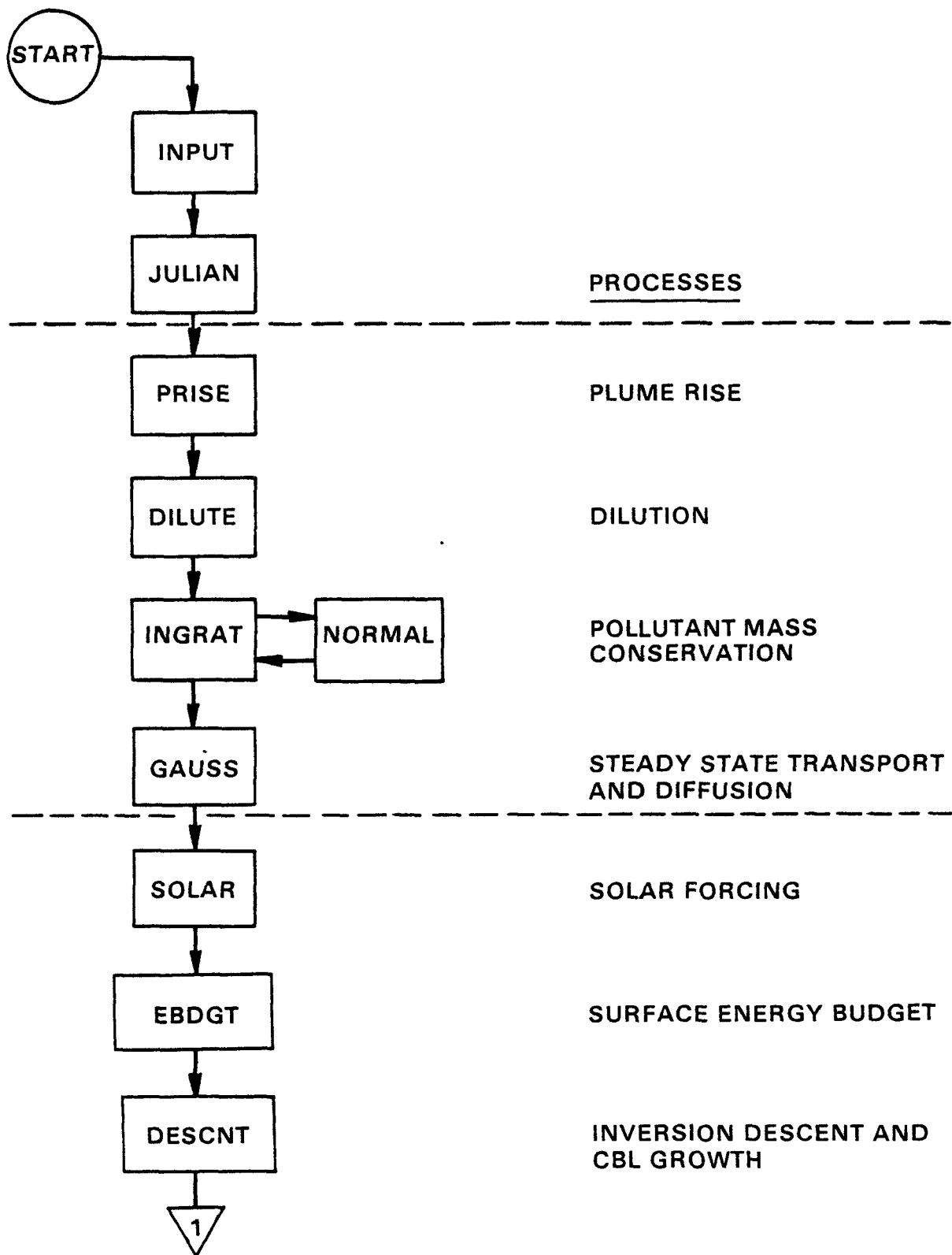


Figure 19. Flow diagram of VALMET model, showing the modular structure of the model and the physical processes parameterized in the modules. The modules indicated between the two-horizontal dashed lines constitute the nocturnal portion of the model. The daytime portion of the model follows the second dashed line.

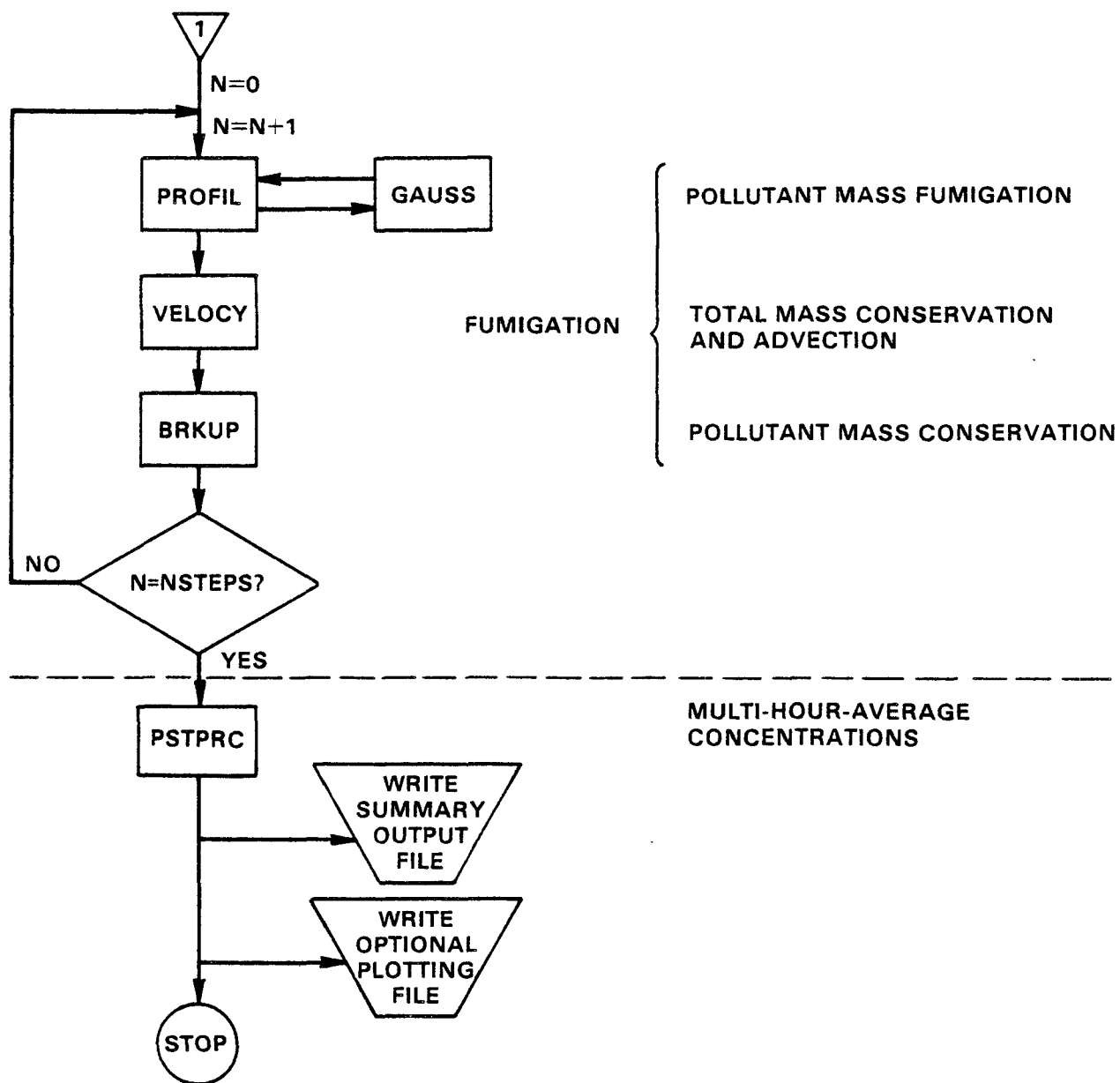


Figure 19. (contd)

When the user runs VALMET from an interactive terminal, a data table appears on the user's screen. This table gives sample input values for a model run. The user may follow directions given on the screen to change any of the input values to simulate air pollution dispersion in any valley of interest, or he may simply specify that the sample (or default) simulation be run.

The input table (Figure 20) is arranged according to categories of input data. Table input values for the sample simulation are generally specified in the MKS system of units, although pressures are given in millibars and parameters involving potential temperatures are given in degrees Kelvin in conformance with general meteorological practice.

Table 5 below gives a full listing of the appropriate units of all input parameters used in VALMET as well as the default values of these parameters. VALMET is programmed so that the user can change input values as many times as necessary until the input table is properly completed. Once the input table is satisfactory to the user, he instructs VALMET to proceed with the model run.

SPECIFICATION OF THE MODEL INPUTS BY THE USER

As a convenience to the user, the VALMET program checks to see that any parameter values input by the user are within a normal atmospheric range of values for that parameter in the units required by VALMET. See Table 6 for a listing of the ranges of values assigned to each parameter. If the input value is outside normal atmospheric ranges, a message is sent to the user to respecify the input value. The intent of this feature is to help the user identify gross input errors caused, for example, by using the wrong units for input variables.

In this section of the report we will instruct the model user how to determine the input parameters that are required by the model. The parameters are entered into the model by the user as he follows instructions given on the interactive terminal screen. The input parameters are discussed in groups, as follows:

Valley Characteristics

The characteristics of the valley topographic cross section must be obtained from topographic maps. The user should plot the terrain cross section at the down-valley distance of interest. From this cross section the user should estimate the valley floor width (estimates to the nearest 100 m should be sufficient) and the two sidewall inclination angles. The user must use his judgment when making these estimates, depending on the representativeness of the topographic cross section plotted. Since the model will deal with the valley sidewalls only to the initial depth of the temperature inversion, the user should ignore the sidewalls that extend above this height when estimating representative sidewall angles.

THE PROGRAM INITIALIZATION PARAMETERS ARE SET TO THE FOLLOWING VALUES:

| | | | | | |
|----------------------|------------|----------|-------------|----------|-------------------|
| SENSIBLE HEAT FLUX | (1) A0 | = 0.24 | (2) K | = 0.15 | |
| VALLEY CHARACTER. | (3) WIDTH | = 600. | (4) ALPHA1 | = 15. | (5) ALPHA2 = 15. |
| MODEL CHARACTER. | (6) NBOX | = 3 | | | |
| INVERSION CHARACTER. | (7) HZERO | = 500. | (8) GAMMA | = 0.025 | (9) BETA = 0.000 |
| SITE LOCATION | (10) LAT | = 40.00 | (11) URLONG | = 105.00 | |
| DATE | (12) MO | = 9 | (13) IDAY | = 21 | (14) IYR = 82 |
| VALLEY ATMOSPHERE | (15) TEMP | = 10.00 | (16) PRESS | = 750.00 | |
| GAUSSIAN PLUME | (17) XC | = 10000. | (18) YZERO | = 0. | (19) UC = 4.00 |
| | (20) Q | = 0.0010 | (21) STAB | = F | (22) US = 4.00 |
| STACK CHARACTER. | (23) H | = 250.00 | (24) STMP | = 100.00 | (25) SRAD = 3.00 |
| | (26) SVEL | = 24.00 | (27) AS | = 0. | |

IF NO CHANGES ARE TO BE MADE IN VALUES IN TABLE ---- ENTER 99

IF "STAB" IS TO BE CHANGED ---- ENTER 98

IF CHANGES OTHER THAN TO "STAB" ARE TO BE MADE ---- ENTER TOT. NUMBER OF CHANGES

Figure 20. Illustration of the VALMET model input table as it appears on the user's interactive screen.

TABLE 5. DEFAULT VALUES OF VALMET INPUT PARAMETERS

| Variable Name | Definition | Units | Default Value |
|------------------|--|--------------------------------|------------------|
| 1. A0 | Fraction of solar flux converted to sensible heat flux | 0-1 | 0.24 |
| 2. K | Fraction of sensible heat flux used to grow CBLs | 0-1 | 0.15 |
| 3. WIDTH | Valley floor width | m | 600 |
| 4. ALPHA1 | Sidewall #1 elevation angle | ° | 15 |
| 5. ALPHA2 | Sidewall #2 elevation angle | ° | 15 |
| 6. NBOX | Number of grid elements on valley floor half-width | - | 3 |
| 7. HZERO | Initial inversion depth | m | 500 |
| 8. GAMMA | Inversion vertical potential temperature gradient | °K/m | 0.025 |
| 9. BETA | Rate of potential temperature increase above valley | °K/s | 0 |
| 10. LAT | Latitude | °N | 40 |
| 11. URLONG | Longitude | °W | 105 |
| 12. MO | Month | 1-12 | 9 |
| 13. IDA | Day of month | 1-31 | 21 |
| 14. IYR | Year | 00-99 | 82 |
| 15. TEMP | Air temperature | °C | 10 |
| 16. PRESS | Air Pressure | mb | 750 |
| 17. X | Down-valley distance from stack | m | 10000 |
| 18. YZERO | Stack offset distance from valley floor centerline | m | 0 |
| 19. UC | Plume-carrying wind speed at receptor cross section | m/s | 4 |
| 20. Q | Stack emission rate | kg/s | 0.001 |
| 21. STAB | Atmospheric stability | D-F | F |
| 22. US | Plume-carrying wind speed at source cross section | m/s | 4 |
| 23. H | Plume centerline height | m | 250 |
| 24. STMP | Stack emission temperature | °C | 100 |
| 25. SRAD | Stack radius | m | 3 |
| 26. SVEL | Stack emission velocity | m/s | 0 |
| 27. AS | Cross-sectional area at source | 10 ³ m ² | 0 |

Date

The user must specify the date of the simulation by giving the month, day and year. The date is necessary in the solar model to calculate day length, time of sunrise, etc. The year is necessary to account for the minor effect of leap years on the simulation.

TABLE 6. LIMITS ON THE VALUES OF INPUT PARAMETERS

| Variable | | Units | Lower Limit | Upper Limit |
|------------|--------------------------------|-------|-------------|-------------|
| Name | | | | |
| 1. A0 | - | | 0 | 1 |
| 2. K | - | | 0 | 1 |
| 3. WIDTH | m | | 0 | 50000 |
| 4. ALPHA1 | ° | | 0 | 90 |
| 5. ALPHA2 | ° | | 0 | 90 |
| 6. NBOX | - | | 1 | 30 |
| 7. HZERO | m | | 0 | 2000 |
| 8. GAMMA | °K/m | | 0 | 0.050 |
| 9. BETA | °K/s | | 0 | 0.0005 |
| 10. LAT | °N | | -90 | 90 |
| 11. URLONG | °W | | -180 | 180 |
| 12. MO | - | | 1 | 12 |
| 13. IDA | - | | 1 | 31 |
| 14. IYR | - | | 0 | 99 |
| 15. TEMP | °C | | -50 | 50 |
| 16. PRESS | mb | | 600 | 1050 |
| 17. X | m | | 100 | 100000 |
| 18. YZERO | m | | -50000 | 50000 |
| 19. UC | m/s | | 0 | 15 |
| 20. Q | kg/s | | 0 | 1 |
| 21. STAB | D-F | | D | F |
| 22. US | m/s | | 0 | 15 |
| 23. H | m | | 0 | 1000 |
| 24. STMP | °C | | 0 | 600 |
| 25. SRAD | m | | 0 | 5 |
| 26. SVEL | m/s | | 0 | 50 |
| 27. AS | 10 ³ m ² | | 0 | 150000 |

Site Location

Both latitude and longitude of the site must be specified by the user in order to support solar radiation calculations within the model. The longitude value is necessary to account for corrections to the time of sunrise.

Model Characteristics

The user must specify the number of grid elements on the valley floor half width in order to define the model's numerical grid. There are several considerations that the user should keep in mind when specifying this number. The implications of the specification can be considered by referring to Figure 12.

The number of grid elements on the valley floor half width (NBOX) is used in the model to figure the length of the grid elements. The length is given by

$$\text{BOXLEN} = w / (\text{NBOX} * 2)$$

where w is the valley floor width. Once BOXLEN is calculated, the model then calculates how many grid elements of this length (NTOTI) will be necessary in order to reach the top of the inversion when the grid elements are arrayed end to end. NTOTI must not exceed 30, as currently dimensioned in the model. On the other hand, NTOTI should not be too small, since this parameter affects the spatial resolution of concentrations calculated within the model. As a rule of thumb, NBOX may be chosen to produce grid elements of 100 or 200 m length.

Valley Atmosphere

The mean temperature and pressure within the valley temperature inversion at sunrise should be estimated using the altitude of the site and knowledge of seasonal changes in atmospheric temperature. Observational data would be useful in estimating both of these parameters, but the accuracy of these estimates is not critical to the model results. The values are used to correct the model concentration values to standard pressure and temperature and to calculate the atmospheric density for use in the inversion breakup or energy budget calculations.

Stack Characteristics

The stack characteristics should be obtained from engineering calculations for the specific air pollution source. The required parameters include physical stack height, effluent temperature, stack inside radius, and exit velocity. If the user does not wish to engage the plume rise module, the stack radius or exit velocity should be specified as zero. The plume center-line height over the entire length of the valley will then be equal to the value specified as the physical stack height. The final parameter that must be specified by the user is the area of the valley cross section at the stack. This area, bounded by the valley floor, the two sidewalls and the temperature inversion top at sunrise, is used in the plume dilution module to calculate clean air volume flux across the cross section at the pollutant source. The area should be calculated from Equation (1), but is input in thousands of square meters (i.e., the results of the calculation with Equation (1) should be divided by 1000 before being input into the model). The model user will need to know the inversion depth at sunrise in order to calculate the area. If the user does not wish to engage the plume dilution module or does not have the wind speed observations on the cross valley section where pollution calculations are to be made, he should specify the cross-sectional area at the stack to be zero. The wind speed specification at

the downwind cross section is then deactivated (i.e., is not used in the model) and the plume is advected down the valley with the wind speed specified at the pollutant source with no plume dilution during transport.

Inversion Characteristics

The user must specify inversion depth and inversion potential temperature gradient at sunrise, as well as the rate of potential temperature increase at the inversion top during the period of inversion breakup. The user should specify these parameters on the basis of observations of temperature inversion development within the valley of interest. These observations are critical to the model results and should be based on vertical soundings taken from the valley floor, if available. The modeler should be cautioned against using observations taken from surface-based instruments, unless these have been shown to be clearly related to vertical profiles over the valley center. A qualified analyst may be able to determine the inversion depth from acoustic sounder records. The modeler must use his judgment in specifying a single number for the potential temperature gradient at sunrise. Actual soundings are often complicated, especially in the lower levels. The potential temperature gradient obtained by subtracting the surface value from the value at the inversion top and dividing by the inversion depth may not be a representative number for the inversion as a whole when a shallow and very strong inversion layer is present near the ground. The temperature gradient is used in the model primarily to calculate the energy deficit within the valley represented by the presence of the temperature inversion. The total energy deficit is obtained under an assumption of cross valley homogeneity by weighting the temperature deficits at various levels by the cross-sectional area of the valley. Since the valley is much wider at its top than near the valley floor, errors made in estimating temperature deficits (i.e., determining a representative potential temperature gradient) at the upper levels are more critical to model results than at the lower levels. A better estimate of the valley energy deficit will be obtained by ignoring shallow, but very strong, temperature inversion layers present on the valley floor if this means that the potential temperature gradient estimate is more accurate for upper levels.

In lieu of observations one may use the observations of Whiteman [9] to obtain first estimates of inversion depths, strengths, and inversion top warming rates in Colorado valleys.

When the model is used to estimate worst-case air pollution concentrations, one should naturally attempt to arrive at worst-case estimates of inversion characteristics parameters.

Gaussian Plume Parameters

The model user must specify Gaussian plume parameters including the distance to the cross section of interest, the stack distance offset from the valley floor centerline, the plume-carrying wind speed, the source emission rate, and the atmospheric stability.

The down-valley distance is determined from a topographic map by measuring the distance from the source to the cross valley section along the valley floor centerline following any curves or turns in the valley's course.

The stack distance offset is determined as the shortest distance from the valley floor centerline to the pollutant source on the valley floor. The sign of the distance follows from the orientation of the valley coordinate system, as discussed in Section 3.

The wind speeds used in VALMET are critical parameters that must be carefully specified from available data. Down-valley wind speeds in Colorado valleys have been shown to vary significantly from valley to valley [9], so that wind speeds in one valley are not necessarily indicative of wind speeds in another valley. In short, observations are necessary for the valley being modeled. Furthermore, the wind speeds vary on a cross valley section due to vertical and horizontal position within the cross section [42]. On a vertical profile through the nocturnal temperature inversion, the peak winds are often located about midway through the inversion depth with lower wind speeds near the ground and at the inversion top. Near-surface wind speeds, therefore, are not generally indicative of wind speeds at a typical plume carrying level. Near-surface wind direction observations, in fact, may be 180 degrees in error shortly after sunrise when wind continues to flow down-valley in the elevated stable core while the winds reverse to up-valley in the CBL which develops over the valley floor. Near-surface wind observations should, therefore, not be used to drive the VALMET model.

Two wind speeds are required inputs for the VALMET model. Both are required in order to allow for plume dilution due to clean air inflow between the source and the cross section where air pollution calculations are made. The user must specify the average nocturnal wind speed at plume-carrying level at both the source and the receptor characteristic of the nocturnal down-valley flow. They may be obtained from a doppler acoustic sounder or from successive tethered sonde or pilot balloon ascents.

The source emission rate may be obtained from engineering calculations for the stack of interest. "Worst-case" pollutant calculations should be made on the basis of worst-case emission rates. The model can not handle emission rates that vary in time, so a realistic time average emission rate is most appropriate for driving the model.

The model uses Pasquill-Gifford diffusion coefficients [26,27,43] to characterize diffusion in the nighttime, high-stability, elevated stable core of the valley temperature inversion. The stability class in this stable region should be D, E, or F following the original definitions of atmospheric stability given in Table 3. The user-input stability class is automatically modified internally within VALMET to account for enhanced diffusion in complex terrain.

Sensible Heat Flux

The final two input parameters in the VALMET model are the two sensible heat flux parameters. The parameters, which are both fractions between 0 and 1, are based on the valley surface energy budget. Little research has yet been done on valley energy budgets and, since the energy budget is known to strongly influence the local diurnal meteorology of valleys, the initiation of such research should be considered an important priority in future studies.

The first sensible heat flux parameter is A_0 , the fraction of extra-terrestrial solar heat flux converted to sensible heat flux within the valley. The conversion, of course, occurs at the valley surfaces (valley floor and sidewalls), but the bulk thermodynamic model used as the basis of VALMET cannot distinguish between energy budgets over the different surfaces. The fraction required in the model, then, is the fraction of the (extraterrestrial) solar heat flux coming downward across the upper surface of the temperature inversion which is converted to sensible heat flux within the valley. This fraction is assumed to be constant during the temperature inversion breakup period. A_0 depends on the transmissivity of the earth's atmosphere to the solar beam, the albedo of the valley surfaces and vegetative cover, and the presence of clouds, as well as the partitioning of the solar beam upon striking the valley surfaces. The long wave radiative balance also plays a role at these surfaces which affects sensible heat flux. Whiteman [9] has analyzed the individual terms in the surface energy budget to determine that the maximum value of A_0 is unlikely to be greater than 0.6. A valley having a low reflectivity would approach this value under clear skies only if the valley had no soil moisture. Whiteman and McKee [3] were able to simulate temperature inversion breakup well in a dry Colorado valley in October using an A_0 value of 0.45. Maximum values of heat flux observed in the 1968 Kansas experiments [44], if assumed to be representative of solar noon values, correspond to A_0 values of about 0.25. The value of A_0 may be smaller in winter when snow cover is present in a valley and the albedo is large. The overall albedo in winter may depend strongly on the presence of forest cover within the valley or the relative proportions of other lower albedo surfaces. Whiteman and McKee [3] were able to simulate inversion breakup in Colorado's snow-covered Yampa Valley using $A_0 = 0.19$.

The modeler may estimate a value of A_0 from the discussion in the paragraph above or, if sufficient meteorological data are available for the valley in question, he may base his estimate on one of two alternate quantitative methods. The first method is described below. Then the second, and more comprehensive method, which also provides a means for estimating the second sensible heat flux parameter, k , is described. The first method of determining A_0 involves the solution of Whiteman and McKee's [3] Equation (21), Equation (28), or a combination of the two for A_0 knowing, for a particular day:

- a) the sunrise temperature inversion potential temperature gradient,
- b) the inversion depth at sunrise,
- c) the valley floor width and sidewall inclination angles,
- d) the solar parameters on the day of interest, and
- e) the observed time of temperature inversion breakup.

By using such meteorological information for a variety of days in different seasons, the modeler may determine a climatology of A_0 values that would be useful in air pollution modeling. For the convenience of the reader, a reprint of the Whiteman and McKee article is included in this report as Appendix C.

The value of the second sensible heat flux parameter, k , is the fraction (0-1) of the sensible heat flux used to cause CBL growth. The remaining fraction (1- k) represents the fraction of sensible heat flux used to transport mass up the valley sidewalls causing the inversion top to sink. The value of k is 1 for flat terrain since temperature inversions are destroyed there entirely by CBL growth, but approaches zero in snow-covered valleys where CBL growth is arrested after reaching a certain height [9]. Whiteman and McKee [3] were able to simulate inversion breakup in a dry Colorado valley using $k = 0.14$. Inversion breakup in the snow-covered Yampa Valley was simulated well using $k = 0$.

The search for a mathematical relationship between k and parameters that are more easily measured is a high priority for future work. The value of k is expected to depend strongly on valley width and, perhaps, on sensible heat flux itself. Given the present lack of an appropriate mathematical relationship, the best approach for determining k is to simply determine the value of k which best fits observations of inversion breakup in the particular valley being modeled. The means by which this can be accomplished was described by Whiteman and McKee [3]. They described how the value of A_0 determines the temperature inversion breakup time, while the value of k determines the height at which the CBL and inversion top meet to cause inversion breakup, and have presented plots showing the effect of varying k and A_0 on temperature inversion breakup. Both the time and height can be observed using an acoustic sounder or multiple serial tethered sonde ascents in the valley of interest. Observed time variations of CBL depth and inversion top height can be fit with a trial and error procedure using Whiteman and McKee's [3] Equations (29) and (30). The reader should refer, again, to Appendix C. These equations are programmed in VALMET module "DESCNT" where they may be solved using a numerical method. The modeler who wishes to use the procedure should convert a copy of subroutine DESCNT to a main program where the subroutine arguments are explicitly specified. The number of time steps to inversion destruction, and the CBL and inversion top heights as a function of time would be required outputs of such a program. The effect of changing A_0 and k could then be easily investigated and fit to actual observations. A time step of 600 seconds would be sufficient for the computations desired. The numerical method requires a CBL height and inversion depth at sunrise as mathematical initial conditions. The valley meteorological data necessary to use this approach to determine k and A_0 include:

- a) inversion depth at sunrise,
- b) inversion potential temperature gradient at sunrise,
- c) valley floor width and sidewall angles,
- d) solar model parameters A_1 and τ ,

- e) the time of inversion destruction, and
- f) the height at which the rising CBL and descending inversion top meet at the time of temperature inversion destruction.

Solar parameters can be determined from model equations provided earlier in this report. Topographic parameters can be determined from a topographic map. The potential temperature gradient at sunrise requires a vertical temperature sounding. The other required parameters can also be obtained from such soundings, if they are made frequently through the valley depth during the temperature inversion breakup period. They may also be determined from monostatic acoustic sounder records by a qualified analyst.

ERROR MESSAGES

The VALMET model has several built-in checking and correction routines which will produce error messages when the model input parameters have been improperly specified by the user, or when the user attempts to use the model in a way unintended by the model developers. These messages are written on the screen of the user's interactive terminal. The error messages and their explanations are given below.

1. PARAMETER NO. nn OUT OF RANGE, PLEASE RESPECIFY

This error message is written from Subroutine INPUT when the user has tried to change the default value of an input parameter (number nn=1 to 27), but has selected a new value that is outside normal ranges of that parameter. The user should check that he has used the right units for the input specification. Execution of the program is not terminated by this error. The user may respecify the input parameters as many times as he wishes before executing the VALMET calculations.

2. STACK MUST BE ON THE VALLEY FLOOR - RESPECIFY YZERO

This error message is written from Subroutine INPUT when the user specifies a stack location that is not on the valley floor. VALMET was not designed to handle this situation, so the user must respecify the stack location. To do this, respecify YZERO to be smaller in absolute value than half the valley width W. Execution of the program is not terminated by this error.

3. DOWNVALLEY WINDSPEED AT STACK HAS BEEN SET TO 1 M/S

This error message is written from Subroutine INPUT when the user has specified a very low (0-1 m/s) plume-carrying wind speed at stack height. The nighttime VALMET simulation has, as its basis, the Gaussian plume formulation, which fails to predict concentrations realistically as winds become calm ($u_s \rightarrow 0$). To obviate this difficulty, VALMET automatically respecifies the wind speed to 1 m/s and continues execution. While the basis for this modification to the wind speed is primarily mathematical, one must recognize that perfectly calm conditions are unusual in the valley atmosphere due to the generation of

the prevalent locally developed circulations. The frequency of occurrence of calm conditions has been overestimated in the past, and is still being overestimated by the performance characteristics of available mechanical wind sensors.

4. TOO MANY GRID ELEMENTS -- PLEASE REDUCE NBOX OR RE-DIMENSION THE MODEL TO ALLOW MORE GRID ELEMENTS

This error message is written from Subroutine INPUT when the input parameters specified by the user result in the model requiring more grid elements than are currently dimensioned in the model (i.e., 30). The total number of grid elements, NTOTI, may not exceed 30 unless the user increases the dimensions in the model by changing the PARAMETER statements so that NB is the new number desired (don't forget to also change NB1, since it should be equal to NB+1). If your computer memory is limited, you must decrease NBOX and live with the poorer spatial resolution which results, as documented at other places in this report. Execution of the model is not terminated by this error. If you reduce NBOX the program will continue to execute, but if you decide to increase the model dimensions you must stop execution and make some basic changes in the VALMET code.

5. YOU HAVE SPECIFIED A WRONG STABILITY CLASS - F WILL BE USED INSTEAD

This error message is written from Subroutine INPUT when the user enters a stability class other than D, E, or F. VALMET automatically uses F stability when this occurs. Execution of the program is not terminated by this error.

6. THE PLUME, AFTER PLUMERISE, IS NOT WITHIN THE STABLE CORE

This error message is written from the main program. If the plume rises above the stable core, or never exceeds the initial CBL height, it is not transported down the valley in stable nighttime conditions and it makes no physical sense to run VALMET under these conditions. Model execution is terminated by this error.

SECTION 5

TECHNICAL DESCRIPTION OF INDIVIDUAL MODULES

VALMET-Main Program

VALMET is the main program that controls the modules or subroutines which, taken together, form the valley air quality model. The function of the main program is to provide the basic structure of the air quality model and to call the specific modules as required. In addition, several computing house-keeping functions are performed in the main program including the establishment of PARAMETER statements and COMMON blocks, and the opening and closing of output files. Model outputs are written from the main program, as well.

Inputs

Inputs to the main program come through Subroutine INPUT, a subroutine that is run interactively by the user and which features a default input table. Data coming into the main program from subroutines usually come through arguments listed in the subroutine call statement. Large arrays of data, however, are frequently transferred from the main program to the subroutines (and vice versa) through COMMON blocks.

Outputs

The results of a model run are written to two output disk files. The first output file, named VALMET.OUT, is a formatted file which contains the results of the model run. After the model is run, the contents of this file may be printed to obtain a summary record of the model run, including model input parameters and outputs. A second file, named VALMET.PLT, is also automatically generated with every computer run. This formatted file contains time series of pollutant concentrations, temperature inversion depths and convective boundary layer depths, as well as many of the basic parameters used in the model run. The file is created for the model user who wishes to develop his own plotting programs to plot the results of a model run. An example program that the authors used to generate the plots used in this report is shown in Appendix B. Since every user's computer installation will have different plotting software and hardware, this approach of creating a basic data file but not including a specific plotting program in the air pollution model seemed the most appropriate way to proceed. Interested users can develop their own specific plotting software using our example.

Conventions

The following indexing conventions are used in VALMET where it has proven convenient:

I=grid element index N or MN=time step index

Variable Name Definitions

| INPUT/ OUTPUT | VARIABLE NAME | DEFINITION |
|------------------|------------------|--|
| I | A0 | Fraction of extraterrestrial solar flux converted to sensible heat flux (0-1) |
| I | A1 | Solar flux on horizontal surface at solar noon (Wm^{-2}) |
| - | A2 | Same as A0 |
| I | AC | Valley cross-sectional area below inversion top at cross-sectional distance XC (m^2) |
| I | ALPHA1 | Sidewall #1 elevation angle (rad) |
| I | ALPHA2 | Sidewall #2 elevation angle (rad) |
| I | AS | Valley cross-sectional area below inversion top at pollution source cross section (m^2) |
| I | BETA | Rate of increase of potential temperature at inversion top ($^{\circ}\text{K/s}$) |
| I | BOXLEN | Length of grid elements (m) |
| - | CCHI | Nocturnal pollutant concentration in a grid element ($\mu\text{g}/\text{m}^3$) |
| - | CHIOFF | Concentration offset value due to reflection off valley floor and sidewalls ($\mu\text{g}/\text{m}^3$) |
| - | CLCONC | Centerline concentration ($\mu\text{g}/\text{m}^3$) |
| - | DELTAT | Time step size (s) |
| I | DLH | Plume rise (m) |
| - | DF | Inverse of dilution factor |
| I | GAMMA | Vertical potential temperature gradient ($^{\circ}\text{K/m}$) |
| I | H | Plume centerline height (m) |
| - | HCBLI | Initial CBL height (m) |
| I | HZERO | Initial depth of inversion (m) |
| - | I | Grid element index |
| - | I1 | Intermediate variable |
| - | IAVG | Averaging period (s) |
| I | IDA | Day of month (1-31) |
| - | IFIX2 | Number of grid elements on sidewall at given time step |
| - | IND | Loop index |
| I | ISTAB | Stability index (1-6) |
| - | ISTABY | Stability index for determination of σ_y (1-6) |
| - | ISTABZ | Stability index for determination of σ_z (1-6) |
| - | IT | Intermediate value used in calculating time |
| - | ITIME | Time unit=LST |

| | | |
|---|---------|---|
| I | IYR | Year (00-99) |
| - | JULDAY | Julian date (1-366) |
| I | K | Fraction of sensible heat flux used to grow CBL (0-1) |
| I | LAT | Latitude (°N) |
| - | MN | N-1 |
| I | MO | Month (1-12) |
| - | N | Time step counter |
| - | NAS | Number of averaging intervals in NINDEX |
| - | NB | Parameter giving the maximum number of model grid elements, for use in dimensioning arrays |
| - | NB1 | NB+1 |
| I | NBOX | Number of grid elements on the valley floor half-width |
| - | ND | Loop index |
| - | NINDEX | Number of time steps in simulation, including exponential decay after breakup |
| - | NS | Parameter giving the maximum number of model time steps, for use in dimensioning arrays |
| - | NSTEPS | Number of time steps required to destroy initial temperature inversion |
| - | NTOT | Total number of grid elements left in the model at a given time step |
| I | NTOTI | Total number of grid elements in the model at initiation |
| - | NTSA | Number of time steps in averaging interval |
| - | NTSR | Time of sunrise (LST) |
| - | NY | Intermediate variable used to count grid elements |
| I | PRESS | Atmospheric pressure at center of temperature inversion (mb) |
| - | PSTD | Standard pressure (1013 mb) |
| I | Q | Stack emission rate (kg/s) |
| - | RHO | Air density (kg/m ³) |
| - | SIGMAY | Sigma y (m) |
| - | SIGMAZ | Sigma z (m) |
| I | SRAD | Stack radius (m) |
| I | STMP | Stack temperature (°K) |
| - | STNDCON | Factor to adjust concentration to standard conditions |
| - | SUM1 | Fraction of plume mass within valley cross section (0-1) |
| - | SUM2 | Fraction of plume mass above valley cross section (0-1) |
| I | SVEL | Stack exit velocity (m/s) |
| - | T1 | Intermediate variable used to calculate time |
| - | T2 | Intermediate variable used to calculate time |
| - | T3 | Intermediate variable used to calculate time |
| - | T4 | Intermediate variable used to calculate time |
| - | TAU | Length of daylight period (s) |
| I | TEMP | Air temperature (°K) |
| - | TMAXC1 | Ending time of the 1-hr average concentration max (h LST) |

| | | |
|---|--------|---|
| - | TMAXC2 | Ending time of the 3-hr average concentration max (h LST) |
| - | TSTD | Standard temperature (293.16°K) |
| - | TSTP | Time in averaging period (s) |
| I | UC | Mean down-valley plume transport velocity at cross section distance XC (m/s) |
| I | URLONG | Longitude (°W) |
| I | US | Mean down-valley plume transport velocity at pollutant source cross section (m/s) |
| I | W | Valley floor width (m) |
| I | XC | Distance from stack to model cross section (km) |
| - | Y | Y-coordinate (m) |
| I | YZERO | Stack offset from valley floor centerline (m) |
| - | Z | Z-coordinate (m) |

Array Name Definitions

| INPUT/ OUTPUT | ARRAY NAME | DEFINITION |
|------------------|---------------|---|
| - | AVG(NB,2) | Maximum 1-hr and 3-hr average concentration array ($\mu\text{g}/\text{m}^3$) |
| - | CCH(2,NB) | Short-term storage location for concentrations at two adjacent time steps ($\mu\text{g}/\text{m}^3$) |
| - | CHI(NB) | Nocturnal steady state concentration array ($\mu\text{g}/\text{m}^3$) |
| - | CHIBAR(NB) | Average pollutant concentration injected into the top of grid elements at each time step ($\mu\text{g}/\text{m}^3$) |
| O | CONC(NS,NB) | Pollution concentration array ($\mu\text{g}/\text{m}^3$) |
| - | HC(NS) | Height of CBL top (m) |
| - | HITEL(NB) | Height of lower side of grid element on sidewall (m) |
| - | HITEU | Height of upper side of grid element on sidewall (m) |
| - | HT(NS) | Height of inversion top (m) |
| - | NDXTIM(NB,2) | Index number of TMAXC1 and TMAXC2 |
| - | NTS(2) | Number of time steps in 1-hr and 3-hr |
| - | SUM(NB) | Summing array to accumulate pollutant concentrations during averaging interval |
| - | TIME(NS) | Midpoint time array for averaging intervals (h MST) |
| - | V(NB1) | Slope flow velocity array (m/s) |

Subroutines Called

BRKUP
DESCNT
DILUTE

EBDGT
GAUSS
INGRAT
INPUT
JULIAN
PRISE
PROFIL
PSTPRC
SOLAR
VELOCITY

Common Blocks

BLK1
BLK2 Not used in main program
BLK3 Not used in main program
BLK4
BLK5
BLK6

INPUT-Input Module

Purpose

The VALMET program runs in an interactive mode in which the user controls program execution from a remote interactive terminal. The user enters model inputs from the remote terminal by following directions given to the user on the terminal screen by subroutine INPUT. Once the input values are specified by the user he can direct the program to begin the air pollution simulation. The functions of the INPUT module are to obtain the proper input data from the model user, to convert the input data to the proper units for processing in later modules of VALMET, to check the input data for errors, and to notify the user of any errors.

Inputs

Inputs to this module come entirely through user input from an interactive terminal, unless default values of the input parameters are selected by the user.

Outputs

Outputs from the module go to the main program through the subroutine argument list.

Variable Name Definitions

| INPUT/ VARIABLE OUTPUT NAME | DEFINITIONS |
|--------------------------------|--|
| I A0 | Fraction of solar flux converted to sensible heat flux (0-1) |
| - AC | Valley cross-sectional area at distance XC (m^2) |
| I ALPHA1 | Sidewall #1 elevation angle ($^\circ$) |
| I ALPHA2 | Sidewall #2 elevation angle ($^\circ$) |
| I AS | Cross-sectional area at source (m^2) |
| I BETA | Rate of potential temperature increase above valley ($^\circ K/s$) |
| - BOXLEN | Grid element length (m) |
| O DELTAT | Time step (s) |
| I GAMMA | Inversion vertical potential temperature gradient ($^\circ K$) |
| I H | Plume centerline height (m) |
| I HCBLI | CBL height at sunrise (m) |
| I HZERO | Initial inversion depth (m) |
| I IDA | Day of month (1-31) |
| O IFIX | Number of grid elements on sidewall |
| O ISTAB | Atmospheric stability (1-6) |
| I IYR | Year (00-99) |
| - J | Index |
| - J6 | Index |

| | | |
|---|--------|--|
| - | J12 | Index |
| - | J13 | Index |
| - | J14 | Index |
| I | K | Fraction of sensible heat flux used to grow CBL (0-1) |
| I | LAT | Latitude (°N) |
| - | LU | Logical unit number |
| I | MO | Month (1-12) |
| I | NBOX | Number of grid elements on valley floor half width |
| - | NTOTI | Total number of grid elements |
| - | NU | Number of input parameters to be changed from default values |
| I | PRESS | Air Pressure (mb) |
| I | Q | Stack emission rate (kg/s) |
| - | RHO | Air density (kg/m ³) |
| - | RNO | NBOX |
| I | SRAD | Stack radius (m) |
| I | STMP | Stack emission temperature (°C) |
| I | SVEL | Stack emission velocity (m/s) |
| I | TEMP | Air temperature (°C) |
| I | UC | Plume-carrying wind speed at cross section (m/s) |
| I | URLONG | Longitude (°W) |
| I | US | Plume-carrying wind speed at source (m/s) |
| I | W | Valley floor width (m) |
| I | XC | Down-valley distance to cross section from stack (m) |
| I | YZERO | Stack offset distance from valley floor centerline (m) |

Array Name Definitions

| INPUT/ OUTPUT | ARRAY NAME | DEFINITIONS |
|------------------|------------|--|
| - | ASTAB(6) | Atmospheric stability array |
| - | CAT(10) | Input parameter category array |
| - | ID(27) | Array of identification numbers for input parameters |
| - | NAM(27) | Input parameter name array |
| - | VAL(27) | Default input value array |
| - | VALLO (27) | Minimum values of input parameters |
| - | VALHI (27) | Maximum values of input parameters |
| - | VALNEW(27) | New values of input parameters |

Subroutine Called

None

Common Blocks

None

JULIAN-Julian Day Module

Purpose

JULIAN calculates the Julian date, given the month, day and year of the air pollution simulation.

Inputs

The month, day, and year are input to the subroutine from the main program through the subroutine argument list.

Outputs

The Julian date is sent to the main program through the subroutine argument list.

Variable Name Definitions

| INPUT/ OUTPUT | VARIABLE NAME | DEFINITION |
|------------------|------------------|---------------------|
| - | A | Leap year indicator |
| I | IDA | Day of month (1-31) |
| I | IYR | Year (00-99) |
| O | JULDAY | Julian date (1-366) |
| I | MO | Month (1-12) |

Array Name Definitions

| INPUT/ OUTPUT | ARRAY NAME | DEFINITION |
|------------------|------------|-----------------------------------|
| - | NDAY(12) | Cumulative days of year, by month |

Subroutines Called

None

Common Blocks

None

PRISE-Plume Rise Module

Purpose

PRISE calculates plume rise using the Briggs plume rise algorithms documented in the MPTER User's Manual, taking account of both plume momentum and buoyancy effects.

Inputs

The inputs to PRISE come through the subroutine argument list and include stack characteristics (radius, exit velocity, exit temperature), ambient atmospheric characteristics (air temperature, wind speed, stability class, potential temperature gradient) and down-valley distance to the cross section of interest.

Outputs

The output of PRISE is the plume centerline rise above the physical stack height. This value is passed to the main program through the subroutine argument list.

FORTRAN Library Subroutines

| Name | Function |
|--------------------|---|
| AMIN1(x1,x2,...xn) | Determine the minimum value of a list of real numbers |

Variable Name Definitions

| INPUT/ OUTPUT | VARIABLE NAME | DEFINITION |
|------------------|------------------|---|
| - | DELTT | Plume temperature excess ($^{\circ}\text{K}$) |
| 0 | DLH | Plume centerline rise above stack height (m) |
| - | DLH1 | Intermediate plume rise variable |
| - | DLH2 | Intermediate plume rise variable |
| - | DTC | Crossover temperature difference ($^{\circ}\text{K}$) |
| - | F | Buoyancy flux (ms^{-3}) |
| - | G | Acceleration due to gravity (ms^{-2}) |
| I | GAMMA | Potential temperature gradient ($^{\circ}\text{K/m}$) |
| I | ISTAB | Vertical atmospheric stability index (3-6) |
| - | S | Stability parameter (s^{-2}) |
| I | SRAD | Stack radius (m) |
| I | STMP | Stack gas exit temperature ($^{\circ}\text{K}$) |
| I | SVEL | Stack gas exit velocity (m/s) |
| I | TEMP | Ambient air temperature ($^{\circ}\text{K}$) |
| - | UCUT | Critical wind speed (m/s) |
| I | US | Ambient plume-carrying wind speed (m/s) |
| - | X | Down-valley distance (m) |

| | | |
|---|----|----------------------------------|
| I | XC | Down-valley distance (km) |
| - | XF | Distance to final plume rise (m) |
| - | XX | Intermediate distance variable |

Array Name Definitions

None

Subroutines Called

None

Common Blocks

None

Special Note

The user might wish to specify an "effective stack height" directly, rather than specifying a physical stack height and allowing this subroutine to calculate the additive plume rise. This can be done by inputting the effective stack height in place of the physical stack height, and inputting a zero value for either stack radius or stack gas exit velocity. PRISE returns a zero value for plume rise when a zero value is input for either of these parameters.

DILUTE-Plume Dilution Module

Purpose

DILUTE calculates the dilution factor necessary to account for clean air dilution of the nocturnal pollutant plume during its transport down the valley due to clean air inflow from valley tributaries, slope flows, or entrainment at the top of the down-valley flow layer.

Inputs

The inputs to DILUTE come from the main program through the subroutine argument list. They include the cross-sectional areas and wind speeds at the pollutant source and the receptor cross sections.

Outputs

The output from DILUTE is the dilution factor calculated from the ratio of volume fluxes at the two cross sections. It is passed to the main program through the subroutine argument list.

Variable Name Definitions

| INPUT/ OUTPUT | VARIABLE NAME | DEFINITION |
|------------------|------------------|---|
| I | AC | Area of valley cross section at distance x (m^2) |
| I | AS | Area of valley cross section at pollutant source (m^2) |
| O | DF | Inverse of dilution factor |
| I | UC | Wind speed at cross section at distance x (m/s) |
| I | US | Wind speed at pollutant source cross section (m/s) |

Array Name Definitions

None

Subroutines Called

None

Common Blocks

None

INGRAT-Valley Plume Reflection Module

Purpose

The purpose of Subroutine INGRAT is to calculate Gaussian diffusion coefficients and to accomplish cross wind integrations of plume mass on a valley cross section in order to determine the amount of plume mass within the valley cross section and the amount of plume mass which has escaped out the top of the valley inversion. These mass calculations are necessary to simulate valley plume channeling so that nocturnal plume reflection off the valley floor and sidewalls can be handled in the main program.

Inputs

Inputs to Subroutine INGRAT come into the subroutine through the subroutine argument list. Outputs include the fraction of plume mass within the valley inversion, the fraction which has diffused out the top of the inversion, and the two dispersion coefficients, sigma y and sigma z.

Variable Name Definitions

| INPUT/ OUTPUT | VARIABLE NAME | DEFINITION |
|------------------|------------------|--|
| I | ALPHA1 | Sidewall #1 elevation angle (rad) |
| I | ALPHA2 | Sidewall #2 elevation angle (rad) |
| - | F | Analytical formula for Gaussian distribution |
| I | H | Plume centerline height (m) |
| I | HZERO | Initial inversion height (m) |
| - | I | Height increment counter |
| I | ISTABY | Horizontal atmospheric stability index (1-6) |
| I | ISTABZ | Vertical atmospheric stability index (1-6) |
| - | NP | Number of height increments to inversion top |
| - | P | Number of height increments to inversion top |
| - | PHIY | Area under Gaussian curve from y1 to y2 |
| - | PHIY1 | Area under Gaussian curve from minus infinity to y1 |
| - | PHIY2 | Area under Gaussian curve from minus infinity to y2 |
| - | PI | Trigonometric constant |
| - | R | Height increment counter |
| O | SIGMAY | Standard deviation of plume concentration in y-direction (m) |
| O | SIGMAZ | Standard deviation of plume concentration in z-direction (m) |
| O | SUM1 | Fraction of pollution within valley inversion (0-1) |
| O | SUM2 | Fraction of pollution diffusing out inversion top (0-1) |
| I | W | Width of valley floor (m) |
| I | XC | Down-valley distance from stack to cross section (km) |
| I | Y1 | Y-coordinate of sidewall #1 at height z (m) |
| - | Y2 | Y-coordinate of sidewall #2 at height z (m) |
| I | YZERO | Off-centerline displacement of stack (m) |
| - | Z | Vertical coordinate (m) |
| - | ZINC | Height increment for integration (m) |

Array Name Definitions

| INPUT/ OUTPUT | ARRAY NAME | DEFINITION |
|------------------|------------|--|
| - | SIGGY(18) | McMullen's coefficients for P-G σ_y |
| - | SIGGZ(18) | McMullen's coefficients for P-G σ_z |

Subroutines Called

NORMAL

Common Blocks

None

NORMAL-Normal or Gaussian Curve Integration Module

Purpose

Subroutine NORMAL is used to calculate the area under a Gaussian or Normal distribution curve from minus infinity to X standard deviations. The polynomial approximation technique used in this subroutine comes from Abramowitz and Stegun [33, p. 932] following a formulation attributed to Hastings [34].

Inputs

The sole input is the standard deviation X where X is between 0 and positive infinity. This input comes into the subroutine through the subroutine argument list.

Outputs

The sole output is the area under the Gaussian curve, PHI. This output is carried back to the calling program (Subroutine INGRAT) through the argument list.

Variable Name Definitions

| INPUT OUTPUT | VARIABLE NAME | DEFINITION |
|-----------------|------------------|------------------------|
| 0 | PHI | Area under curve (0-1) |
| - | PI | Trigonometric constant |
| - | SIGH | Intermediate variable |
| - | T | Intermediate variable |
| I | X | Standard deviation |

Array Name Definitions

| INPUT/ OUTPUT | VARIABLE NAME | DEFINITION |
|------------------|------------------|----------------------------|
| - | C(6) | Coefficients of polynomial |

Subroutines Called

None

Common Blocks

None

GAUSS-Gaussian Plume Module

Purpose

This subroutine uses a Gaussian plume algorithm to calculate pollutant concentration at an arbitrary receptor location $P(x,y,z)$. The present version uses Pasquill-Gifford dispersion coefficients, sigma y and sigma z, calculated using McMullen's [28] method.

Inputs

The subroutine requires information on the coordinates of the receptor and source, the plume centerline height, source strength, wind velocity, dispersion coefficients, atmospheric temperature, and atmospheric pressure. The inputs come into the subroutine through the subroutine argument list.

Outputs

The subroutine output is the pollutant concentration at the receptor in micrograms per cubic meter. The output is sent to the calling program (MAIN or PROFIL) through the subroutine argument list.

Variable Name Definitions

| INPUT/ OUTPUT | VARIABLE NAME | DEFINITION |
|------------------|------------------|--|
| O | CHI | Pollutant concentration ($\mu\text{g}/\text{m}^3$) |
| - | CHIOQ | Concentration/source strength ($\mu\text{g s m}^{-3} \text{ kg}^{-1}$) |
| I | DF | Inverse of plume dilution factor |
| - | G1 | Off-centerline term in y direction |
| - | G4 | Off-centerline term in z direction |
| I | H | Plume centerline height (m) |
| I | Q | Source strength (kg/s) |
| I | SIGMAY | Sigma y (m) |
| I | SIGMAZ | Sigma z (m) |
| I | US | Wind speed (m/s) |
| I | Y | Receptor coordinate (m) |
| I | YZERO | Stack offset distance from valley floor centerline (m) |
| I | Z | Receptor coordinate (m) |

Array Name Definitions

None

Subroutines Called

None

Common Blocks

None

SOLAR-Extraterrestrial Solar Radiation Module

Purpose

The purpose of Subroutine SOLAR is to calculate the time of sunrise, length of day, and extraterrestrial solar flux on a horizontal surface at solar noon given the day of year and the latitude and longitude of the site. The outputs of SOLAR are necessary to drive the daytime portion of VALMET.

Inputs

Necessary subroutine inputs include the latitude and longitude of the site and the Julian date of the simulation. These three inputs come into SOLAR through the subroutine argument list.

Outputs

Outputs from Subroutine SOLAR include the local standard time of sunrise, the length of the daytime period, and the extraterrestrial solar flux on a horizontal surface at solar noon.

Variable Name Definitions

| INPUT/ OUTPUT | VARIABLE NAME | DEFINITION |
|------------------|------------------|---|
| 0 | A1 | Solar flux on horizontal surface at solar noon (W/m ²) |
| - | CONV | Conversion factor-degrees to radians (rad/deg) |
| - | COSZ | Cosine of zenith angle |
| - | D | Julian date (1-366) |
| - | D2 | Date interpolation variable for equation of time |
| - | DECLIN | Declination (rad) |
| - | DECMAX | Maximum declination (rad) |
| - | DZERO | Julian date of vernal equinox |
| - | ECCENT | Eccentricity of earth's orbit |
| - | ID | Date interpolation variable for equation of time |
| - | IT | Time unit conversion variable |
| I | JULDAY | Julian date (1-365) |
| I | LAT | Latitude (°N) |
| - | LONCOR | Longitude correction (h) |
| - | LONG | Longitude of earth in its orbit around sun (rad) |
| 0 | NTSR | Time of sunrise (hhmm) |
| - | OMD | Earth's position in orbit around sun on date of interest (rad) |
| - | OMDZRO | Earth's position in orbit around sun at date of vernal equinox (rad) |
| - | OMEGA | Revolution rate of earth (rad/day) |
| - | ONEHR | Conversion factor (rad/h) |
| - | PI | Trigonometric constant |

- RDVCSQ Earth-sun distance factor
- SC Solar constant (W/m^2)
- SR Hour angle of sunrise (rad)
- STDLON Longitude of standard meridian of time zone ($^\circ\text{W}$)
- T1 Time unit conversion variable
- T2 Time unit conversion variable
- 0 TAU Length of daylight period (h)
- TIMCOR Correction due to equation of time (h)
- TMNOON Local standard time of solar noon (h)
- I URLONG Longitude of site ($^\circ\text{W}$)

Array Name Definitions

| INPUT/ OUTPUT | ARRAY NAME | DEFINITION |
|------------------|------------|---|
| - | EQNTIM(25) | Equation of time correction at 15-day intervals (h) |

Subroutines Called

None

Common Blocks

None

EBDGT-Surface Energy Budget Module

Purpose

The purpose of EBDGT is to determine the fraction of extraterrestrial solar heat flux that is converted to sensible heat flux in the valley of interest. It is this sensible heat flux that drives the post-sunrise inversion breakup that leads to air pollution fumigations on the valley floor and sidewalls. The fraction depends on factors associated with the surface energy budget, including surface albedo, soil moisture, surface cover, cloud cover, atmospheric transmissivity, and long-wave radiative transfer within the valley. The present version of the subroutine is not fully developed and does not yet explicitly include these factors. The present skeletal version of the subroutine merely specifies a fraction that the user has previously input using guidance given in earlier sections of this report. Further development of this subroutine is a suggested priority for future work.

Inputs

The fraction of extraterrestrial solar flux converted to sensible heat flux in the valley is the sole input to the present version of EBDGT, and is input to the subroutine through the subroutine argument list.

Outputs

The present version of EBDGT simply outputs to the main program the user-specified input value. The output is transferred to the main program through the subroutine argument list.

Variable Name Definitions

| INPUT/ OUTPUT | VARIABLE NAME | DEFINITIONS |
|------------------|------------------|---|
| I | A0 | Fraction of extraterrestrial solar flux converted to sensible heat flux (0-1) |
| 0 | A2 | Same as A0 (0-1) |

Array Name Definitions

None

Subroutines Called

None

Common Blocks

None

DESCNT-Inversion Descent and CBL Growth Module

Purpose

DESCNT uses Whiteman and McKee's [3] bulk thermodynamic model of temperature inversion breakup to calculate post-sunrise changes in valley inversion and CBL depths. The method considers that the valley temperature inversion represents an energy deficit relative to the warmer air above the inversion. The energy deficit is destroyed after sunrise by solar energy input into the valley as it is converted to sensible heat flux at valley surfaces. The energy is used in two ways: (1) it is used to grow CBLs over valley surfaces and (2) it is used to cause air to flow upslope in the valley sidewall CBLs. Air flowing up the sidewalls in the CBLs causes corresponding descending motions over the valley center, resulting in a descending inversion top after sunrise. The module uses a numerical method for the calculations, and incorporates the effects of warming above the valley in retarding the inversion breakup.

Inputs

The inputs to DESCNT include solar flux parameters, valley characteristics parameters, model time step, initial CBL and inversion top heights, an above valley warming rate parameter, inversion potential temperature gradient, and mean valley air temperature and pressure. These inputs are passed to the subroutine through the subroutine argument list.

Outputs

The main outputs of DESCNT are CBL heights and inversion top heights as a function of time (actually, time step). These outputs are passed back to the main program in arrays located in common block BLK1. The number of time steps required to destroy the valley inversion is also an output of the subroutine, passed to the main program through the subroutine argument list.

Variable Name Definitions

| INPUT/ OUTPUT | VARIABLE NAME | DEFINITIONS |
|------------------|------------------|---|
| I | A0 | Fraction of A1 converted to sensible heat flux (0-1) |
| I | A1 | Solar flux on horizontal surface at solar noon (Wm^{-2}) |
| I | ALPHA1 | Sidewall #1 elevation angle (rad) |
| I | ALPHA2 | Sidewall #2 elevation angle (rad) |
| I | BETA | Rate of temperature change at inversion top ($^{\circ}\text{K/s}$) |
| - | C | Intermediate factor |
| - | CP | Specific heat at constant pressure ($\text{J kg}^{-1} \text{K}^{-1}$) |
| I | DELTAT | Time step (s) |
| - | DHC | Change in CBL height (m) |
| - | DHDT | Change of CBL height with time (m/s) |
| - | DHT | Change in inversion top height (m) |

| | | |
|---|--------|--|
| - | DHTDT | Change in inversion top height with time (m/s) |
| - | FACT1 | Multiplicative factor |
| - | FACT2 | Multiplicative factor |
| - | FDENOM | Intermediate variable-denominator |
| - | FNUM | Intermediate variable-numerator |
| I | GAMMA | Vertical potential temperature gradient ($^{\circ}\text{K/m}$) |
| - | HCBL | Height of CBL top (m) |
| I | HCBLI | Initial CBL height (m) |
| - | HTOP | Height of inversion top (m) |
| I | HZERO | Initial height of inversion top (m) |
| I | K | Fraction of sensible heat flux going into CBL growth (0-1) |
| - | N | Time step counter |
| O | NSTEPS | Number of time steps required to destroy inversion |
| - | PI | Trigonometric constant |
| I | PRESS | Average pressure at inversion center at sunrise (mb) |
| I | RHO | Air density (kg/m^3) |
| - | T | Elapsed time since sunrise (s) |
| I | TAU | Length of daylight period (s) |
| - | THTOT | Potential temperature/ambient temperature |
| - | TI | Time of sunrise (s) |
| I | W | Valley floor width (m) |

Array Name Definitions

| INPUT/ OUTPUT | ARRAY NAME | DEFINITIONS |
|------------------|------------|------------------------------------|
| O | HC(NS) | Array of CBL heights (m) |
| O | HT(NS) | Array of inversion top heights (m) |

Subroutines Called

None

Common Blocks

BLK1

PROFIL-Concentration Profile Module

Purpose

The purpose of Subroutine PROFIL is to calculate the pollutant concentration injected into the top of each of the model grid elements at each time step.

Inputs

Subroutine PROFIL requires a number of inputs, dealing primarily with the valley characteristics, grid element locations and specifications, and Gaussian plume characteristics. Subroutine PROFIL is called for each model time step and does calculations for each of the grid elements. All inputs come into the subroutine through the subroutine argument list.

Outputs

For each model time step, Subroutine PROFIL calculates the pollutant concentration injected into the top of each of the growing grid elements. To maintain accuracy in the calculations, the concentration for each grid element is calculated as the average of four concentration determinations made at the various sides of the quadrilateral Gaussian plume element which sinks into the grid element.

Variable Name Definitions

| INPUT/ OUTPUT | VARIABLE NAME | DEFINITIONS |
|------------------|------------------|--|
| - | ALPHA | Average of ALPHA1 and ALPHA2 |
| I | ALPHA1 | Sidewall #1 elevation angle (rad) |
| I | ALPHA2 | Sidewall #2 elevation angle (rad) |
| I | BOXLEN | Grid element length (m) |
| I | CHIOFF | Offset air pollution concentration due to reflections ($\mu\text{g}/\text{m}^3$) |
| - | CH1Y1 | Concentration at P(X,Y1,Z) ($\mu\text{g}/\text{m}^3$) |
| - | CH1Y2 | Concentration at P(X,Y2,Z) ($\mu\text{g}/\text{m}^3$) |
| - | CH1Z1 | Concentration at P(X,Y,Z1) ($\mu\text{g}/\text{m}^3$) |
| - | CH1Z2 | Concentration at P(X,Y,Z2) ($\mu\text{g}/\text{m}^3$) |
| I | DF | Inverse of plume dilution factor |
| I | H | Plume centerline height (m) |
| I | HCL | CBL height at lower time step (m) |
| I | HCU | CBL height at upper time step (m) |
| I | HTL | Inversion top height at lower time step (m) |
| I | HTU | Inversion top height at upper time step (m) |
| I | HZERO | Inversion depth at sunrise (m) |
| - | I | Grid element index |
| I | NBOX | Number of grid elements on valley floor half-width |
| I | NTOT | Number of model grid elements at a given time step |

| | | |
|---|--------|--|
| I | NTOTI | Initial number of model grid elements |
| I | PRESS | Ambient pressure (mb) |
| I | Q | Source strength (kg/s) |
| I | SIGMAY | Sigma y (m) |
| I | SIGMAZ | Sigma z (m) |
| I | TEMP | Ambient temperature (°K) |
| I | US | Down-valley wind speed at stack cross section (m/s) |
| - | Y | Y-coordinate of receptor (m) |
| - | Y1 | Y-coordinate at left side of sinking mass element (m) |
| - | Y2 | Y-coordinate at right side of sinking mass element (m) |
| I | YZERO | Y-distance of stack from valley floor centerline (m) |
| - | Z | Z-coordinate of receptor (m) |
| - | Z1 | Effective z-coordinate at bottom of sinking mass element (m) |
| - | Z2 | Effective z-coordinate at top of sinking mass element (m) |

Array Name Definitions

| INPUT/ OUTPUT | ARRAY NAME | DEFINITIONS |
|------------------|------------|---|
| 0 | CHIBAR(NB) | Average concentration injected into top of each grid element ($\mu\text{g}/\text{m}^3$) |

Subroutines Called

GAUSS

Common Blocks

BLK2

VELOCITY-Upslope Flow Velocity Module

Purpose

Subroutine VELOCITY uses the mass continuity equation for air to calculate the slope flow velocity profile, under the assumption that the convective boundary layer depth does not vary as a function of distance up the slope. An implicit assumption is that all mass lost from the valley inversion cross section as the inversion top sinks is transported from the valley in the upslope flows which develop in the convective boundary layers over the slopes. The upslope velocities are calculated at the boundaries between grid elements.

Inputs

The inputs to this subroutine come through the subroutine argument list and through the common block labeled BLK1. BLK1 provides the inversion top and CBL heights for every time step. Inputs from the argument list include the time step index number, the time step length, and information about the size and location of the grid elements.

Output

The output of VELOCITY is an array of upslope wind velocities calculated at the NTOTI+1 boundaries between the NTOT grid elements. The subroutine is called from the main program at each model time step, and the calculated velocities are passed back to the main program through the common block labeled BLK3.

Variable Name Definitions

| INPUT/ OUTPUT | VARIABLE NAME | DEFINITIONS |
|------------------|------------------|--|
| I | BOXLEN | Length of grid elements (m) |
| - | CIH | Inversion top displacement during time step (m) |
| I | DELTAT | Time step (s) |
| - | I | Grid element index |
| I | MN | N-1 |
| I | N | Time step index |
| I | NBOX | Number of grid elements on valley floor half-width |
| I | NTOT | Total number of grid elements in simulation at a given time step |
| I | NTOTI | Number of grid elements in simulation at beginning of simulation |

Array Name Definitions

| INPUT/ OUTPUT | ARRAY NAME | DEFINITIONS |
|------------------|------------|-----------------------------------|
| I | HC(NS) | CBL height array (m) |
| I | HT(NS) | Inversion top height array (m) |
| O | V(NB1) | Upslope wind velocity array (m/s) |

Subroutines Called

None

Common Blocks

BLK1
BLK3

BRKUP-Pollutant Mass Budget Module

Purpose

The purpose of Subroutine BRKUP is to calculate pollutant concentrations in each of the grid elements using a pollutant mass balance. The calculations are made for each model time step, taking account of pollution sinking into the top of each grid element, CBL growth, upslope advection of pollution, mixing within each grid element and carryover of pollution in each grid element from the previous time step. A currently unused feature of the pollution mass budget in each grid element is the provision for sources and sinks of pollution within the element. A special feature of BRKUP is the exponential decay of air pollution concentrations in grid elements that are dropped from the simulation as the top of the inversion sinks below the grid element.

Inputs

Inputs to the subroutine coming through the subroutine argument list include time step index, number of grid elements on the valley floor half-width, total number of grid elements at model initiation, the grid element length, and model time step length. Other inputs are available through labeled common blocks BLK1, BLK2, and BLK3. BLK1 provides information on CBL and inversion depths for each time step. BLK2 provides information generated in Subroutine PROFIL on the amount of air pollution mass sinking into the top of each grid element at the given time step. BLK3 provides the upslope wind velocities used to advect pollutant mass up the valley sidewalls at the given time step. These velocities were generated in Subroutine VELOCY.

Outputs

BRKUP calculates air pollution concentrations in the model grid elements for each time step. These calculations constitute the main output of the VALMET model, and are output to the main program through the subroutine argument list. The main program performs further calculations on these concentrations to determine 5-min-average concentrations which are stored in the main program for further processing into maximum 1- and 3-h averages.

Variable Name Definitions

| INPUT/ OUTPUT | VARIABLE NAME | DEFINITIONS |
|------------------|------------------|--|
| - | A | Pollutant mass within the grid element at previous time step (μg) |
| - | B | Pollutant mass coming from adjacent downhill grid element (μg) |
| I | BOXLEN | Grid element length (m) |
| - | C | Pollutant mass sinking through growing top of CBL (μg) |
| - | D | Pollutant mass transported into adjacent uphill grid element (μg) |

- DELTAH Entrainment at top of grid element (m)
- I DELTAT Time step (s)
- I Grid element index
- I MN Index of previous time step
- I N Current time step index
- I NBOX Number of grid elements on valley half-width
- I NTOTI Total number of grid elements at model initiation
- S Exponential decay time constant (s^{-1})

Array Name Definitions

| INPUT/ OUTPUT | ARRAY NAME | DEFINITIONS |
|------------------|------------|---|
| 0 | CCH(2,NB) | Grid element concentration array ($\mu g/m^3$) |
| - | CHIBAR(NB) | Average pollutant concentration injected into top of grid element ($\mu g/m^3$) |
| - | HC(NS) | CBL height array (m) |
| - | HT(NS) | Inversion top height array (m) |
| - | V(NB1) | Upslope velocity array (m/s) |

Subroutines Called

None

Common Blocks

BLK1
BLK2
BLK3

PSTPRC-Post Processor Module

Purpose

This subroutine is a post-processor. It processes the time series of calculated 5-min-average concentrations for each grid element to obtain maximum short-term (1- and 3-hr) average concentrations which can be compared to regulatory standards. The maximum 1- and 3-hr-average concentrations are determined by means of a moving average of the 5-min-average concentration time series, determining maximum values for each of the grid elements. A time index value is saved for each of the maximum values so that the time of occurrence of the maximum can be calculated in the main program. The subroutine is written so that the averaging intervals can be easily changed, if necessary.

Procedure

The moving average is calculated by stepping backwards through the 5-min-average concentration array using a 1- and 3-hr averaging "window", beginning at the last 5-min average calculated for each grid element. As they travel backwards through the 5-min concentration array the 1- and 3-hr averaging intervals will eventually pass the time of sunrise. The nocturnal steady state concentrations are added into the average at that point.

Inputs

The inputs to PSTPRC include the series of 5-min-average concentrations for each of the grid elements, the steady-state nocturnal concentrations in each grid element, the averaging interval (300 s), total number of grid elements and index number of the last 5-min concentration values. The time series of 5-min averaged values is input through common block BLK2. The nocturnal concentrations are input through common block BLK. The other parameters are input through the subroutine argument list.

Outputs

The outputs of Subroutine PSTPRC are passed to the main program through common block BLK6. They include the maximum 1- and 3-hr average concentrations for each grid element, the time index numbers for each of these concentrations, and the number of 5-min time steps in the regulatory averaging intervals (1- and 3-hr).

Variable Name Definitions

| INPUT/ OUTPUT | VARIABLE NAME | DEFINITIONS |
|------------------|------------------|---|
| - | I | Index for grid elements |
| - | K | Index for averaging intervals =1 for 1-hr averages =2 for 3-hr averages |

| | | |
|---|--------|--|
| - | N | Index for 5-min-average time series |
| I | NAS | Number of elements in 5-min series |
| - | NSTART | NAS+1 |
| - | NTIMES | Time index intermediate variable |
| I | NTOTI | Total number of grid elements in model at sunrise |
| - | ONEHR | Number of seconds in 1 hr (s) |
| - | Q1 | Intermediate summation variable |
| - | SUM | Summation variable for concentrations |
| - | THREE | Number of seconds in 3 hr (s) |
| - | TS | Number of 5-min-averages in averaging interval |
| I | TSTP | Averaging interval of basic model concentration array =5 min= 300 s |

Array Name Definitions

| INPUT/ OUTPUT | ARRAY NAME | DEFINITIONS |
|------------------|--------------|---|
| 0 | AVG(NB,2) | Maximum 1- and 3-hr-averages for each grid element ($\mu\text{g}/\text{m}^3$) |
| I | CHI(NB) | Nocturnal concentrations in grid elements ($\mu\text{g}/\text{m}^3$) |
| I | CONC(NA,NB) | Array of 5-min-average concentrations ($\mu\text{g}/\text{m}^3$) |
| 0 | NDXTIM(NB,2) | Array of time index values for maximum 1- and 3-hr averages |
| 0 | NTS(2) | Number of 5-min intervals in 1 and 3 hr |
| - | SUMM(NB,2) | Summing variable for 5-min-average concentration |

Subroutines Called

None

Common Blocks

BLK4
BLK5
BLK6

SECTION 6

SAMPLE MODEL RUNS

In this section we present sample model runs to illustrate model performance and model outputs. In the first model run we present the model results for a run using default input parameters. The first-time model user may compare his results with the results from this run to see that the model is operating properly at his installation. In the second sample run we make calculations for a downwind distance of 30 km rather than the default 10 km, but maintain all other default values for model inputs.

SIMULATION NUMBER 1

The first simulation to be illustrated was obtained using default input values obtained from Table 5. A full listing of the summary output file (VALMET.OUT) generated from this simulation is given below in Figure 21. This output file would be printed by the model user at the completion of the model run and consists of three pages of printer output. Outputs shown in the figure include:

1. a model input table,
2. a listing of numerical simulation parameters,
3. a summary listing of nocturnal model output values,
4. a listing of the output values from the solar model,
5. an output table of maximum 1- and 3-hr-average concentrations in each grid element, and
6. a table of 5-min-average (300 s) concentrations as a function of time for each model grid element.

The user who wishes to get a graphical depiction of model results may manually plot the model results from the output listing. Alternatively, he may develop a plotting program using as input the special file of model output data, VALMET.PLT, that is generated with each model run. Figures 22 and 23 illustrate the types of plots that may be generated using such a plotting program. A listing of the plotting program that generated these figures is given in Appendix B.

THE PROGRAM INITIALIZATION PARAMETERS ARE SET TO THE FOLLOWING VALUES:

SENSIBLE HEAT FLUX (1) A0 = 0.24 (2) K = 0.15
 VALLEY CHARACTER. (3) WIDTH = 500. (4) ALPHA1 = 15. (5) ALPHA2 = 15.
 MODEL CHARACTER. (6) BOX = 3
 INVERSION CHARACTER. (7) IZERO = 500. (8) GAMMA = 0.025 (9) BETA = 0.000
 SITE LOCATION (10) LAT = 40.00 (11) URLONG = 105.00
 DATE (12) MO = 9 (13) DAY = 21 (14) IYR = 82
 VALLEY ATMOSPHERE (15) TEMP = 10.00 (16) PRESS = 750.00
 GAUSSIAN PLUME (17) XC = -10000. (18) YZERO = 0. (19) UC = 4.00
 (20) Q = -0.0010 (21) STAB = F (22) US = 4.00
 STACK CHARACTER. (23) H = -250.00 (24) STMP = 100.00 (25) SRAD = 3.00
 (26) JVEL = 0.00 (27) AS = 0.

NUMERICAL SIMULATION PARAMETERS:
 TIMESTEPS ARE 10.0 SECONDS LONG
 NUMBER OF GRID ELEMENTS = 20
 GRID ELEMENTS ARE 100.0 METERS LONG
 NUMBER OF TIMESTEPS FROM SUNRISE TO INVERSION DESTRUCTION = 1337
 NUMBER OF TIMESTEPS IN SIMULATION (INCLUDES EXPONENTIAL DECAY AFTER INVERSION DESTRUCTION) = 1697
 CONCENTRATION AVERAGING INTERVAL = 300 SECONDS
 NUMBER OF AVERAGING INTERVALS IN THE SIMULATION = 57

PLUME DIFFUSION DURING NOCTURNAL TRAVEL:
 A PLUME CENTERLINE CONCENTRATION OF 1.20 MICROGRAMS PER CUBIC METER OCCURS 250. M ABOVE THE VALLEY FLOOR CENTER.
 AT THE TRAVEL DISTANCE OF 10.0 KM 95.0% OF THE PLUME IS CONTAINED WITHIN THE VALLEY INVERSION CROSS SECTION.
 AT THE TRAVEL DISTANCE OF 10.0 KM 0.1% OF THE PLUME HAS DIFFUSED OUT THE TOP OF THE VALLEY.
 THE REMAINING 4.8% OF THE PLUME MASS IS MIXED UNIFORMLY THROUGHOUT THE INVERSION CROSS
 SECTION TO PRODUCE AN OFFSET CONCENTRATION OF 0.010 MICROGRAMS PER CUBIC METER.
 AREA AT SIMULATION CROSS SECTION IN THOUSANDS OF SQ METERS IS 1234.
 CLEAR AIR DILUTION FACTOR IS 1.000

SOLAR MODEL RESULTS:
 TIME OF SUNRISE = 550 LST
 LENGTH OF DAYLIGHT PERIOD = 12.10 HRS
 EXTRATERRESTRIAL SOLAR FLUX ON HORIZONTAL SURFACE AT SOLAR NOON = 1055.1 WATTS PER SQUARE METER

MODEL OUTPUT: CONCENTRATIONS IN MICROGRAMS/CUBIC METER:

| GRID ELEMENT NUMBER | HEIGHT ABOVE VALLEY FLOOR (M) | MAXIMUM 1-HOUR AVERAGE | TIME OF OCCURRENCE (LST) | TIME OF MAXIMUM 3-HOUR AVERAGE | TIME OF OCCURRENCE (LST) |
|---------------------------|-------------------------------------|------------------------------|--------------------------------|---|--------------------------------|
| 1 | 0.- | 0.64 | 8.21-9.21 | 0.36 | 6.79-9.79 |
| 2 | 0.- | 0.69 | 8.21-9.21 | 0.39 | 6.79-9.79 |
| 3 | 0.- | 0.69 | 8.21-9.21 | 0.39 | 6.79-9.79 |
| 4 | 0.- | 0.66 | 8.21-9.21 | 0.38 | 6.71-9.71 |
| 5 | 27.-54. | 0.60 | 8.13-9.13 | 0.36 | 6.62-9.62 |
| 6 | 54.-80. | 0.54 | 8.13-9.13 | 0.34 | 6.46-9.46 |
| 7 | 80.-107. | 0.47 | 8.04-9.04 | 0.31 | 6.29-9.29 |
| 8 | 107.-134. | 0.41 | 7.96-8.96 | 0.29 | 6.13-9.13 |
| 9 | 134.-161. | 0.36 | 7.88-8.88 | 0.26 | 5.96-8.96 |
| 10 | 161.-187. | 0.31 | 7.71-8.71 | 0.24 | 5.79-8.79 |
| 11 | 187.-214. | 0.26 | 7.54-8.54 | 0.21 | 5.63-8.63 |
| 12 | 214.-241. | 0.23 | 7.38-8.38 | 0.18 | 5.54-8.54 |
| 13 | 241.-268. | 0.19 | 7.21-8.21 | 0.15 | 5.38-8.38 |
| 14 | 268.-295. | 0.16 | 7.04-8.04 | 0.12 | 5.21-8.21 |
| 15 | 295.-321. | 0.14 | 6.88-7.88 | 0.09 | 5.04-8.04 |
| 16 | 321.-348. | 0.12 | 6.63-7.63 | 0.07 | 4.88-7.88 |
| 17 | 348.-375. | 0.10 | 6.46-7.46 | 0.05 | 4.71-7.71 |
| 18 | 375.-402. | 0.07 | 6.29-7.29 | 0.03 | 4.46-7.46 |
| 19 | 402.-428. | 0.04 | 6.04-7.04 | 0.02 | 4.13-7.13 |
| 20 | 428.-455. | 0.02 | 5.63-6.63 | 0.01 | 3.63-6.63 |

Figure 21. Listing of summary output file generated by Sample 1.

300 SECOND AVERAGE POLLUTANT CONCENTRATIONS ($\mu\text{g}/\text{m}^3$) IN MODEL GRID ELEMENTS AS A FUNCTION OF TIME INDICATED TIME IS AT THE MIDPOINT OF 300 SECOND AVERAGING PERIOD PRE-SUNRISE STEADY STATE CONCENTRATIONS ARE GIVEN IN FIRST LINE

[illegible]

Figure 21. continued

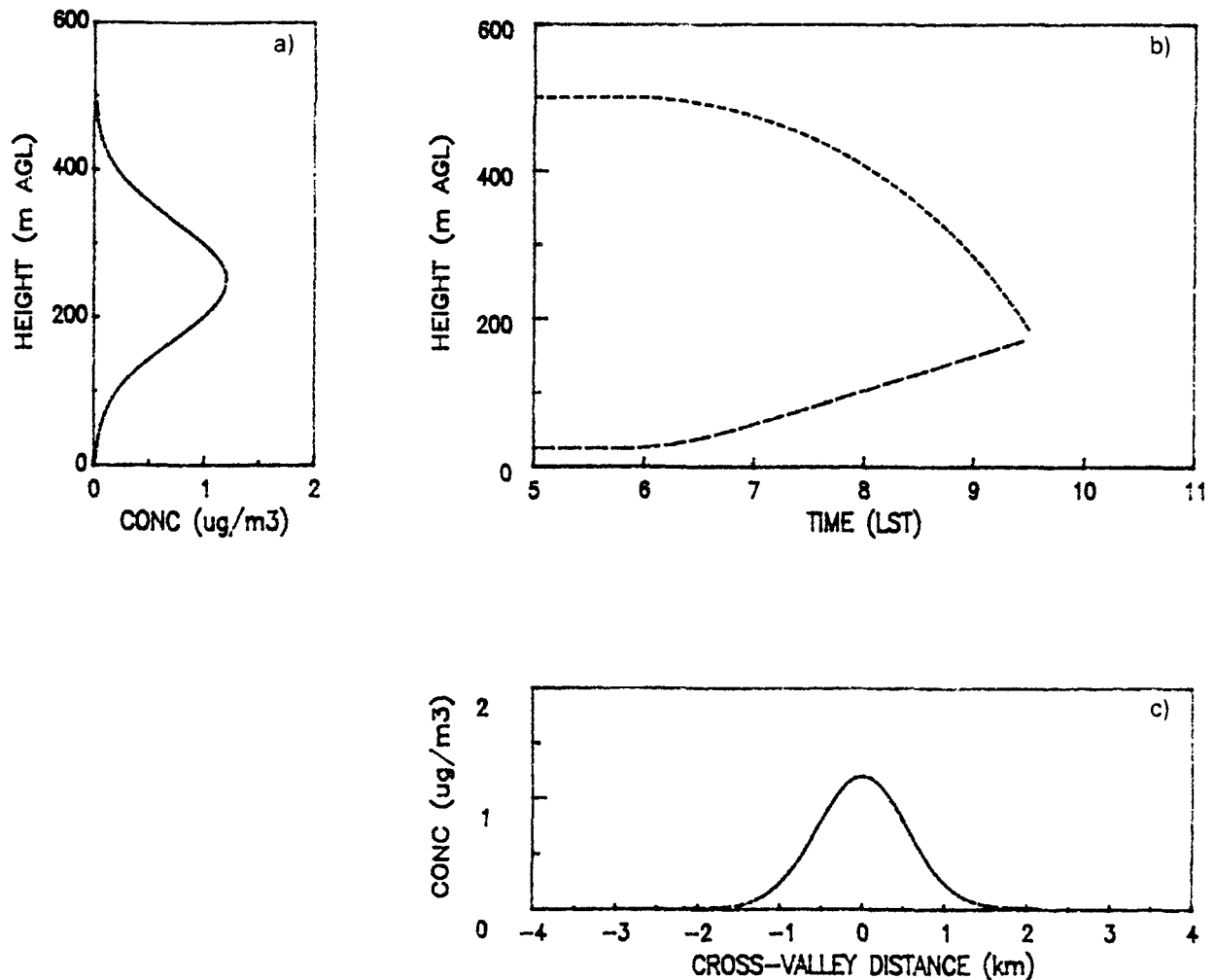


Figure 22. Plots of Sample Simulation 1: (a) nocturnal vertical concentration profile through plume centerline, (b) CBL height (long dashes) and inversion height (short dashes) as a function of time, and (c) nocturnal cross-valley concentration profile through plume centerline.

Figure 22 illustrates some of the characteristics of the simulation. It presents plots of the nocturnal vertical air pollution concentration profile at the valley center (Figure 22a), the nocturnal cross-valley concentration profile through the plume centerline (Figure 22c), and plots of CBL height (long dashes) and inversion top height (short dashes) as a function of time (Figure 22b).

Figure 23 presents plots of the 5-min-average pollution concentrations for selected model grid elements. Twenty grid elements are necessary for the

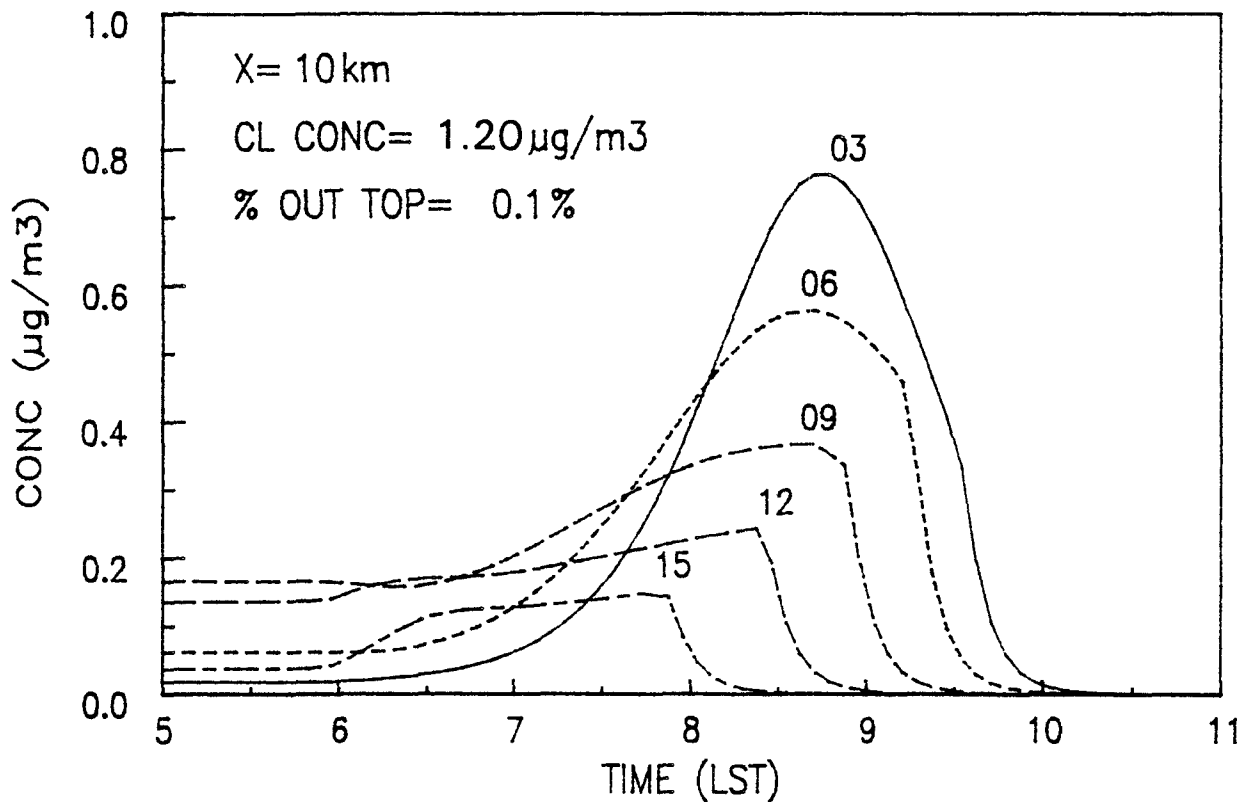


Figure 23. Pollutant concentration versus time for selected grid elements for Sample Simulation 1. The down-valley distance, centerline concentration and fraction of mass diffusing out the top of the valley inversion during the plume's nocturnal transport are indicated on the figure.

default simulation--three on the valley floor and 17 on the valley sidewall. Plots are shown for grid elements 3, 6, 9, 12, and 15. Sunrise on the date of the simulation was at 0550 am LST. Low steady-state concentrations are seen in the figure before sunrise, with time-varying concentrations arising from fumigations and upslope advection after sunrise. Nocturnal concentrations on the valley floor and sidewalls are low since the plume, traveling down the valley centerline at 250 m height, has diffused insufficiently both vertically and horizontally to produce high concentrations on the valley surfaces. The predominant feature of the concentration curves at the 10 km travel distance is the post-sunrise fumigation of the pollutant plume on the valley floor and sidewalls. The highest concentrations occur on the valley floor as the high concentrations at plume centerline subside into the growing CBL. The highest concentration shown occurred in grid element number 3 and is $0.77\text{ }\mu\text{g}/\text{m}^3$. This may be compared to the nocturnal plume centerline concentration of $1.20\text{ }\mu\text{g}/\text{m}^3$. Grid elements on the valley sidewalls are strongly affected by upslope advection. For example, the concentration in grid element 15 increases rapidly just following sunrise as the higher concentrations in downslope grid elements

(e.g., see grid element 12) are advected up the sidewall. Another feature of the simulations, apparent in the figure, is the exponential decay of concentrations in individual grid elements as the temperature inversion top subsides below their elevation. This occurs earliest at the highest grid elements. The exponential decay in concentrations simulates the effect of a sudden increase in mixing depth that occurs when the temperature inversion descends below the grid element. The concentration in grid element 3 begins to drop rapidly to zero at the time of temperature inversion destruction (0933 LST).

SIMULATION NUMBER 2

The results of sample simulation number 2 are shown below in Figures 24 and 25, in the same way that the results of simulation number 1 were illustrated. Input parameters for this simulation, 30-km down-valley from the pollutant source, differ from the previous simulation only in down-valley distance.

At the 30 km cross section, the nocturnal plume had diffused sufficiently during travel that substantial reflections had occurred from the valley surfaces. The vertical and horizontal concentration profiles through the plume centerline (Figure 24) show that the concentrations were more uniform within the valley than at the 10-km section. At the 30-km section, 2.7% of the plume had diffused out the top of the valley inversion, and the plume centerline concentration was $0.39 \mu\text{g}/\text{m}^3$. The CBL growth, inversion top descent, and inversion breakup occur exactly as shown in the first simulation. Concentrations (Figure 25) differ during both the pre-sunrise and post-sunrise periods, however, due to the different nocturnal concentration profiles within the cross section at the longer travel distance. Nocturnal concentrations are higher at the valley surfaces due to the broader distribution of the plume about its centerline. The highest concentration in sidewall grid element 12 occurs during the night. Since the pollutant is more evenly distributed across the cross section, the effects of fumigations are less pronounced than at the 10-km cross section. Again, as at the 10-km cross section, the greatest effect of fumigation is on the valley floor.

The example shown here as simulation number 2 is used merely to illustrate the effect of changing down-valley distance, other parameters remaining constant. Other parameters could have been changed along with the down-valley distance (such as valley width, for example) to simulate the physical characteristics of a real valley more accurately.

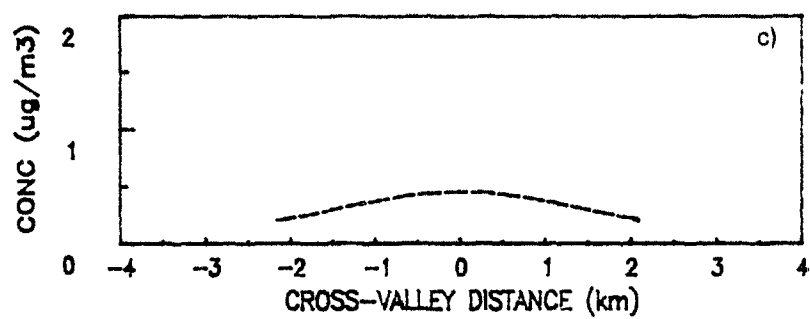
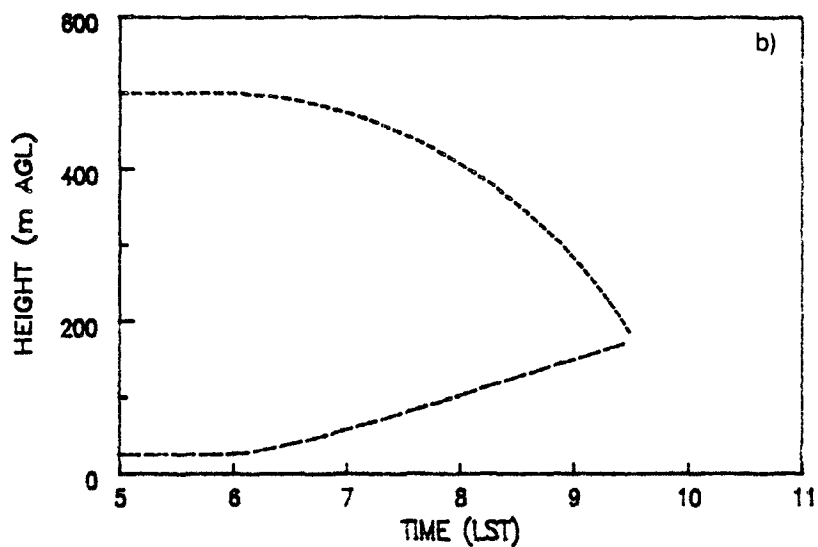
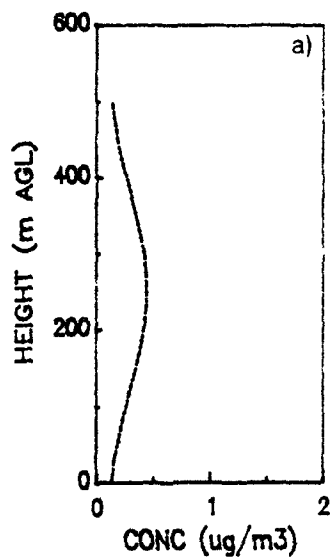


Figure 24. Same as Figure 22, for Sample Simulation 2.

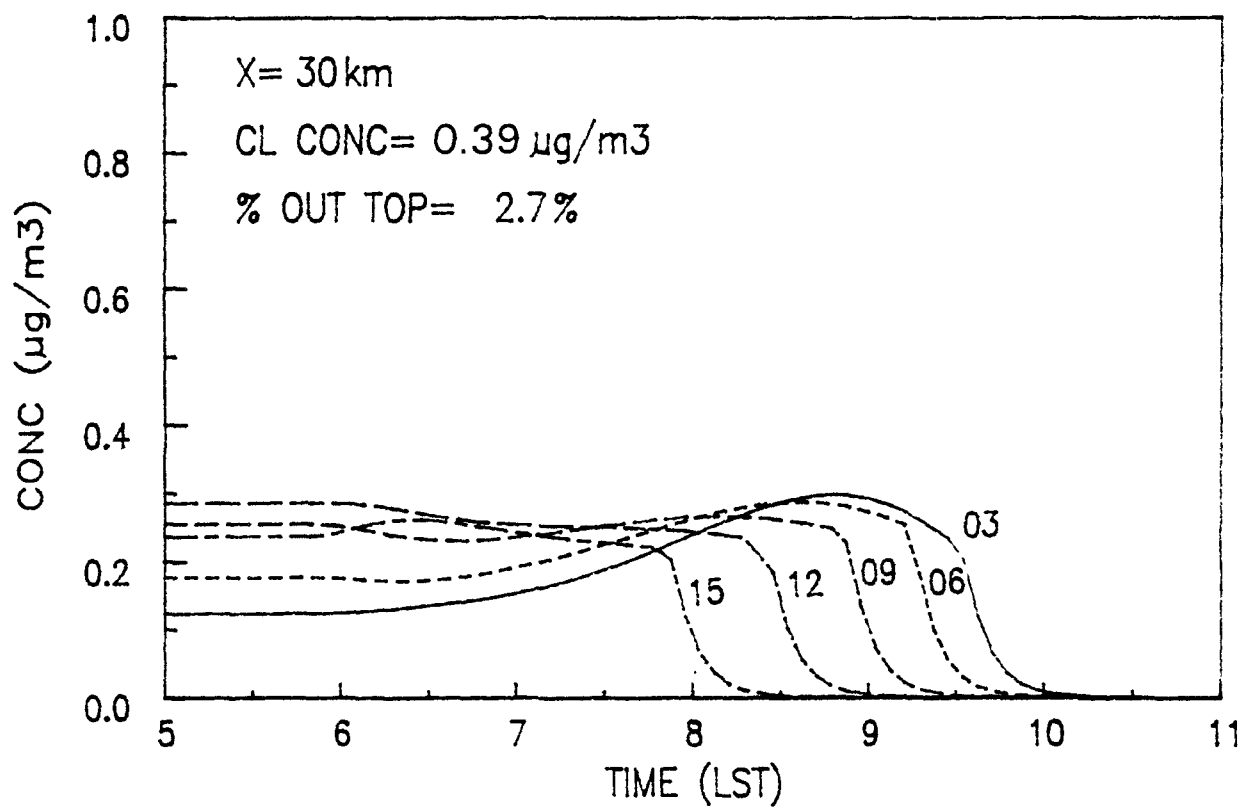


Figure 25. Same as Figure 23, for Sample Simulation 2.

SECTION 7

FURTHER WORK

In this section, we will discuss the need for the further development and testing of the VALMET model. VALMET, as described in this report, is a working model able to simulate many of the observed features of the meteorology of Colorado's deep valleys. The model has been developed in a modular fashion so that the modules can be upgraded as we learn more about valley meteorology. The model, while incorporating what are thought to be the relevant physical processes that lead to air pollution transport and dispersion, has not yet been fully tested against actual air quality data. Nevertheless, some initial results [52,53,54] are now available from meteorological and tracer experiments conducted in the Brush Creek Valley of Colorado in 1982. The tracer experiments, supported by the EPA in cooperation with the U.S. Department of Energy's (DOE) Atmospheric Studies in Complex Terrain (ASCOT) Program, were designed to provide the data necessary to perform an initial evaluation of the VALMET model. The evaluation is not yet complete, but is sufficient to provide us with initial guidance on the further development of VALMET. In addition to the 1982 tracer experiments, a more comprehensive set of tracer and meteorological experiments was conducted in the same valley in September and October of 1984 as part of DOE's ASCOT program. The 1984 ASCOT data are not yet available, but they will constitute an important resource to further test the model. A portion of the tracer experiment, supported by the EPA, was designed specifically to test the VALMET and MELSAR [55] air quality models developed in its GRAMA program. In the following, we will briefly summarize the results from the 1982 experiments, pointing out the implications for future modifications to the VALMET model. Suggested modifications resulting from these experiments and from other sources will then be individually discussed.

GUIDANCE FROM THE 1982 EXPERIMENTS

The 1982 tracer experiments were designed to provide the data required to evaluate the initial version of VALMET [52]. We did not consider it sufficient to simply collect tracer concentration data on a cross-valley arc and compare this with model calculations. Rather, the approach taken was to collect meteorological and tracer data to test the full range of meteorological assumptions and parameterizations used in modules within the model. For example, the model predicts that convective boundary layers will grow over heated surfaces after sunrise, that upslope flows will develop within these boundary layers, that pollutants from the elevated nocturnal plume will fumigate into the convective boundary layers, and that they will be transported out of the valley by the upslope flows. Thus, within the

restraints of the resources available, it was necessary to observe the development of convective boundary layers over the slopes, the upslope wind systems, fumigation of pollutants, and transport of pollutants up the slope. In addition, it was necessary to simulate an elevated release of pollutants and to observe the characteristics of the nocturnal plume.

The EPA tracer experiments were conducted in a valley chosen by DOE using criteria unrelated to the testing of the VALMET model. The Brush Creek Valley was a useful "target of opportunity" for the initial evaluation of VALMET, but, as is usual with such opportunities, there were advantages and disadvantages to the choice of this particular valley.

There were several advantages to choosing the Brush Creek Valley for the initial evaluation of VALMET. First, the valley has a rather simple topography. The narrow, 25-km-long valley has no major changes in valley orientation along its length. It has nearly equal sidewall inclinations. The valley drains a plateau, so that the ridges are at a constant altitude regardless of location along the valley axis. The valley has no major tributaries. Second, the valley axis is oriented from NW to SE so that the sidewalls would be exposed to quite different insolation during the post-sunrise temperature inversion breakup period. The effect of this unequal heating was a major uncertainty in the model formulation. On the basis of meteorological data collected in wider Colorado valleys, and numerical model results, the VALMET model was developed under an assumption of horizontal homogeneity of atmospheric structure on a valley cross section. This assumption could be readily tested in the Brush Creek Valley, where the narrowness of the valley and the NW-SE orientation of the valley would clearly maximize any horizontal gradients in atmospheric structure between the sidewalls. Third, the Brush Creek Valley would be heavily instrumented with meteorological sensors by the ASCOT program. Access to their meteorological data would be a great benefit to the model evaluation effort.

Along with the above advantages, there was a major disadvantage to conducting an initial evaluation of VALMET using data from the Brush Creek Valley. This disadvantage was related to the short segment of the valley that was accessible for tracer instrumentation. VALMET is a two-dimensional model, predicting concentrations on a cross section oriented perpendicular to the valley axis some distance down-valley from a source. Restrictive assumptions are present in VALMET regarding a required homogeneity of the temperature and wind structure in the along-valley direction. The Brush Creek Valley, however, is a short tributary valley that flows into the Roan Valley a few kilometers below the valley cross section where most measurements were made. Consequently, tracer plume carried down the Brush Creek Valley during the night would be carried into Roan Creek. Reversal of the down-valley winds (to up-valley) after sunrise would result in a large part of the tracer plume being carried up the Roan Creek Valley, rather than being carried back up the Brush Creek Valley as assumed in the model. Evaluation of VALMET would be complicated by this violation of a major assumption in the model, which had been designed for longer valleys.

The full evaluation of the VALMET model will be the subject of future work. It is appropriate here, however, to make some initial qualitative statements concerning the evaluation of the model. First, with respect to the nocturnal portion of the model, the nocturnal plume was carried down the valley, as expected. The nocturnal plume, although released above the valley center, was found to be displaced somewhat towards one sidewall as it was transported down the valley. No completely satisfactory physical explanation for this phenomenon has yet been offered, and no mechanism is available in the VALMET model to model it. The valley is not strictly linear, but turns slightly with down-valley distance. Because the plume was displaced towards the "outside" of the turn, it is conceivable that inertial effects are responsible for the displacement of the plume from the valley centerline. Further information on this phenomenon will be available from the 1984 experiments.

The nocturnal plume was carried down the valley in a rather strong "jet" of down-valley winds, with the level of maximum winds at about release height. The nocturnal model, based on the Gaussian formulation, is incapable of treating vertical shears in transport winds but, when winds at release height are used for transport, the model approximates transport and diffusion along the valley direction fairly well.

Assumptions in the daytime portion of the model were verified with actual meteorological and tracer data [53,54]. The post-sunrise period was characterized by the growth of convective boundary layers over the sunlit valley surfaces. The tracer plume fumigated the valley sidewalls as convective boundary layers grew upwards into the remnants of the nocturnal temperature inversion containing the elevated tracer plume. Tracer was carried from the valley by upslope flows, which developed within the growing convective boundary layers. Corresponding subsiding motions over the valley center were noted in the temperature profiles at several of the tethered balloon sites, but the limited vertical resolution of the tracer plume did not allow this feature to be seen in the tracer concentration analyses.

Due to the northwest-southeast orientation of the deep, steep-walled valley, very significant differences occurred in the timing and rates of convective boundary layer growth on the opposing sidewalls following sunrise. As a result of the unequal heating of the different sidewalls, a cross-valley flow developed, carrying the elevated plume towards the warmer sidewall [53]. Due to the cross valley advection, tracer concentrations were higher on this sidewall than predicted by the model. A future modification of the VALMET model will be required to handle this situation properly in narrow valleys where post-sunrise insolation on the opposing sidewalls is quite different. The Brush Creek tracer experiments were the first direct experimental confirmation of the importance of this physical effect on tracer plume dispersion.

The short length of the Brush Creek Valley, as expected, affected the results of the tracer experiments. The primary effect, from initial analyses, seems to be that the tracer concentrations in the valley fell more rapidly than expected after the post-sunrise wind reversal. This is thought

to be due to the nocturnal plume being carried largely up Roan Creek after the wind reversal rather than reversing direction to come back up Brush Creek.

SUGGESTED MODIFICATIONS TO THE VALMET MODEL

The basic modeling approach in VALMET is to explicitly parameterize a number of physical processes acting to disperse pollutants in the valley atmosphere. Based on the parameterizations now included in the model and initial results from the 1982 tracer experiments, a number of suggestions can be made for model improvement. Some of these suggestions are presented below. The simpler modifications are listed first.

Deposition

Deposition of pollutants during transport could be incorporated into the model at two points. Deposition during along-valley transport of the plume could be included in modules INGRAT and NORMAL, while deposition occurring in the slope flows could be rather easily incorporated into module BRKUP using a surface sink term in the pollutant mass budget calculations.

Emission Above or Below Stable Core

The present model assumes implicitly that pollutants are emitted into the stable core, which is then advected down-valley. Concentrations are produced by fumigation of pollutants from this elevated plume as the CBL grows upward into it. Modifications to the model will be required if the emissions fail to enter the stable core. This will happen at the stack location ($x=0$) once the CBL grows to the effective stack height. Pollutants would then be emitted into the CBL. Similarly, once the inversion top sinks below the effective stack height, the pollutants are dispersed above the valley inversion and do not affect the stable core.

Calculations of air pollution concentrations down-valley of the stack should take account of these possibilities by modifying pollutant calculations when changes in the stable core concentration profiles are advected over the cross section of interest. The advection time depends on the distance x down-valley of the stack and the wind speed in the stable core, such that the advection time is

$$t_1 - t_0 = x/u_s$$

where t_0 is the time of sunrise and t_1 is the time when the inversion top descends below the effective stack height or the CBL grows above the effective stack height. When calculations are made far downwind of the stack ($x \gg 0$), or down-valley flows are weak (u_s small) the travel time will be so long that the inversion will be broken before any change in concentration calculations is necessary. It may be necessary, however, to modify the model calculations in short, well-drained valleys. Similarly, the model, when applied to ground level sources, will need modification to account for the post-sunrise emission directly into the CBL.

Energy Budget

The energy budget model needs a great deal of further work. It presently includes a simple bulk parameterization of the fraction of extraterrestrial solar radiation converted to sensible heat flux at the valley surfaces. This fraction, in general, should vary throughout the day and should depend on cloudiness, soil moisture, albedo, ground heat flux, vegetation, atmospheric absorption of the solar beam, etc. It may be worthwhile to adapt existing surface energy budget parameterization schemes for use in the energy budget module. This will, of course, increase the input requirements of the overall model. A different approach is possible. One could look at existing data sets and try to determine the value of this fraction leading to the "worst-case" pollution episodes in different parts of the country. The model could then be used with these fractions to simulate such conditions. Such an empirical approach should also be focused on determining the other free parameter in the model, the fraction k of sensible heat flux causing CBLs to grow. A major effort is required to do a good job on either approach.

Cross Valley Flows

The model should be modified to incorporate cross valley flows in the stable core. Such flows have been postulated by others [45] and were clearly observed in the 1982 Brush Creek tracer experiments. They are expected to be strongest in valleys where differential heating occurs on the sidewalls in the morning. An example would be a north-south valley where the morning sun would shine on one sidewall while the other was still in the shade. The existence of such flows may strongly affect post-sunrise concentrations on the sidewall since the plume, containing high concentrations, is advected towards the most-strongly sunlit sidewall. Several methods seem possible for incorporating the modification into VALMET, but little observational information is available to test the different methods. Guidance may be available from the more-sophisticated primitive equation models [46-49].

Turbulent Erosion of the Valley Inversion by Overlying Flows

Too little is presently known about postulated turbulent erosion [15,50] of the top of a valley temperature inversion to include it in the present version of the model. It is not clear that it should be incorporated anyway, since the model is more conservative without it. Lenschow et al. [50] have developed an approach that could be rather easily incorporated into the present model if a means could be found to relate a local Richardson number at the top of the inversion to the rate of turbulent erosion. No way is yet available to do this. Additionally, recent primitive equations modeling indicates that turbulent erosion is not a major factor affecting temperature inversion breakup under conditions of light to moderate winds aloft when inversions are strong.^(a) Fluid modeling experiments may be useful here in the future.

(a) Personal communication with T. B. McKee, Colorado State University, Fort Collins, Colorado, 1983.

Effect of Tributary Flows on the Enhancement of Diffusion

The present version of the model incorporates a simple means of handling dilution due to valley tributary flows. The model does not treat the effect of these tributary flows on enhancing diffusion within the main valley. At present there seems to be too few observational data to incorporate this effect or the related thermodynamic effects caused by converging air masses of different temperature or stratification. The DOE ASCOT program may look into these effects in their future Colorado field programs.

Diffusion Coefficients

The diffusion coefficients in the model need improvement. At present we are modifying Pasquill-Gifford [43] flat terrain coefficients on the basis of the Huntington canyon data of Start et al. [20] and other data summarized by others [29-31]. We need to look at more data or conduct specific diffusion experiments to determine the most appropriate values of these coefficients. Alternatives to the Gaussian plume equation should also be seriously considered.

Time-Varying Wind Speeds in the Stable Core

The model could be modified to handle time-varying wind speeds in the stable core. There is no doubt that the down-valley wind speeds in the stable core decrease after sunrise during the temperature inversion destruction period, since this has been frequently observed [9]. It is not entirely clear what the effect of this decrease will be on calculations, since the wind speed, in addition to modifying plume concentration calculations, will also affect plume rise calculations.

Temperature Inversion Buildup

The present version of the model simulates the nocturnal steady-state period and the inversion breakup or morning transition period. The model could be extended to simulate the temperature inversion formation and growth period, when down-valley winds first become established within a valley. A large quantity of data on this period was collected in Whiteman's National Science Foundation-supported dissertation program in 1977 and 1978. The data have been processed, but not analyzed. A case study [6] indicated some promising research approaches that could lead to an air pollution model for the inversion buildup period.

Differential Heating

One might expect CBLs to grow at different rates over the different sidewalls of a valley, especially when the energy budgets of the sidewalls are substantially different. This might occur frequently in north-south oriented valleys where the differential insolation on the sidewalls varies strongly with time (see Figure 26 for an example). The present version of VALMET has as its basis a bulk energy budget model of the valley inversion that does not treat the sidewall energy budgets separately. A major

modification to the model would be required to simulate CBLs growing at different rates on the individual sidewalls. This would require an additional free parameter in the model, specifying the fraction of sensible heat used for growing CBLs over one sidewall, as opposed to the other. At present there seem to be no vertical structure data available taken on a single day on two opposite sidewalls. Without this kind of data it is difficult to come up with accurate parameterizations of the differential CBL growth. Brehm [51], based on the Innsbruck, Austria, Slopewind Experiment of 1978, has presented a conceptual model showing differential CBL growth on opposite sidewalls (Figure 27). His conceptual model also shows subsidence in the stable core. Bader and McKee [47], however, in their two-dimensional simulation of valley inversion breakup, noted no significant differential boundary layer growth over opposite valley sidewalls even when substantially different sensible heat flux functions were used on the different valley sidewalls. They explained this as due to the effects of horizontally propagating gravity waves that act to keep isotherms horizontal within the stable core. They also noted the existence of multiple closed cross valley circulations within the stable core early in the post-sunrise period that acted to warm the valley temperature inversion differentially with height, destabilizing the valley atmosphere. This process acts in consort with stable core subsidence to warm the valley atmosphere. As shown by the different conclusions reached in these two studies, it seems appropriate to verify differential CBL growth using specially designed field studies.

Stacks Located on Sidewalls

The model could be modified to handle emissions from stacks located above the valley floor on the sidewalls. In view of the results from the 1982 tracer experiments, this modification should be combined with a new treatment of differential heating and cross valley flows, since the development of cross valley flows due to differential heating may strongly affect concentrations on the sidewalls in the vicinity of the elevated stack.

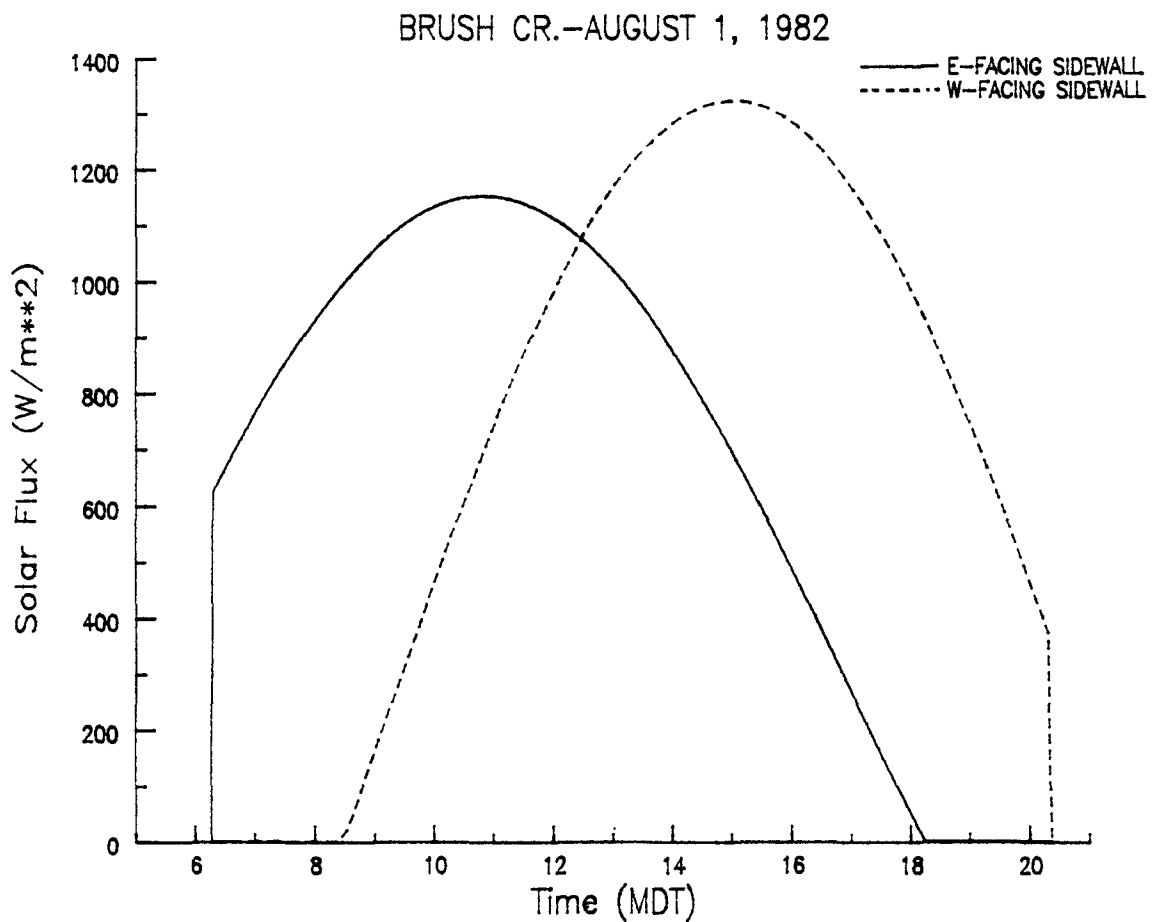


Figure 26. Illustration of differential solar flux on opposing sidewalls for Brush Creek Colorado on August 4, 1982. The Brush Creek Valley drains from NW to SE. The curves represent extra-terrestrial solar flux (i.e., they assume no atmosphere) and were determined using a solar radiation model.

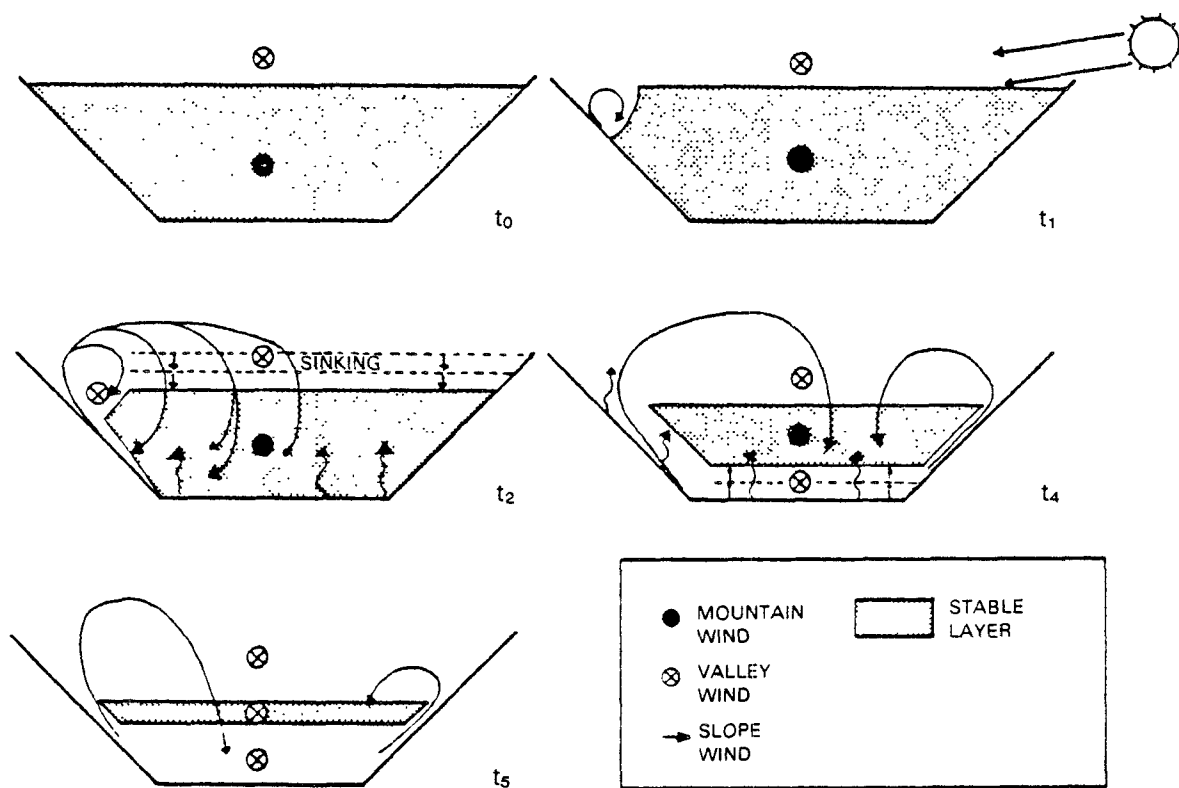


Figure 27. Brehm's [51] conceptual model of temperature inversion destruction in Austria's Inn Valley, showing differential CBL growth over the opposite sidewalls and continued down-valley flow in the elevated stable core.

REFERENCES

1. Hewson, E. W., and G. C. Gill. 1944. "Meteorological Investigations in Columbia River Valley Near Trail, B.C.," Bur. Mines Bull., U.S. Department of Interior, 453, 23-228.
2. Bierly, E. W., and E. W. Hewson. 1962. "Some Restrictive Meteorological Conditions to be Considered in the Design of Stacks." J. Applied Meteor., 1, 383-390.
3. Whiteman, C. D., and T. B. McKee. 1982. "Breakup of Temperature Inversions in Deep Mountain Valleys: Part II. Thermodynamic Model." J. Applied Meteor., 21, 290-302.
4. U.S. Environmental Protection Agency. 1978. Handbook for Preparing Office of Research and Development Reports, Revised. Report EPA-600/9-78-032, December 1978, U.S. Environmental Protection Agency, Cincinnati, Ohio.
5. Peterson, W. B., J. S. Irwin, D. B. Turner and J. A. Catalano. 1982. Handbook for Preparing Users' Guides for Air Quality Models. August 1982, U.S. Environmental Protection Agency, Research Triangle Park, North Carolina.
6. Whiteman, C. D. 1981. "Temperature Inversion Buildup in Valleys of the Rocky Mountains." Preprints, Second Conference on Mountain Meteorology. Nov. 9-12, 1981, Steamboat Springs, Colorado, pp. 276-272.
7. Whiteman, C. D. and T. B. McKee. 1977. "Observations of Vertical Atmospheric Structure in a Deep Mountain Valley." Arch. Meteor. Geophys. Bioklimat., Ser. A, 26, 29-50.
8. Whiteman, C. D., and T. B. McKee. 1979. Temperature Inversion Destruction in Mountain Valleys - Implications for Air Pollution Dispersion. Proceedings of the Tenth International Technical Meeting on Air Pollution Modeling and Its Application, NATO/CCMS Pilot Study, Oct. 23-26, 1979, Rome, Italy, 217-224.
9. Whiteman, C. D. 1980. Breakup of Temperature Inversions in Colorado Mountain Valleys. Ph.D. Dissertation, Colorado State University, pp. 250. Available from University Microfilms, Ann Arbor, Michigan, or as Atmospheric Science Paper No. 328 from Department of Atmospheric Science, Colorado State University, Fort Collins, Colorado.

10. Whiteman, C. D. 1982. "Breakup of Temperature Inversions in Deep Mountain Valleys: Part I. Observations." J. Applied Meteorology, 21, 270-289.
11. Whiteman, C. D., and T. B. McKee. 1978. "Air Pollution Implications of Inversion Descent in Mountain Valleys." Atmospheric Environment, 12, 2151-2158.
12. Whiteman, C. D., and T. B. McKee. 1981. "Valley Wind Systems Under Temperature Inversion Conditions." Proceedings, Symposium on Intermediate Range Atmospheric Transport Processes and Technology Assessment. October 1-3, 1980, Gatlingburg, Tennessee, pp. 351-358.
13. Whiteman, C. D., and R. L. Drake. 1981. The Green River Ambient Model Assessment Program September 1981 Progress Report on Local Scale Modeling Activities. PNL-4058. September 1981. Pacific Northwest Laboratory, Richland, Washington, 249 pp.
14. Whiteman, C. D., and K. J. Allwine. 1982. Green River Ambient Model Assessment Program FY-1982 Progress Report. PNL-4520. October 1982. Pacific Northwest Laboratory, Richland, Washington, 187 pp.
15. Davidson, B., and P. K. Rao. 1958. Preliminary Report on Valley Wind Studies in Vermont, 1957. Final Report AFCRC-RT-58-29, Contract AF 19(604)-1971, College of Engineering, New York University, 54 pp.
16. Beuttner, J. K., and N. Thyer. 1966. Valley Winds in the Mount Rainier Area. Arch. Meteor. Geophys. Bioklimat., Ser. B., 14(2):125-147.
17. Tyson, P. D., and R. A. Preston-Whyte. 1972. "Observations of Regional Topographically-Induced Wind Systems in Natal." J. Applied Meteor., 11, 643-650.
18. Sterten, A. K. 1963. A Further Investigation of the Mountain and Valley Wind System in South-Eastern Norway. Intern Rapport K-254, Forsvarets Forskningsinstitut, Norwegian Defence Research Establishment, Kjeller, Norway, 51 pp.
19. Urfer-Henneberger, C. 1970. Neuere Beobachtungen über die Entwicklung des Schonwetterwindsystems in einem V-förmigen Alpental (Dischmatal bei Davos). Arch. Meteor. Geophys. Bioklimat., Ser. B, 18, 21-42.
20. Start, G. E., C. R. Dickson and L. L. Wendell. 1975. "Diffusion in a Canyon Within Rough Mountainous Terrain." J. Applied Meteor., 14(3):333-346.
21. Briggs, G. A. 1969. Plume Rise. AEC Critical Review Series, TID-25075.
22. Briggs, G. A. 1971. "Some Recent Analyses of Plume Rise Observations." In: Proceedings of the Second International Clean Air Congress, H. M. Englund and W. T. Beery, eds. Academic Press, New York, pp. 1029-1032.

23. Briggs, G. A. 1973. "Diffusion Estimation for Small Emissions." Atmos. Turbulence and Diffusion Laboratory, Contribution File No. (Draft) 79. Oak Ridge, Tennessee, 59 pp.
24. Briggs, G. A. 1975. "Plume Rise Predictions." Lectures on Air Pollution and Environmental Impact Analysis, D. A. Haugen, ed. American Meteorological Society, Boston, Massachusetts, pp. 59-111.
25. Pierce, T. E., and D. B. Turner. 1980. User's Guide for MPTER: A Multiple Point Gaussian Dispersion Algorithm with Optional Terrain Adjustment. EPA-600/8-80-016. April 1980, U.S. Environmental Protection Agency, Research Triangle Park, North Carolina.
26. Turner, D. B. 1969. Workbook on Atmospheric Dispersion Estimates. Public Health Service Publications No. 999-AP-26.
27. Slade, D. H. (ed.). 1968. Meteorology and Atomic Energy 1968. U.S. Atomic Energy Commission, Division of Technical Information, Oak Ridge, Tennessee, 445 pp.
28. McMullen, R. W. 1975. "The Change of Concentration Standard Deviations with Distance." J. Air Poll. Control Assoc., 25(10):1057-1058.
29. Minnott, D. H., D. L. Shearer and Y. Gotaas. 1979. "Measurements of the Vertical Dispersion Rate in Deep-Valley Terrain." Preprint Volume: Fourth Symposium on Turbulence, Diffusion and Air Pollution. January 15-18, 1979, Reno, Nevada. Published by American Meteorological Society, Boston, Massachusetts.
30. Minnott, D. H., D. L. Shearer and R. S. Marker. 1977. Development of Vertical Dispersion Coefficients for Deep-Valley Terrain. Report C00-4026-3 prepared for U.S. Energy Research and Development Administration by TRC Environmental Consultants, Inc.
31. Shearer, D. L., D. H. Minnott and G. R. Hilst. 1977. Development of Vertical Dispersion Coefficients for Rolling Terrain Environments. The Research Corporation of New England (TRC) Report C00-4026-1, January 1977.
32. Gotaas, Y. 1972. A Model of Diffusion in a Valley from a Continuous Point Source." Arch. Meteor. Geophys. Bioklimat., Ser. A, 21, 13-26.
33. Abramowitz, M., and I. A. Stegun. 1965. Handbook of Mathematical Functions with Formulas, Graphs, and Mathematical Tables. Dover Publications, Inc., New York, 1046 pp.
34. Hastings, C., Jr. 1955. Approximations for Digital Computers. Princeton University Press, Princeton, New Jersey.
35. Sellers, W. D. 1965. Physical Climatology. The University of Chicago Press. Chicago, Illinois, 272 pp.

36. Kreith, F., and J. F. Kreider. 1978. Principles of Solar Engineering. Hemisphere Publishing Corp., Washington, D.C., 778 pp.
37. McCullough, E. C. 1968. Total Daily Radiant Energy Available Extraterrestrially as a Harmonic Series in the Day of the Year. Arch. Meteor. Geophys. Bioklimat., Ser. B, 16, 129-243.
38. Waugh, A. E. 1973. Sundials: Their Theory and Construction. New York, Dover Publications, Inc., 228 pp.
39. Thompson, P. D. 1961. Numerical Weather Analysis and Predictions. The MacMillan Co., 170 pp.
40. Haltiner, G. J. 1971. Numerical Weather Prediction. John Wiley and Sons, Inc., New York, 317 pp.
41. Friedman, F. L., and E. B. Koffman. 1981. Problem Solving and Structured Programming in FORTRAN, Second Edition. Addison-Wesley Publishing Co., Reading, Massachusetts.
42. Müller, H., R. Reiter, R. Sladkovic, and K. Munzert. 1982. "Aerologische Untersuchungen des Tagesperiodischen Windsystems im Loisachtal." XVII Internationale Tagung für Alpine Meteorologie. Berchtesgaden, 21-25 September 1982. Annalen der Meteorologie, (Neue Folge), Nr. 19, 186-188.
- 43.. Hanna, S. R., G. A. Briggs and R. P. Hosker, Jr. 1982. Handbook on Atmospheric Diffusion. DOE/TIC-11223. Technical Information Center, U.S. Department of Energy. 102 pp.
44. Sundararajan, A., and S. A. Macklin. 1976. "Comments on the Heat Flux and Friction Velocity in Free Convection Near the Ground." J. Applied Meteor., 33, 715-718.
45. Gleeson, T. A. 1951. "On the Theory of Cross-Valley Winds Arising From Differential Heating of the Slopes." J. Meteor., 8(6), 398-405.
46. Bader, D. C. 1981. Simulation the Daytime Boundary Layer Evolution in Deep Mountain Valleys. M.S. Thesis, Atmospheric Science Department, Colorado State University, Fort Collins, Colorado.
47. Bader, D. and T. B. McKee. 1983. "Dynamical Model Simulation of the Morning Boundary Layer Development in Deep Mountain Valleys." J. Climate and Appl. Meteor., 22(3), 341-351.
48. McNider, R. T. 1981. "Investigation of the Impact of Topographic Circulations on the Transport and Dispersion of Air Pollutants." Ph.D. Thesis. Department of Environmental Science, University of Virginia, Charlottesville, Virginia (available from University Microfilm, Ann Arbor, Michigan).

49. McNider, R. T., and R. A. Pielke. 1981. "Diurnal Boundary-Layer Development Over Sloping Terrain." J. Atmos. Sci., 38(10), 2198-2212.
50. Lenschow, D. H., and B. B. Stankov. 1979. "The Rapid Morning Boundary-Layer Transition." J. Atmos. Sci., 36, 2108-2124.
51. Brehm, M. 1981. Hangwindexperiment Innsbruck 1978 - Gebirgswindsystem und Inversionsauflosung. Ph.D. Dissertation, Ludwig-Maximilians-Universitat, Munich, West Germany.
52. Whiteman, C. D., R. N. Lee, M. M. Orgill and B. D. Zak. 1984. Green River Air Quality Model Development. Meteorological and Tracer Data - July/August 1982 Field Study in Brush Valley, Colorado. PNL-5163. Pacific Northwest Laboratory, Richland, Washington, 139 pp.
53. Whiteman, C. D., A. H. Huber, R. W. Fisher, and B. D. Zak. 1984. "Atmospheric Tracer Experiments in a Deep Narrow Valley." Conference Volumes: (Joint Session) Fourth Joint Conference on Applications of Air Pollution Meteorology and Third Conference on Mountain Meteorology, October 16-19, 1984, Portland, Oregon, pp. J1-J4.
54. Orgill, M. M., R. N. Lee, R. I. Schreck, K. J. Allwine and C. D. Whiteman. 1984. "Early Morning Ventilation of an SF₆ Tracer from a Mountain Valley." Conference Volumes: (Joint Session) Fourth Joint Conference on Applications of Air Pollution Meteorology and Third Conference on Mountain Meteorology, October 16-19, 1984, Portland, Oregon, pp. J36 J-39.
55. Allwine, K. J., and C. D. Whiteman. 1984. Technical Description of MELSAR: A Mesoscale Air Quality Model for Complex Terrain. PNL-5048, Pacific Northwest Laboratory, Richland, Washington.

APPENDIX A
FORTRAN LISTING OF VALMET


```

1      PROGRAM VALMET
2      C*****
3      C**** THIS COMPUTER MODEL PREDICTS AIR POLLUTION CONCENTRATIONS ON A *
4      C**** VALLEY FLOOR AND SIDEWALLS ARISING FROM AN ELEVATED CONTINUOUS *
5      C**** POINT SOURCE OF POLLUTION DURING NOCTURNAL STEADY-STATE *
6      C**** DOWN-VALLEY DRAINAGE FLOWS AND DURING THE POST-SUNRISE *
7      C**** TEMPERATURE INVERSION BREAKUP PERIOD. A MODIFIED GAUSSIAN PLUME *
8      C**** ALGORITHM IS USED DURING THE NOCTURNAL PERIOD. A NUMERICAL SCHEME *
9      C**** IS USED FOR THE CALCULATIONS AFTER SUNRISE WHEN FUMIGATIONS OCCUR. *
10     C**** SIMPLE PARAMETERIZATIONS ARE USED IN THE POST-SUNRISE SIMULATIONS *
11     C**** TO ACCOUNT FOR SOLAR FORCING, SENSIBLE HEAT FLUX, CBL GROWTH, *
12     C**** INVERSION DESCENT, AND UPSLOPE TRANSPORT AND DIFFUSION. A USER'S *
13     C**** MANUAL IS NOW AVAILABLE FOR THIS MODEL. CONTACT C.D. WHITEMAN *
14     C**** OR K.J. ALLWINE, GEOSCIENCES RESEARCH AND ENGINEERING DEPARTMENT, *
15     C**** BATTELLE PACIFIC NORTHWEST LABORATORIES, RICHLAND, WA 99352. *
16     C**** VERSION 1.1 DECEMBER 1, 1984 *
17     C*****
18
19     PARAMETER(NS=6000,NA=100,NB=30,NB1=31)
20
21     COMMON/BLK1/HC(NS),HT(NS)
22     COMMON/BLK2/CHIBAR(NB)
23     COMMON/BLK3/V(NB1)
24     COMMON/BLK4/CONC(NA,NB)
25     COMMON/BLK5/CHI(NB)
26     COMMON/BLK6/AVG(NB,2),NDXTIM(NB,2),NTS(2)
27
28     REAL HITEL(NB),HITEU(NB),TIME(NS)
29     REAL K,LAT
30     REAL SUM(NB),CCH(2,NB)
31     CHARACTER*3 ITIME
32
33     C**** OPEN FILES
34     OPEN(UNIT=2,NAME='VALMET.OUT',TYPE='NEW',FORM='FORMATTED')
35     OPEN(UNIT=3,NAME='VALMET.PLT',TYPE='NEW',FORM='FORMATTED')
36
37     C**** INITIALIZE PARAMETERS
38     HCBLI=25.
39     ITIME='LST'
40     C**** STANDARD TEMPERATURE AND PRESSURE
41     PSTD=1013.
42     TSTD=20.+273.16
43
44     C**** READ INPUT DATA FROM SUBROUTINE
45     CALL INPUT(HCBLI,H,W,ALPHA1,ALPHA2,DELTAT,NBOX,HZERO,
46     +         GAMMA,BETA,LAT,URLONG,MO,IDA,IYR,K,RHO,PRESS,
47     +         Q,ISTAB,XC,UC,STMP,SRAD,SVEL,TEMP,A0,YZERO,US,
48     +         AS,BOXLEN,NTOTI,AC)
49     C     NUMBER OF TIMESTEPS IN THE CONCENTRATION AVERAGING PERIOD
50     NTSA=30
51     C     CONCENTRATION AVERAGING INTERVAL IN SECONDS
52     IAVG=NTSA*INT(DELTAT)
53     C     FACTOR TO CONVERT TO STANDARD CONDITIONS
54     STNDCON=PSTD/PRESS*TEMP/TSTD
55
56
57     C**** CALCULATE JULIAN DATE
58     CALL JULIAN(MO,IDA,IYR,JULDAY)
59
60     C**** PLUME RISE
61     CALL PRISE(TEMP,SVEL,SRAD,STMP,XC,US,ISTAB,GAMMA,DLH)
62     H=H+DLH
63     IF(H.GT.HZERO.OR.H.LE.HCBLI)THEN
64     WRITE(6,115)

```

```

65      115 FORMAT(1H0,'THE PLUME, AFTER PLUMERISE, IS NOT WITHIN',
66      + ' THE STABLE CORE')
67      STOP 4
68      ENDIF
69
70      C**** ADJUST STABILITY CATEGORIES TO ACCOUNT FOR ENHANCED
71      C      DIFFUSION IN COMPLEX TERRAIN, AFTER START ET AL.(1975).
72      ISTABY=ISTAB-2
73      ISTABZ=ISTAB-1
74
75      C**** VOLUMETRIC DILUTION DUE TO SLOPE FLOW CONVERGENCE, TRIBUTARY
76      C**** FLOWS, OR ENTRAINMENT.
77      CALL DILUTE(US,UC,AS,AC,DF)
78
79      C**** DETERMINE DIFFUSION COEFFICIENTS AND CALCULATE THE FRACTION
80      C**** OF POLLUTANT MASS IN THE VALLEY CROSS-SECTION THAT HAS
81      C**** DIFFUSED "BEYOND" THE VALLEY WALLS AND "BELOW" THE GROUND.
82      CALL INGRAT(XC,YZERO,ISTABY,ISTABZ,W,ALPHA1,ALPHA2,
83      +           HZERO,H,SUM1,SUM2,SIGMAY,SIGMAZ)
84
85      C**** DISTRIBUTE THE LOST MASS FRACTION BACK INTO THE CROSS-
86      C**** SECTION. USE WELL-MIXED ASSUMPTION.
87      CHIOFF=(1.-SUM1-SUM2)*Q*1.E09/(US*DF*AC)
88
89      C**** USE GAUSSIAN PLUME EQUATION TO CALCULATE THE MAXIMUM
90      C**** CENTERLINE CONCENTRATION WITHIN THE VALLEY CROSS-SECTION
91      CALL GAUSS(YZERO,H,YZERO,H,Q,US,DF,SIGMAY,SIGMAZ,
92      +          CLCONC)
93      CLCONC=(CLCONC+CHIOFF)*STNDCON
94
95      C**** USING GAUSSIAN PLUME EQUATION, CALCULATE STEADY-STATE
96      C**** NOCTURNAL CONCENTRATIONS AT POINTS ON THE VALLEY FLOOR AND
97      C**** SIDEWALLS CORRESPONDING TO THE GRID ELEMENTS USED FOR THE
98      C**** AFTER-SUNRISE CALCULATIONS.
99      DO 1 I=1,NTOTI
100     IF(I.LE.NBOX) THEN
101     C VALLEY FLOOR
102     Z=0.
103     Y=(BOXLEN/2.)+BOXLEN*(I-1)
104     CALL GAUSS(Y,Z,YZERO,H,Q,US,DF,SIGMAY,SIGMAZ,CCHI)
105     CCHI=CCHI+CHIOFF
106     C SIDEWALLS
107     ELSE
108     Z=(BOXLEN*TAN(ALPHA1))/2.+(I-NBOX-1)*BOXLEN*TAN(ALPHA1)
109     Y=W/2.+Z/TAN(ALPHA1)
110     CALL GAUSS(Y,Z,YZERO,H,Q,US,DF,SIGMAY,SIGMAZ,CCHI)
111     CCHI=CCHI+CHIOFF
112     ENDIF
113     CHI(I)=CCHI
114     1 CONTINUE
115
116     C**** THE FIRST ELEMENT IN THE MODEL OUTPUT CONCENTRATION ARRAY IS
117     C**** DEFINED AS THE STEADY-STATE NOCTURNAL CONCENTRATION.
118     DO 2 I=1,NTOTI
119     CONC(1,I)=CHI(I)
120     CCH(1,I)=CHI(I)
121     2 CONTINUE
122
123     C**** CALCULATE SOLAR PARAMETERS FOR THE SITE AND DATE.
124     CALL SOLAR(LAT,URLONG,JULDAY,NTSR,TAU,A1)
125     TAU=TAU*3600.
126     T4=NTSR
127     IT=NTSR/100
128     T2=IT

```

```

129      T1=T4/100
130      T3=(T1-T2)*100./60.+T2
131
132      C**** ENERGY BUDGET
133      CALL EBDGT(A0,A2)
134      A0=A2
135
136      C**** USE BULK THERMODYNAMIC MODEL TO DETERMINE INVERSION TOP
137      C**** DESCENT AND CBL RISE AS FUNCTION OF TIME. THE NUMBER OF
138      C**** TIME STEPS REQUIRED TO DESTROY THE INVERSION IS ONE OF
139      C**** THE OUTPUTS OF THE THERMODYNAMIC MODEL.
140      CALL DESCNT(A0,A1,ALPHA1,ALPHA2,BETA,DELTAT,GAMMA,
141      +          HCBLI,HZERO,K,W,PRESS,RHO,TAU,NSTEPS)
142      NINDX=NSTEPS+NINT(3600./DELTAT)
143      NAS=NINDX/NTSA+1
144
145      C**** CALCULATE AIR POLLUTION CONCENTRATION AS A FUNCTION OF TIME
146      C**** AFTER SUNRISE.
147      N=1
148      DO 9 IND=1,NAS
149
150      C      INITIALIZE CONCENTRATION SUMMING ARRAY TO ZERO
151      DO 3 I=1,NTOTI
152      SUM(I)=0.
153      3 CONTINUE
154
155      C      LOOP ON NUMBER OF TIMESTEPS PER AVERAGING PERIOD
156      DO 7 ND=1,NTSA
157      N=N+1
158      MN=N-1
159
160      IF(N.GT.NSTEPS)THEN
161      DO 4 I=1,NTOTI
162      V(I)=999.9
163      4 CONTINUE
164      GO TO 5
165      ENDIF
166
167      IFIX2=(HT(MN)-HC(MN))/(BOXLEN*TAN(ALPHA1))
168      NTOT=NBOX+IFIX2
169
170      C**** CALCULATE POLLUTANT MASS COMING INTO GROWING BOX AT ITS TOP.
171      CALL PROFIL(NBOX,NTOTI,NTOT,BOXLEN,HC(MN),ALPHA1,
172      +          ALPHA2,HZERO,H,HC(N),HT(MN),HT(N),YZERO,Q,
173      +          US,DF,SIGMAY,SIGMAZ,CHIOFF)
174
175      C**** CALCULATE VELOCITIES AT BOX SEPTA.
176      CALL VELOCY(N,MN,NTOTI,NBOX,NTOT,BOXLEN,DELTAT)
177
178      C**** CALCULATE POLLUTANT MASS BUDGET FOR EACH BOX.
179      5 CALL BRKUP(N,MN,NTOTI,BOXLEN,DELTAT,CCH)
180
181      DO 6 I=1,NTOTI
182      SUM(I)=CCH(2,I)+SUM(I)
183      CCH(1,I)=CCH(2,I)
184      6 CONTINUE
185
186      7 CONTINUE
187
188      DO 8 I=1,NTOTI
189      CONC(IND,I)=SUM(I)/REAL(NTSA)*STNDCON
190      8 CONTINUE
191

```

```

192     IF(IND.EQ.1) THEN
193         TIME(IND)=T3+REAL(NTSA)*DELTAT/2./3600.
194     ELSE
195         TIME(IND)=TIME(IND-1)+REAL(NTSA)*DELTAT/3600.
196     ENDIF
197
198     9 CONTINUE
199
200     C**** EMPLOY THE POST-PROCESSOR TO CALCULATE MAXIMUM 1- AND 3-HOUR
201     C**** AVERAGE CONCENTRATIONS FOR REGULATORY APPLICATIONS.
202     TSTP=REAL(NTSA)*DELTAT
203     CALL PSTPRC(TSTP,NTOTI,NAS)
204
205     C**** WRITE OUT RESULTS TO UNIT 2.
206     WRITE(2,100) DELTAT,NTOTI,BOXLEN,NSTEPS,NINDX
207     100 FORMAT(1H0,'NUMERICAL SIMULATION PARAMETERS:',/,1X,
208     + 'TIMESTEPS ARE',F5.1,' SECONDS LONG',/,1X,'NUMBER OF GRID',
209     + ' ELEMENTS=',I3,/,1X,'GRID ELEMENTS ARE',F6.1,' METERS',
210     + ' LONG',/,1X,'NUMBER OF TIMESTEPS FROM SUNRISE TO INVERSION',
211     + ' DESTRUCTION=',I6,/,1X,'NUMBER OF TIMESTEPS IN SIMULATION',
212     + ' (INCLUDES EXPONENTIAL DECAY AFTER INVERSION DESTRUCTION)=',
213     + I6)
214     WRITE(2,101) IAVG,NAS
215     101 FORMAT(1H,'CONCENTRATION AVERAGING INTERVAL=',I5,' SECONDS',
216     +/,1H,'NUMBER OF AVERAGING INTERVALS IN THE SIMULATION=',I4)
217     WRITE(2,102) CLCONC,H,XC,(SUM1*100.)
218     102 FORMAT(1H0,'PLUME DIFFUSION DURING NOCTURNAL TRAVEL:',/,1H,
219     + 'A PLUME CENTERLINE CONCENTRATION OF',F7.2,
220     + ' MICROGRAMS PER CUBIC METER OCCURS',F6.0,' M ABOVE ',
221     + 'THE VALLEY FLOOR CENTER.',/,1H,'AT THE TRAVEL DISTANCE OF'
222     + ',F6.1,' KM',F5.1,'% OF THE PLUME IS CONTAINED WITHIN THE'
223     + ' VALLEY INVERSION CROSS SECTION.')
224     WRITE(2,103) XC,(SUM2*100.),((1.-SUM1-SUM2)*100.),CHIOFF
225     103 FORMAT(1H,'AT THE TRAVEL ',
226     + 'DISTANCE OF',F6.1,' KM',F5.1,'% OF THE PLUME HAS DIFFUSED',
227     + ' OUT THE TOP OF THE VALLEY.',/,1H,'THE REMAINING',F5.1,
228     + '% OF THE PLUME MASS IS MIXED UNIFORMLY THROUGHOUT THE ',
229     + 'INVERSION CROSS',/,1H,'SECTION TO PRODUCE AN OFFSET CONC',
230     + 'ENTRATION OF',F7.3,' MICROGRAMS PER CUBIC METER.')
231     WRITE(2,104) (AC/1000.),(1./DF)
232     104 FORMAT(1H,'AREA AT SIMULATION CROSS SECTION IN THOUSANDS OF ',
233     + 'SQ METERS IS',F8.0,/,1H,'CLEAN AIR DILUTION FACTOR IS',F8.3)
234     WRITE(2,105) NTSR,ITIME,(TAU/3600.),A1
235     105 FORMAT(1H0,'SOLAR MODEL RESULTS:',/,1H,'TIME OF SUNRISE=',
236     + I6,1X,A3,/,1X,'LENGTH OF DAYLIGHT PERIOD=',F6.2,' HRS',/,
237     + 1H,'EXTRATERRESTRIAL SOLAR FLUX ON HORIZONTAL SURFACE AT',
238     + ' SOLAR NOON=',F7.1,' WATTS PER SQUARE METER')
239     WRITE(2,106)
240     106 FORMAT(1H0,'MODEL OUTPUT: CONCENTRATIONS IN MICROGRAMS/CUBIC',
241     + ' METER:',/,1H,2X,'GRID',5X,'HEIGHT ABOVE',3X,'MAXIMUM',4X,
242     + 'TIME OF',5X,'MAXIMUM',4X,'TIME OF',/,1H,1X,'ELEMENT',
243     + 3X,'VALLEY FLOOR',4X,'1-HOUR',2X,'OCCURRENCE',5X,'3-HOUR',
244     + 2X,'OCCURRENCE',/,1H,1X,'NUMBER',9X,'(M)',7X,'AVERAGE',
245     + 5X,'(LST)',6X,'AVERAGE',5X,'(LST)')
246
247     DO 10 I=1,NTOTI
248     IF(I.LE.NBOX) THEN
249         HITEL(I)=0.
250         HITEU(I)=0.
251     ELSE
252         HITEL(I)=(I-NBOX-1)*BOXLEN*TAN(ALPHAL)
253         HITEU(I)=(I-NBOX)*BOXLEN*TAN(ALPHAL)
254     ENDIF
255     10 CONTINUE

```

```

256
257 DO 11 I=1,NTOTI
258 TMAXC1=TIME(NDXTIM(I,1))
259 TMAXC2=TIME(NDXTIM(I,2))
260 WRITE(2,107) I,HITEL(I),HITEU(I),AVG(I,1),TMAXC1-1.,
261 + TMAXC1,AVG(I,2),TMAXC2-3.,TMAXC2
262 107 FORMAT(1H ,I4,9X,F4.0,'-',F4.0,2(2X,F8.2,2X,F5.2,'-',F5.2))
263 11 CONTINUE
264
265 WRITE(2,108) IAVG,IAVG
266 108 FORMAT(1H1,/,15X,I5,' SECOND AVERAGE POLLUTANT CONCENTRATIONS',
267 + ' (ug/m3) IN MODEL GRID ELEMENTS AS A FUNCTION OF TIME',/,
268 + 1H ,32X,'INDICATED TIME IS AT THE MIDPOINT OF',I5,' SECOND',
269 + ' AVERAGING PERIOD',/,1H ,32X,'PRE-SUNRISE STEADY STATE',
270 + ' CONCENTRATIONS ARE GIVEN IN FIRST LINE')
271 WRITE(2,109)
272 109 FORMAT(1H0,2X,'TIME',2X,(20('BOX',3X)),/,1H ,2X,'LST',4X,
273 + '01',4X,'02',4X,'03',4X,'04',4X,'05',4X,'06',4X,'07',4X,
274 + '08',4X,'09',4X,'10',4X,'11',4X,'12',4X,'13',4X,'14',4X,
275 + '15',4X,'16',4X,'17',4X,'18',4X,'19',4X,'20')
276
277 IF(NTOTI.LE.20) THEN
278 NY=NTOTI
279 ELSE
280 NY=20
281 ENDIF
282
283 WRITE(2,110) T3,(CHI(I),I=1,NY)
284 110 FORMAT(1H ,1X,'<',F4.2,20F6.2)
285 DO 12 MN=1,NAS
286 WRITE(2,111) TIME(MN),(CONC(MN,I),I=1,NY)
287 111 FORMAT(1H ,21F6.2)
288 12 CONTINUE
289
290 IF(NTOTI.GE.21) THEN
291 WRITE(2,112)
292 112 FORMAT(1H1,/,/,2X,'TIME',2X,(20('BOX',3X)),/,1H ,2X,
293 + 'LST',4X,'21',4X,'22',4X,'23',4X,'24',4X,'25',4X,'26',
294 + 4X,'27',4X,'28',4X,'29',4X,'30',4X,'31',4X,'32',4X,'33',
295 + 4X,'34',4X,'35',4X,'36',4X,'37',4X,'38',4X,'39',4X,'40')
296 WRITE(2,113) T3,(CHI(I),I=21,NTOTI)
297 113 FORMAT(1H ,1X,'<',F4.2,20F6.2)
298 DO 13 MN=1,NAS
299 WRITE(2,114) TIME(MN),(CONC(MN,I),I=21,NTOTI)
300 114 FORMAT(1H ,21F6.2)
301 13 CONTINUE
302 ENDIF
303
304 CLOSE(UNIT=2)
305
306 C**** WRITE OUT RESULTS TO UNIT 3 FOR PLOTTING.
307 I1=1
308 TIME(1)=T3
309 WRITE(3,201) NSTEPS,NTSR,NINDX,NTOTI,NAS,ITIME
310 201 FORMAT(1H ,5I8,A3)
311 WRITE(3,202) CLCONC,DELTAT,SUM1,SUM2,XC,CHIOFF,
312 + SIGMAZ,SIGMAY,ALPHA1,ALPHA2,W,HZERO,H
313 202 FORMAT(1H ,13F10.5)
314 DO 14 I=1,NTOTI
315 WRITE(3,203) I,I1,T2,CHI(I)
316 DO 14 IND=1,NAS
317 WRITE(3,203) I,IND+1,TIME(IND),CONC(IND,I)
318 203 FORMAT(1H ,I2,I5,F12.7,F12.7)
319 14 CONTINUE

```

```
320      DO 15 I=1,NSTEPS
321      WRITE(3,204) HC(I),HT(I)
322 204  FORMAT(1H ,6(2F9.3))
323      15 CONTINUE
324      CLOSE(UNIT=3)
325
326      STOP 'NORMAL EXIT'
327      END
```

```

1 C+*****
2 SUBROUTINE INPUT(HCBLI,H,W,ALPHA1,ALPHA2,DELTAT,
3 1 NBOX,HZERO,GAMMA,BETA,LAT,URLONG,MO,IDA,IYR,K,RHO,
4 2 PRESS,Q,ISTAB,XC,UC,STMP,SRAD,SVEL,TEMP,A0,YZERO,US,
5 3 AS,BOXLEN,NTOTI,AC)
6
7 PARAMETER (NS=6000,NA=100,NB=30,NB1=31)
8
9 C**** THIS SUBROUTINE CONTROLS AN INTERACTIVE TERMINAL THROUGH WHICH
10 C**** INPUT DATA ARE RECEIVED BY THE MODEL.
11
12 REAL K, LAT, VAL(27), VALNEW(27), VALLO(27), VALHI(27)
13 REAL ASTAB(6)
14 INTEGER ID(27)
15 CHARACTER*7 NAM(27)
16 CHARACTER*20 CAT(10)
17
18 C*****INPUT DEFINITIONS*****
19 C ALPHA1 VALLEY SIDEWALL SLOPE(DEG ELEVATION) *
20 C ALPHA2 OTHER VALLEY SIDEWALL SLOPE (DEG) *
21 C AS CROSS SECTIONAL AREA AT SOURCE (THOUSANDS OF M2) *
22 C BETA RATE OF TEMP RISE ABOVE VALLEY (DEG K/SEC) *
23 C DELTAT TIME STEP (SEC) *
24 C GAMMA VERTICAL POTENTIAL TEMPERATURE GRADIENT (DEG K/M) *
25 C H INITIAL HT OF POLLUTION MAX CONCENTRATION(M). *
26 C HZERO INITIAL INVERSION HEIGHT(M) *
27 C IDA DAY OF MONTH (1-31) *
28 C ISTAB ATMOSPHERIC STABILITY CLASS (1-6), E.G., 6=F *
29 C IYR YEAR (00-99) *
30 C K FRACTION OF SENSIBLE HEAT GOING INTO CBL GROWTH (0-1) *
31 C LAT LATITUDE (DEG N) *
32 C MO MONTH OF YEAR (1-12) *
33 C NBOX NUMBER OF BOXES ON HALF OF THE VALLEY FLOOR. *
34 C PRESS PRESSURE (MB) *
35 C Q POLLUTANT SOURCE STRENGTH (KG/SEC) *
36 C RHO DENSITY (KG/M**3) *
37 C SRAD STACK RADIUS (M) *
38 C STMP STACK EFFLUENT TEMPERATURE (DEG C) *
39 C SVEL STACK EXIT VELOCITY (M/S) *
40 C TEMP AMBIENT AIR TEMPERATURE (DEG C) *
41 C UC DOWNVALLEY WIND VELOCITY AT CROSS SECTION (M/SEC) *
42 C URLONG LONGITUDE (DEG W) *
43 C US PLUME-CARRYING DOWNVALLEY WINDSPEED AT STACK (M/S) *
44 C W FULL WIDTH OF VALLEY FLOOR (M) *
45 C YZERO OFF-CENTERLINE DISPLACEMENT OF STACK (M) *
46 C XC DOWNVALLEY DISTANCE FROM SOURCE TO CROSS SECTION (M) *
47 C*****
48
49 C**** SPECIFY NAMES OF CATEGORIES AND PARAMETERS.
50 DATA CAT /'SENSIBLE HEAT FLUX ','VALLEY CHARACTER. ',
51 1 'MODEL CHARACTER. ','INVERSION CHARACTER.',
52 2 'SITE LOCATION ','DATE ',
53 3 'VALLEY ATMOSPHERE ','GAUSSIAN PLUME ',
54 4 'STACK CHARACTER. ','/'
55 DATA NAM /'A0 '=','K '=','WIDTH '=','ALPHA1=',
56 1 'ALPHA2=','NBOX '=','HZERO '=','GAMMA '=','
57 2 'BETA '=','LAT '=','URLONG=','MO '=','IDAY '=','
58 3 'IYR '=','TEMP '=','PRESS '=','XC '=','YZERO '=','
59 4 'UC '=','
60 5 'Q '=','STAB '=','US '=','H '=','STMP '=','
61 6 'SRAD '=','SVEL '=','AS '='/'
62

```

```

63 C**** SET DEFAULT VALUES.
64 DATA VAL / .24, .15, 600., 15., 15., 3., 500., .025, 0.,
65 1 40.00, 105.00, 9., 21., 82., 10., 750., 10000.,
66 2 0., 4., .001, 'F', 4., 250., 100., 3., 0., 0./
67
68 C**** SET LOWER LIMITS OF PARAMETERS
69 DATA VALLO / 5*0., 1., 3*0., -90., -180., 1., 1., 0., -50.,
70 1 600., 100., -50000., 2*0., 'D', 6*0./
71
72 C**** SET UPPER LIMITS OF PARAMETERS
73 DATA VALHI / 1., 1., 50000., 90., 90., 30., 2000., .050, .0005,
74 1 90., 180., 12., 31., 99., 50., 1050., 100000., 50000.,
75 2 15., 1., 'F', 15., 1000., 600., 5., 50., 150000./
76
77 C**** NAME STABILITY CATEGORIES.
78 DATA ASTAB / 'A', 'B', 'C', 'D', 'E', 'F'/
79
80 C**** WRITE OUT TABLE OF INPUT VALUES.
81 LU=6
82 10 WRITE(LU,100)
83 WRITE(LU,110) CAT(1), (J, NAM(J), VAL(J), J=1,2)
84 WRITE(LU,120) CAT(2), (J, NAM(J), VAL(J), J=3,5)
85 J6=6
86 NBOX=INT(VAL(6))
87 WRITE(LU,130) CAT(3), J6, NAM(6), NBOX
88 WRITE(LU,140) CAT(4), (J, NAM(J), VAL(J), J=7,9)
89 WRITE(LU,150) CAT(5), (J, NAM(J), VAL(J), J=10,11)
90 J12=12
91 J13=13
92 J14=14
93 MO=INT(VAL(12))
94 IDA=INT(VAL(13))
95 IYR=INT(VAL(14))
96 WRITE(LU,160) CAT(6), J12, NAM(12), MO, J13, NAM(13), IDA, J14, NAM(14), IYR
97 WRITE(LU,170) CAT(7), (J, NAM(J), VAL(J), J=15,16)
98 WRITE(LU,180) CAT(8), (J, NAM(J), VAL(J), J=17,19)
99 WRITE(LU,190) (J, NAM(J), VAL(J), J=20,22)
100 WRITE(LU,192) CAT(9), (J, NAM(J), VAL(J), J=23,25)
101 WRITE(LU,194) (J, NAM(J), VAL(J), J=26,27)
102 IF(LU.EQ.2) GO TO 70
103
104 100 FORMAT(/,1H,'THE PROGRAM INITIALIZATION PARAMETERS ARE SET TO THE
105 1 FOLLOWING VALUES:',/)
106 110 FORMAT(1H,A20,2(2X,'(',I2,')',1X,A7,F6.2))
107 120 FORMAT(1H,A20,3(2X,'(',I2,')',1X,A7,F6.0))
108 130 FORMAT(1H,A20,2X,'(',I2,')',1X,A7,I6)
109 140 FORMAT(1H,A20,2X,'(',I2,')',1X,A7,F6.0,2(2X,'(',I2,')',1X,A7,
110 1 F6.3))
111 150 FORMAT(1H,A20,2(2X,'(',I2,')',1X,A7,F6.2))
112 160 FORMAT(1H,A20,3(2X,'(',I2,')',1X,A7,I6))
113 170 FORMAT(1H,A20,2(2X,'(',I2,')',1X,A7,F6.2))
114 180 FORMAT(1H,A20,2X,'(',I2,')',1X,A7,F6.0,
115 1 2X,'(',I2,')',1X,A7,F6.0,
116 2 2X,'(',I2,')',1X,A7,F6.2)
117 190 FORMAT(1H,20X,2X,'(',I2,')',1X,A7,F6.4,
118 1 2X,'(',I2,')',1X,A7,A6,
119 2 2X,'(',I2,')',1X,A7,F6.2)
120 192 FORMAT(1H,A20,3(2X,'(',I2,')',1X,A7,F6.2))
121 194 FORMAT(1H,20X,2X,'(',I2,')',1X,A7,F6.2,
122 1 2X,'(',I2,')',1X,A7,F6.0)
123

```



```

124 C**** DETERMINE IF CHANGES TO INPUT VALUES ARE TO BE MADE.
125 WRITE(6,200)
126 200 FORMAT(/,1H,'IF NO CHANGES ARE TO BE MADE IN VALUES IN TABLE',
127 1 ' ---- ENTER 99',/,1H,'IF "STAB" IS TO BE CHANGED ---- ENTER',
128 2 ' 98',/,1H,'IF CHANGES OTHER THAN TO "STAB" ARE TO BE MADE',
129 3 ' --- ENTER TOT. NUMBER OF CHANGES')
130 READ(5,*) NU
131 IF(NU.EQ.99) GO TO 40
132 IF(NU.EQ.98) GO TO 30
133
134 C**** CHANGE VALUES IN TABLE.
135 WRITE(6,210)
136 210 FORMAT(/,1H,'SPECIFY ID. NUMBER OF PARAMETER TO BE CHANGED',
137 1 ' FOLLOWED BY THE NEW VALUE.',/,1H,'ALL CHANGES ARE ENTERED',
138 2 ' SEPARATED BY COMMAS (E.G., 1,200.,2,50.,4,600., ETC).')
139 READ(5,*) (ID(J),VALNEW(J),J=1,NU)
140
141 DO 20 J=1,NU
142
143 IF(VALNEW(J).LT.VALLO(ID(J)).OR.VALNEW(J).GT.VALHI(ID(J)))THEN
144 WRITE(6,240) ID(J)
145 240 FORMAT(/,1H,'PARAMETER NO. ',I2,' OUT OF RANGE, PLEASE',
146 1 ' RESPECIFY')
147 GO TO 20
148 ENDIF
149
150 VAL(ID(J))=VALNEW(J)
151
152 IF(ID(J).EQ.18)THEN
153 IF(ABS(VAL(18)).GT.VAL(3)/2.)THEN
154 WRITE(6,250)
155 250 FORMAT(/,1H,'STACK MUST BE ON VALLEY FLOOR-RESPECIFY YZERO')
156 ENDIF
157 ENDIF
158
159 IF(ID(J).EQ.22)THEN
160 IF(VAL(22).LE.1.)THEN
161 VAL(22)=1.
162 WRITE(6,260)
163 260 FORMAT(/,1H,'DOWNVALLEY WINDSPEED AT STACK HAS BEEN SET',
164 + ' TO 1 M/S')
165 ENDIF
166 ENDIF
167
168 20 CONTINUE
169 GO TO 10
170
171 C**** CHANGE STABILITY DESIGNATION.
172 30 CONTINUE
173 WRITE(6,220)
174 220 FORMAT(/,1H,'SPECIFY NEW STABILITY: D, E OR F ')
175 READ(5,230) VAL(21)
176 230 FORMAT(A4)
177 GO TO 10
178
179 C**** SET VALUES FOR EACH PARAMETER.
180 40 CONTINUE
181 C SENSIBLE HEAT FLUX
182 A0=VAL(1)
183 K=VAL(2)
184 C VALLEY PHYSICAL CHARACTERISTICS
185 W=VAL(3)
186 ALPHA1=(VAL(4)/360.)*6.28
187 ALPHA2=(VAL(5)/360.)*6.28

```

```

188 C MODEL CHARACTERISTICS
189     NBOX=INT(VAL(6))
190     RNO=NBOX
191 C LENGTH OF BOXES.
192     BOXLEN=.5*W/RNO
193 C TIME STEP
194     DELTAT=((W/2.)/RNO)/10.
195 C INVERSION CHARACTERISTICS
196     HZERO=VAL(7)
197     GAMMA=VAL(8)
198     BETA=VAL(9)
199 C CROSS-SECTIONAL AREA OF VALLEY
200     AC= HZERO*W+(.5*(HZERO)**2)*(1./TAN(ALPHA1)+
201       + 1./TAN(ALPHA2))
202 C TOTAL NUMBER OF WHOLE BOXES IN MODEL AT INITIATION.
203     IFIX=(HZERO-HCBLI)/(BOXLEN*TAN(ALPHA1))
204     NTOTI=NBOX+IFIX
205     IF (NTOTI.GT.NB) THEN
206       WRITE(6,280)
207       280 FORMAT(/,1H , 'TOO MANY GRID ELEMENTS-- PLEASE REDUCE NBOX',
208         + ' OR RE-DIMENSION THE MODEL TO ALLOW MORE GRID ELEMENTS')
209       GO TO 10
210     ENDIF
211 C SITE LOCATION
212     LAT=VAL(10)
213     URLONG=VAL(11)
214 C DATE
215     MO=INT(VAL(12))
216     IDA=INT(VAL(13))
217     IYR=INT(VAL(14))
218 C VALLEY ATMOSPHERE
219     TEMP=VAL(15)
220     PRESS=VAL(16)
221     RHO=PRESS/(TEMP+273.16)/2.8704
222 C GAUSSIAN PLUME
223     XC=VAL(17)
224     YZERO=VAL(18)
225     UC=VAL(19)
226     Q=VAL(20)
227     DO 50 J=4,6
228     IF (VAL(21).EQ.ASTAB(J)) GO TO 60
229     50 CONTINUE
230     WRITE(6,290)
231     290 FORMAT(/,1H , 'YOU HAVE SPECIFIED A WRONG STABILITY CLASS-
232       1 F WILL BE USED INSTEAD')
233     J=6
234     60 ISTAB=J
235 C STACK CHARACTERISTICS
236     US=VAL(22)
237     H=VAL(23)
238     STMP=VAL(24)
239     SRAD=VAL(25)
240     SVEL=VAL(26)
241     AS=VAL(27)*1000.
242     LU=2
243     GO TO 10
244
245 C*** CONVERT DOWN-VALLEY DISTANCES TO KILOMETERS
246     70 XC=XC/1000.
247

```

```
248 C**** CONVERT TEMPERATURES TO DEGREES K
249     TEMP=TEMP+273.16
250     STMP=STMP+273.16
251
252     RETURN
253     END
```

```

1 C+++++
2 SUBROUTINE JULIAN(MO,IDA,IYR,JULDAY)
3 C THIS SUBROUTINE CALCULATES THE JULIAN DATE GIVEN THE
4 C MONTH, DAY, AND YEAR.
5
6 DIMENSION NDAY(12)
7
8 DATA NDAY/0,31,59,90,120,151,181,212,243,273,304,334/
9
10 JULDAY=IDA+NDAY(MO)
11 C ADJUST FOR LEAP YEAR
12 A=FLOAT(IYR)/4-IYR/4
13 IF(A.EQ.0. .AND. MO.GE.3) JULDAY=JULDAY+1
14
15 RETURN
16 END

```

```

1  C+++++
2  SUBROUTINE PRISE(TEMP,SVEL,SPAD,STMP,XC,US,ISTAB,GAMMA,DLH)
3  C**** THIS SUBROUTINE IS USED TO CALCULATE PLUME RISE. IT IS
4  C**** DERIVED FROM THE PLUME RISE ALGORITHM IN THE E.P.A. MODEL
5  C**** "MPTR".
6
7  C**** DEFINITIONS *****
8  C THE INPUT VARIABLES ARE: *
9  C GAMMA - POTENTIAL TEMPERATURE GRADIENT (DEG K/M). *
10 C ISTAB - P-G STABILITY (1,2,3,4,5 OR 6). *
11 C SVEL - STACK EXIT VELOCITY (M/S). *
12 C SRAD - INSIDE STACK RADIUS (M). *
13 C STMP - STACK EXIT TEMPERATURE (DEG K). *
14 C TEMP - AMBIENT AIR TEMPERATURE (DEG K). *
15 C US - AMBIENT WIND SPEED (M/S). *
16 C XC - DISTANCE TO DOWNVALLEY CROSS SECTION (KM). *
17 C THE OUTPUT IS: *
18 C DLH - PLUME CENTER-LINE RISE ABOVE STACK HEIGHT (M). *
19 C*****
20
21 DATA G/9.8/
22
23 IF(SVEL.EQ.0..OR.SRAD.EQ.0.) THEN
24 DLH=0.
25 RETURN
26 ENDIF
27
28 X=XC*1000.
29 DELTT=STMP-TEMP
30 F=G*SVEL*SRAD*SRAD*DELTT/STMP
31
32 C **COMPUTE FOR NEUTRAL-UNSTABLE
33 IF(ISTAB.LE.4) THEN
34 IF(F.GE.55.) THEN
35 DTC=0.00575*STMP*SVEL**.6667/((2.*SRAD)**.3333)
36 ELSE
37 DTC=0.0297*STMP*SVEL**.3333/((2.*SRAD)**.6667)
38 ENDIF
39 IF(DELT.T.LE.DTC.OR.STMP.LE.TEMP) THEN
40 C *MOMENTUM DOMINATED
41 DLH=6.*SRAD*SVEL/US
42 ELSE
43 C *BOUYANCY DOMINATED
44 IF(F.GE.55.) THEN
45 XF=3.5*34.*F**(.4)
46 ELSE
47 XF=3.5*14.*F**(.625)
48 ENDIF
49 XX=AMIN1(X,XF)
50 DLH=1.6*(F**.3333)*(XX**.6667)/US
51 ENDIF
52
53 C **COMPUTE FOR STABLE CONDITIONS
54 ELSE
55 S=G*GAMMA/TEMP
56 DTC=0.01958*TEMP*SVEL*SQRT(S)
57 IF(DELT.T.LE.DTC.OR.STMP.LE.TEMP) THEN
58 C *MOMENTUM DOMINATED
59 DLH1=6.*SRAD*SVEL/US
60 DLH2=(1.5*((SVEL**2*SRAD**2*TEMP)/(STMP*US))**.3333)
61 + / (S**.1667)
62 DLH=AMIN1(DLH1,DLH2)

```

```

63      ELSE
64      C      *BOUYANCY DOMINATED
65      UCUT=((2.6/4.)**3)*(F**.25)*(S**.125)
66      IF(US.GT.UCUT) THEN
67      XF=((2.6/1.6)**1.5)*US/SQRT(S)
68      ELSE
69      XF=((4./1.6)**1.5)*(US**1.5)/((S**(9./16.))*(F**.125))
70      ENDIF
71      XX=AMIN1(X,XF)
72      DLH=1.6*(F**.3333)*(XX**.6667)/US
73      ENDIF
74      ENDIF
75
76      RETURN
77      END

```

```

1  C+++++++++++++++++++++++++++++++++++++
2      SUBROUTINE DILUTE(US,UC,AS,AC,DF)
3  C**** CALCULATE DILUTION FACTOR TO ACCOUNT FOR CLEAN AIR DILUTION OF THE
4  C**** NOCTURNAL POLLUTANT PLUME DURING ITS TRANSPORT DOWN THE VALLEY AS
5  C**** A RESULT OF CLEAN AIR FLUX INTO THE VALLEY FROM TRIBUTARIES, SLOPE
6  C**** FLOWS, AND/OR ENTRAINMENT AT THE TOP OF THE DOWN VALLEY FLOW
7  C**** LAYER.
8
9      IF (AS.EQ.0.) THEN
10         DF=1.
11     ELSE
12         DF=(UC*AC)/(US*AS)
13         IF (DF.LT.1.) DF=1.
14     ENDIF
15     RETURN
16     END

```

```

1 C+++++
2 SUBROUTINE INGRAT(XC,YZERO,ISTABY,ISTABZ,W,ALPHA1,
3 1 ALPHA2,HZERO,H,SUM1,SUM2,SIGMAY,SIGMAZ)
4 C**** CALCULATE GAUSSIAN DIFFUSION COEFFICIENTS AND DO A
5 C**** CROSSWIND INTEGRATION WITHIN THE VALLEY CROSS-SECTION
6 C**** TO CALCULATE THE MASS OF POLLUTION FLOWING THROUGH
7 C**** THE SECTION (KG/SEC). SIMILARLY, DO A CROSS-WIND INTEGRATION
8 C**** ABOVE THE VALLEY TO CALCULATE THE MASS OF POLLUTION FLOWING
9 C**** ABOVE THE VALLEY. THE REMAINING MASS (CALCULATED FROM THE
10 C**** EQUATION OF CONTINUITY AS Q MINUS THESE TWO QUANTITIES) CAN
11 C**** BE FOLDED BACK INTO THE CROSS-SECTION. THIS IS DONE IN THE
12 C**** MAIN PROGRAM UNDER AN INSTANTANEOUS PERFECT-MIXING
13 C**** ASSUMPTION.
14
15 REAL SIGGY(18),SIGGZ(18)
16
17 DATA SIGGY/ 5.357, 0.8828, -0.0076, 5.058, 0.9024, -0.0096,
18 1 4.651, 0.9181, -0.0076, 4.230, 0.9222, -0.0087,
19 2 3.922, 0.9222, -0.0064, 3.533, 0.9181, -0.0070/
20 DATA SIGGZ/ 6.035, 2.1097, 0.2770, 4.694, 1.0629, 0.0136,
21 1 4.110, 0.9201, -0.0020, 3.414, 0.7371, -0.0316,
22 2 3.057, 0.6794, -0.0450, 2.621, 0.6564, -0.0540/
23
24 C**** DEFINITIONS *****
25 C H PLUME CENTERLINE HEIGHT (M) *
26 C HZERO INITIAL INVERSION HEIGHT (M) *
27 C ISTABY HORIZONTAL STABILITY INDEX (1-6) *
28 C ISTABZ VERTICAL STABILITY INDEX (1-6) *
29 C SIGMAY STD DEVIATION OF PLUME CONC IN Y DIRECTION (M) *
30 C SIGMAZ STD DEVIATION OF PLUME CONC IN Z DIRECTION (M) *
31 C ALPHA1 VALLEY SIDEWALL SLOPE (RAD) *
32 C ALPHA2 OTHER VALLEY SIDEWALL SLOPE (RAD) *
33 C W FULL WIDTH OF VALLEY FLOOR (M) *
34 C XC DOWNVALLEY DISTANCE OF CROSS SECTION (KM) *
35 C YZERO OFF-CENTERLINE DISPLACEMENT OF STACK (M) *
36 C Y,Z COORDINATE AXES (M) *
37 C ZINC VERTICAL HEIGHT INCREMENT FOR INTEGRATION (M) *
38 C*****
39
40 C**** CALCULATE THE SIGMAS USING MCMULLEN'S METHOD (1975)*****
41 SIGMAY=EXP(SIGGY(3*ISTABY-2)+SIGGY(3*ISTABY-1)*LOG(XC)+
42 1 SIGGY(3*ISTABY)*(LOG(XC))**2)
43 SIGMAZ=EXP(SIGGZ(3*ISTABZ-2)+SIGGZ(3*ISTABZ-1)*LOG(XC)+
44 1 SIGGZ(3*ISTABZ)*(LOG(XC))**2)
45
46 C**** INITIAL VALUES
47 PI=3.14159
48 P=100.
49 NP=P
50 ZINC=HZERO/P
51 SUM1=0.
52
53 C**** RATE OF MASS FLOW ACROSS THE VALLEY SECTION
54 DO 1 I=1,NP
55 R=1
56 Z=(R-1.)*ZINC
57 F=(1./(SQRT(2.*PI)*SIGMAZ))*EXP(-.5*((Z-H)/SIGMAZ)**2)
58 Y1=(W/2.+Z/TAN(ALPHA1)-YZERO)/SIGMAY
59 Y2=(-W/2.-Z/TAN(ALPHA2)-YZERO)/SIGMAY

```



```

60
61      IF (Y1.LT.0.) THEN
62      Y1=-Y1
63      CALL NORMAL(Y1,PHIY1)
64      PHIY1=1.-PHIY1
65      ELSE
66      CALL NORMAL(Y1,PHIY1)
67      ENDIF
68
69      IF (Y2.LT.0.) THEN
70      Y2=-Y2
71      CALL NORMAL(Y2,PHIY2)
72      PHIY2=1.-PHIY2
73      ELSE
74      CALL NORMAL(Y2,PHIY2)
75      ENDIF
76
77      PHIY=PHIY1-PHIY2
78      SUM1=SUM1+PHIY*F*Z INC
79      1 CONTINUE
80
81      C**** RATE OF MASS FLOW ABOVE THE CROSS SECTION.
82      SUM2=0.
83      DO 2 I=1,NP
84      R=I
85      Z=(R-1.)*Z INC*2.+HZERO
86      ARG=-.5*((Z-H)/SIGMAZ)**2
87      IF (ARG.LT.-80.) THEN
88      F=0.
89      ELSE
90      F=(1./(SQRT(2.*PI)*SIGMAZ))*EXP(ARG)
91      ENDIF
92      Y1=5.
93      Y2=-5.
94
95      IF (Y1.LT.0.) THEN
96      Y1=-Y1
97      CALL NORMAL(Y1,PHIY1)
98      PHIY1=1.-PHIY1
99      ELSE
100     CALL NORMAL(Y1,PHIY1)
101     ENDIF
102
103     IF (Y2.LT.0.) THEN
104     Y2=-Y2
105     CALL NORMAL(Y2,PHIY2)
106     PHIY2=1.-PHIY2
107     ELSE
108     CALL NORMAL(Y2,PHIY2)
109     ENDIF
110
111     PHIY=PHIY1-PHIY2
112     SUM2=SUM2+PHIY*F*Z INC*2.
113     2 CONTINUE
114
115     RETURN
116     END

```

```

1 C+++++
2 SUBROUTINE NORMAL(X,PHI)
3 C**** CALCULATE THE INTEGRAL OF THE AREA UNDER THE GAUSSIAN CURVE
4 C**** FROM MINUS INFINITY TO X. THE POLYNOMIAL APPROXIMATION
5 C**** USED HERE COMES FROM ABRAMOWITZ AND STEGUN, 1965,
6 C**** HANDBOOK OF MATHEMATICAL FUNCTIONS, DOVER PRESS, NINTH
7 C**** PRINTING, P. 932. THEY ATTRIBUTE THE FORMULA TO HASTINGS (1975).
8
9 REAL C(6)
10
11 DATA C/0.2316419, 0.31938153, -0.356563782,
12 1 1.781477937, -1.821255978, 1.330274429/
13
14 PI=3.14159
15 T=1./(1.+C(1)*X)
16 SIGH=(1./SQRT(2.*PI))*EXP(-X**2/2.)
17 PHI=1.-SIGH*(C(2)*T+C(3)*T**2+C(4)*T**3+C(5)*T**4+C(6)*T**5)
18
19 RETURN
20 END

```

```

1 C+++++
2 SUBROUTINE GAUSS(Y,Z,YZERO,H,Q,US,DF,SIGMAY,SIGMAZ,CHI)
3 C**** THIS PROGRAM USES THE WELL-KNOWN GAUSSIAN PLUME EQUATIONS
4 C**** (TURNER, 1969) TO CALCULATE VALLEY POLLUTION CONCENTRATION
5 C**** DOWNVALLEY OF A POLLUTANT SOURCE.
6
7 C**** DEFINITIONS *****
8 C CHI POLLUTANT CONCENTRATION (MICROGRAMS/M**3) *
9 C CHIOQ CHI OVER Q (S/M**3) *
10 C CHIOQN NORMALIZED AND STP CORRECTED CONCENTRATION (S/M**3) *
11 C DF DILUTION FACTOR *
12 C H PLUME CENTERLINE HEIGHT (M) *
13 C Q SOURCE STRENGTH (KG/S) *
14 C SIGMAY SIGMA Y (M) *
15 C SIGMAZ SIGMA Z (M) *
16 C US WINDSPEED AT SOURCE (M/SEC) *
17 C YZERO OFF-CENTERLINE DISPLACEMENT OF STACK (M) *
18 C XC,Y,Z COORDINATES OF RECEPTOR (KM,M,M) *
19 C*****
20
21 C**** CALCULATE INDIVIDUAL TERMS IN THE GAUSSIAN PLUME EQUATION ***
22 C G1 : OFF CENTERLINE IN Y DIRECTION *
23 C G4 : OFF CENTERLINE IN Z DIRECTION *
24 C*****
25
26 C**** GAUSSIAN PLUME EQUATION
27 G1=EXP(-0.5*((Y-YZERO)/SIGMAY)**2)
28 G4=EXP(-0.5*((Z-H)/SIGMAZ)**2)
29 CHIOQ=1./(2.*3.14*SIGMAY*SIGMAZ*US*DF)*(G1)*(G4)
30
31 C**** CONCENTRATION IN MICROGRAMS PER CUBIC METER
32 CHI=CHIOQ*Q*1.E09
33
34 RETURN
35 END

```

```

1 C+*****
2 SUBROUTINE SOLAR(LAT,URLONG,JULDAY,NTSR,TAU,A1)
3 C**** CALCULATE TIME OF SUNRISE, LENGTH OF DAY, AND SOLAR FLUX ON
4 C**** HORIZONTAL SURFACE AT SOLAR NOON FOR ANY SITE GIVEN LATITUDE,
5 C**** LONGITUDE, AND JULIAN DATE. THIS SUBROUTINE USES MCCULLOUGH'S 1968
6 C**** APPROXIMATIONS AS GIVEN IN ARCH. METEOR. GEOPHYS. BIOKLIMAT.,
7 C**** SER. B, 16, 129-143. REFER TO WHITEMAN, 1980, ATMOSPHERIC
8 C**** SCIENCE PAPER NO. 328, COLORADO STATE UNIVERSITY, FORT
9 C**** COLLINS, COLORADO, 250 PP.
10
11 REAL EQNTIM(25)
12 REAL LAT, LONG, LONCOR
13
14 C**** EQUATION OF TIME IN HRS FAST OR SLOW. .HHHH VALUES GIVEN FOR
15 C**** EVERY 15 JULIAN DAYS, FOR EXAMPLE, 1,16,31,46.....360.
16 DATA EQNTIM/-0.0533,-0.1589,-0.2233,-0.2378,-0.2064,-0.1442,
17 1 -0.0689,+0.0003,+0.0475,+0.0622,+0.0425,-0.0028,
18 2 -0.0558,-0.0961,-0.1058,-0.0789,-0.0186,+0.0639,
19 3 +0.1517,+0.2258,+0.2683,+0.2647,+0.2094,+0.1094,
20 4 -0.0131/
21
22 C**** CONSTANTS
23 C JULIAN DATE OF VERNAL EQUINOX.
24 DZERO=80.
25 PI=3.14159
26 C CONVERSION-DEGREES TO RADIANS.
27 CONV=PI/180.
28 C ECCENTRICITY OF EARTHS ORBIT
29 ECCENT=.0167
30 C MAX DECLINATION.
31 DECMA=(23.+27./60.)*PI/180.
32 C REVOLUTION RATE OF EARTH.
33 OMEGA=2.*PI/365.
34 C SOLAR CONSTANT IN WATTS/M**2
35 SC=1367.
36 C 15 DEGREES OF LONGITUDE IS EQUIVALENT TO 1 HOUR.
37 ONEHR=15.*PI/180.
38 C LONGITUDE OF STANDARD MERIDIAN FOR YOUR TIME ZONE.
39 STDLON=105.
40 LAT=LAT*CONV
41
42 C JULIAN DATE
43 D=JULDAY
44
45 C**** MAKE COMPUTATIONS.
46 OMD=OMEGA*D
47 OMDZRO=OMEGA*DZERO
48 C RATIO OF RADIUS VECTORS SQUARED. ACCOUNTS FOR VARYING DISTANCE
49 C BETWEEN EARTH AND SUN.
50 RDVCSQ=1./(1.-ECCENT*COS(OMD))**2
51 LONG=OMEGA*(D-DZERO)+2.*ECCENT*(SIN(OMD)-SIN(OMDZRO))
52 DECLIN=A SIN(SIN(DECMA)*SIN(LONG))
53 SR=-ABS(ACOS(-TAN(LAT)*TAN(DECLIN)))
54 C LENGTH OF DAYLIGHT PERIOD
55 TAU=-SR*2./ONEHR
56
57 C**** CALCULATE TIME OF SOLAR NOON AT SITE AS A PRELIMINARY TO CALCULATING
58 C**** THE LOCAL TIME FOR ANY GIVEN HOUR ANGLE.
59 LONCOR=(STDLON-URLONG)*1./15.
60 IF(D.GT.361.) GO TO 1
61 ID=((D-1.)/15.)+1.
62 D2=(ID-1)*15+1
63 TIMCOR=(EQNTIM(ID+1)-EQNTIM(ID))*(D-D2)/15.+EQNTIM(ID)

```

```

64      1 IF(D.EQ.362.) TIMCOR=-0.0211
65      IF(D.EQ.363.) TIMCOR=-0.0292
66      IF(D.EQ.364.) TIMCOR=-0.0372
67      IF(D.EQ.365.) TIMCOR=-0.0453
68      TMNOON=12.00-LONCOR-TIMCOR
69
70      C**** CALCULATE SOLAR FLUX AT SOLAR NOON
71      COSZ=SIN(LAT)*SIN(DECLIN)+COS(LAT)*COS(DECLIN)*1
72      C SOLAR FLUX AT SOLAR NOON
73      A1=SC*RDVCSQ*COSZ
74      IF(A1.LT.0.) A1=0.0
75      T1=(12.+(SR/ONEHR)+(TMNOON-12.00))
76      IT=T1
77      T2=IT
78      C TIME OF SUNRISE.
79      NTSR=(T1-T2)*60.+(T2*100.)
80
81      RETURN
82      END

```

```

1 C+++++++++++++++++++++++++++++++++++++
2   SUBROUTINE EBDGT(A0,A2)
3 C**** DETERMINE FRACTION OF EXTRATERRESTRIAL SOLAR FLUX THAT PRODUCES
4 C**** SURFACE SENSIBLE HEAT FLUX.
5 C**** AT PRESENT, THIS SUBROUTINE IS NOT BEING USED, SINCE THE USER NOW
6 C**** SIMPLY INPUTS FRACTION A0. IN FUTURE, THIS SUBROUTINE WOULD BE
7 C**** DEVELOPED TO EXPLICITLY INCORPORATE FEATURES OF THE SURFACE ENERGY
8 C**** BUDGET SUCH AS ALBEDO, SOIL MOISTURE AND CLOUD COVER.
9
10      A2=A0
11
12      RETURN
13      END

```

```

1 C+++++
2 SUBROUTINE DESCNT(A0,A1,ALPHA1,ALPHA2,BETA,DELTAT,GAMMA,
3 1 HCBLI,HZERO,K,W,PRESS,RHO,TAU,NSTEPS)
4 C**** THIS PROGRAM CALCULATES THE HEIGHTS OF THE INVERSION TOP
5 C**** AND CBL TOP AS A FUNCTION OF TIME AFTER SUNRISE AS VALLEY
6 C**** INVERSIONS ARE DESTROYED, USING WHITEMAN'S (1980)
7 C**** NUMERICAL METHOD AS GIVEN IN HIS EQUATIONS 41-50.
8
9 PARAMETER (NS=6000)
10
11 COMMON/BLK1/HC(NS),HT(NS)
12
13 REAL K
14
15 C**** DEFINITIONS *****
16 C A0 FRACTION (0-1) OF A1 CONVERTED TO SENSIBLE HEAT FLUX *
17 C A1 SOLAR FLUX ON HORIZ SFC AT SOLAR NOON (W/M2) *
18 C ALPHA1 SIDEWALL NO. 1 INCLINATION ANGLE (RAD) *
19 C ALPHA2 SIDEWALL NO. 2 INCLINATION ANGLE (RAD) *
20 C BETA RATE OF TEMP CHANGE AT INVERSION TOP (K/SEC) *
21 C CP SPECIFIC HEAT AT CONSTANT PRESSURE (J/KG/K) *
22 C DELTAT TIME STEP (SEC) *
23 C GAMMA VERT POT TEMPERATURE GRADIENT IN INVERSION (K/M) *
24 C HC CBL HEIGHT (M) *
25 C HCBL HEIGHT OF CBL TOP (M) *
26 C HCBLI INITIAL CBL HEIGHT (M) *
27 C HT INVERSION TOP HEIGHT (M) *
28 C HTOP HEIGHT OF INVERSION TOP (M) *
29 C HZERO INITIAL HEIGHT OF INVERSION TOP (M) *
30 C K FRACTION (0-1) OF SENS HT FLUX GOING INTO CBL GROWTH *
31 C N TIMESTEP COUNTER *
32 C NSTEPS NUMBER OF TIME STEPS REQD TO DESTROY INVERSION *
33 C PRESS AVG PRESSURE (MB) AT INV CENTER AT SUNRISE *
34 C PI TRIGONOMETRIC CONSTANT *
35 C RHO AIR DENSITY (KG/M3) *
36 C TAU LENGTH OF DAYLIGHT PERIOD (SEC). 43200SEC=12HR *
37 C T ELAPSED TIME SINCE SUNRISE (SEC) *
38 C TI TIME OF SUNRISE (SEC) *
39 C W VALLEY FLOOR WIDTH (M) *
40 C*****
41
42 C**** INPUT PARAMETERS
43 CP=1005.
44 PI=3.14
45 N=0
46 TI=0.
47 T=0.
48
49 C**** CALCULATE SECONDARY PARAMETERS
50 FACT1=A0*A1/(RHO*CP)
51 THTOT=(1000./PRESS)**.286
52 C=(1./TAN(ALPHA1))+(1./TAN(ALPHA2))
53
54 C**** DO CALCULATIONS
55 HTOP=HZERO
56 HCBL=HCBLI
57 GO TO 2
58 1 CONTINUE
59 T=T+DELTAT
60 2 CONTINUE
61 N=N+1
62 FACT2=FACT1*SIN(PI*(T-TI)/TAU)
63

```

```

64      IF (K.NE.0.) THEN
65          DHDТ=FACT2*ТHTOT*K*(W+HCBЛ*С)/
66      1  (GAMMA*HCBЛ*(W+(HCBЛ*С)/2.))
67      ELSE
68          DHDТ=0.
69      ENDIF
70
71      FNUM=(W+HTOP*С-K*(W+HCBЛ*С))*FACT2-((BETA*
72      1  (HZERO-HTOP)*(W+((HZERO+HTOP)/2.)*С))/(2.*ТHTOT))
73      FDENOM=HTOP*GAMMA*(W+(HTOP*С)/2.)
74      1+(BETA*(Т-ТI)*(W+HTOP*С))/2.
75      DHTDT=-ТHTOT*FNUM/FDENOM
76      DHT=DHTDT*DELTAT
77      HTOP=HTOP+DHT
78      HT(N)=HTOP
79      DHC=DHDТ*DELTAT
80      HCBЛ=HCBЛ+DHC
81      HC(N)=HCBЛ
82
83      C***** STOP CALCULATIONS WHEN INVERSION TOP SINKS BELOW CBL TOP
84      IF (HTOP.LE.HCBЛ) THEN
85          NSTEPS=N
86          RETURN
87      ELSE
88          GO TO 1
89      ENDIF
90
91      END

```



```

1 C+*****
2 SUBROUTINE PROFIL(NBOX,NTOTI,NTOT,BOXLEN,HCL,ALPHA1,
3 1ALPHA2,HZERO,H,HCU,HTL,HTU,YZERO,Q,US,DF,
4 2SIGMAY,SIGMAZ,CHIOFF)
5 C**** THIS SUBROUTINE DETERMINES THE AVERAGE POLLUTANT CONCENTRATION
6 C**** INJECTED INTO THE TOP OF EACH BOX.
7
8 PARAMETER (NB=30)
9
10 COMMON/BLK2/CHIBAR(NB)
11
12 C**** DEFINITIONS *****
13 C HCL CBL HEIGHT AT LOWER TIME STEP (M) *
14 C HCU CBL HEIGHT AT UPPER TIME STEP (M) *
15 C HTL INVERSION TOP HEIGHT AT LOWER TIME STEP (M) *
16 C HTU INVERSION TOP HEIGHT AT UPPER TIME STEP (M) *
17 C Y1 Y COORD AT LEFT SIDE OF SINKING MASS ELEMENT (M) *
18 C Y2 Y COORD AT RIGHT SIDE OF SINKING MASS ELEMENT (M) *
19 C Z1 EFFECTIVE Z COORD AT BOTTOM OF SINKING MASS ELEMENT (M) *
20 C Z2 EFFECTIVE Z COORD AT TOP OF SINKING MASS ELEMENT (M) *
21 C*****
22
23 ALPHA=(ALPHA1+ALPHA2)/2.
24
25 C**** CALCULATE CHIBAR FOR THE BOXES ON THE VALLEY FLOOR.
26 DO 1 I=1,NTOTI
27 Y1=(I-1)*BOXLEN
28 Y2=I*BOXLEN
29 Y=(Y1+Y2)/2.
30
31 IF(I.GT.NTOT) THEN
32 CHIBAR(I)=999.9
33 GO TO 1
34 ELSE IF(I.GT.NBOX .AND. I.LE.NTOT) THEN
35 Z1=HCL+HZERO-HTL+(FLOAT(I-(NBOX+1))+.5)*BOXLEN*TAN(ALPHA)
36 Z2=HCU+HZERO-HTU+(FLOAT(I-(NBOX+1))+.5)*BOXLEN*TAN(ALPHA)
37 ELSE
38 Z1=HZERO-HTL+HCL
39 Z2=HZERO-HTU+HCU
40 ENDIF
41
42 Z=(Z1+Z2)/2.
43 CALL GAUSS(Y,Z1,YZERO,H,Q,US,DF,SIGMAY,SIGMAZ,CHIZ1)
44 CALL GAUSS(Y,Z2,YZERO,H,Q,US,DF,SIGMAY,SIGMAZ,CHIZ2)
45 CALL GAUSS(Y1,Z,YZERO,H,Q,US,DF,SIGMAY,SIGMAZ,CHIY1)
46 CALL GAUSS(Y2,Z,YZERO,H,Q,US,DF,SIGMAY,SIGMAZ,CHIY2)
47 CHIBAR(I)=(CHIZ1+CHIZ2+CHIY1+CHIY2)/4. + CHIOFF
48
49 1 CONTINUE
50 RETURN
51 END

```

```

1 C+*****
2 SUBROUTINE VELOCITY(N,MN,NTOTI,NBOX,NTOT,BOXLEN,DELTAT)
3 C**** THIS SUBROUTINE CALCULATES VELOCITY AT EACH SEPTUM BASED ON
4 C**** MASS CONTINUITY.
5
6 PARAMETER (NS=6000,NB1=31)
7
8 COMMON/BLK1/HC(NS),HT(NS)
9 COMMON/BLK3/V(NB1)
10
11 V(1)=0.
12 CIH=HT(MN)-HT(N)
13 IF(NTOT.EQ.NBOX.AND.HT(N).LE.HC(N)) GO TO 3
14
15 DO 2 I=1,NTOTI
16 IF(I.GT.NTOT) GO TO 1
17 V(I+1)=(I*BOXLEN*CIH/DELTAT)/HC(N)
18 GO TO 2
19 1 V(I+1)=999.9
20 2 CONTINUE
21 GO TO 5
22
23 3 DO 4 I=1,NTOTI
24 V(I+1)=999.9
25 4 CONTINUE
26
27 5 RETURN
28 END

```

```

1 C+*****
2 SUBROUTINE BRKUP(N,MN,NTOTI,BOXLEN,DELTAT,CCH)
3 C**** THIS SUBROUTINE CALCULATES POLLUTANT CONCENTRATIONS IN EACH
4 C**** OF THE GRID ELEMENTS (BOXES) USING A POLLUTANT MASS BALANCE.
5
6 PARAMETER (NS=6000,NB=30,NB1=J1)
7
8 REAL CCH(2,NB)
9
10 COMMON/BLK1/HC(NS),HT(NS)
11 COMMON/BLK2/CHIBAR(NB)
12 COMMON/BLK3/V(NB1)
13
14 C*DEFINITIONS *****
15 C A IS THE POLLUTANT MASS WITHIN THE BOX AT THE PREVIOUS TIME STEP. *
16 C B IS THE MASS COMING FROM THE ADJACENT DOWNHILL BOX. *
17 C C IS THE MASS COMING INTO TOP OF BOX DUE TO SINKING INVERSION *
18 C AND/OR GROWING CBL *
19 C D IS THE MASS GOING OUT UPHILL SIDE OF THE BOX. *
20 C E IS THE MASS SOURCE OR SINK FROM SURFACE OF BOX. *
21 C*****
22
23 E=0.0
24 DELTAH=HC(N)-HC(MN)+HT(MN)-HT(N)
25 DO 4 I=1,NTOTI
26 IF(V(I+1).EQ.999.9) GO TO 3
27 A=CCH(1,I)*BOXLEN*HC(MN)
28 IF(I.EQ.1) GO TO 1
29 B=D
30 GO TO 2
31 1 B=0.0
32 2 C=CHIBAR(I)*DELTAT*BOXLEN
33 D=(DELTAT/BOXLEN*V(I+1)+(HC(N)-HC(MN))/HC(N))*A
34 1 +(DELTAT/BOXLEN*V(I+1))*(B+C)
35 CCH(2,I)=(A+B+C+E-D)/(BOXLEN*HC(N))
36 GO TO 4
37 C**** EXPONENTIAL DECAY
38 3 S=ALOG(.90)
39 CCH(2,I)=CCH(1,I)*EXP(S*DELTAT/10.)
40 4 CONTINUE
41
42 RETURN
43 END

```

```

1 C+++++
2 SUBROUTINE PSTPRC(TSTP,NTOTI,NAS)
3 C**** THIS SUBROUTINE PROCESSES THE TIME SERIES OF CALCULATED
4 C**** 5-MINUTE (300 S) AVERAGE CONCENTRATIONS TO OBTAIN MAXIMUM
5 C**** SHORT TERM (1 AND 3 HOUR) AVERAGE CONCENTRATIONS WHICH CAN
6 C**** BE COMPARED TO REGULATORY STANDARDS.
7
8 PARAMETER (NA=100,NB=30,NB1=31)
9
10 REAL SUMM(NB,2)
11
12 COMMON/BLK4/CONC(NA,NB)
13 COMMON/BLK5/CHI(NB)
14 COMMON/BLK6/AVG(NB,2),NDXTIM(NB,2),NTS(2)
15
16 C**** TIME IN SECONDS
17 ONEHR=3600.
18 THREE=10800.
19
20 C**** NUMBER OF TIMESTEPS
21 NTS(1)=ONEHR/TSTP
22 NTS(2)=THREE/TSTP
23 NSTART=NAS+1
24
25 C**** CALCULATE MAX 1-HR AND 3-HR AVERAGE CONCENTRATIONS
26 DO 7 K=1,2
27 TS=NTS(K)
28 DO 7 I=1,NTOTI
29 SUM=0.
30
31 C**** AVERAGING INTERVAL LESS THAN LENGTH OF DAYTIME CONC SERIES.
32 IF(NSTART.GT.NTS(K)) THEN
33 DO 1 N=NAS,NSTART-NTS(K),-1
34 SUM=SUM+CONC(N,I)
35 1 CONTINUE
36 SUMM(I,K)=SUM
37 Q1=SUM
38 NTIMES=NAS
39 DO 2 N=NAS,NTS(K)+1,-1
40 SUMM(I,K)=SUMM(I,K)+CONC(N-NTS(K),I)-CONC(N,I)
41 IF(SUMM(I,K).GT.Q1)THEN
42 Q1=SUMM(I,K)
43 NTIMES=N-1
44 ENDIF
45 2 CONTINUE
46 DO 3 N=NTS(K),1,-1
47 SUMM(I,K)=SUMM(I,K)+CHI(I)-CONC(N,I)
48 IF(SUMM(I,K).GT.Q1)THEN
49 Q1=SUMM(I,K)
50 NTIMES=N-1
51 ENDIF
52 3 CONTINUE
53 C**** AVERAGING INTERVAL LONGER THAN DAYTIME CONC SERIES
54 ELSE
55 4 DO 5 N=NAS,1,-1
56 SUM=SUM+CONC(N,I)
57 5 CONTINUE
58 SUMM(I,K)=SUM+CHI(I)*(NTS(K)-NAS)
59 Q1=SUM
60 NTIMES=NAS
61 DO 6 N=NAS,1,-1
62 SUMM(I,K)=SUMM(I,K)+CHI(I)-CONC(N,I)
63 IF(SUMM(I,K).GT.Q1)THEN

```

```

64         Q1=SUMM(I,K)
65         NTIMES=N-1
66         ENDIF
67     6     CONTINUE
68     ENDIF
69
70         NDXTIM(I,K)=NTIMES
71         AVG(I,K)=Q1/TS
72     7     CONTINUE
73
74         RETURN
75     END

```

APPENDIX B

FORTRAN LISTING OF VALMET OUTPUT PLOTTING PROGRAM

```

1  C      PROGRAM PLOTT.FOR
2
3  C      THIS PROGRAM IS DESIGNED TO PRODUCE PLOTS OF CONCENTRATION
4  C      VERSUS TIME FOR ARBITRARY GRID ELEMENTS IN MODEL VALMET.
5  C      THIS PROGRAM ALSO PRODUCES A SINGLE PAGE CONTAINING THREE OTHER PLOTS:
6  C      CONC VS HEIGHT, CONC VS X-VALLEY DISTANCE, AND HEIGHT VS TIME.
7
8      PARAMETER (NS=6000,NA=100,NB=30)
9
10     DIMENSION TTIME(NA),CONC(NA,NB),CONCEN(NA),XBORD(5),
11     1  YBORD(5),NBOX(10),XMAXI(10),YMAXI(10)
12     DIMENSION X1(4),X2(4),Y1(4),Y2(4),ICNT(3,2)
13     1  ,T(3,4),Z(1000),TIC(3,2),
14     2  Y(1000),CHIZ(1000),CHIZ(1000),HC(NS),HT(NS),
15     3  TIME(NS),SZ1(3),SZ2(3),TIK(3,2)
16
17     CHARACTER*20 INFILE
18     CHARACTER*3 ITIME
19     CHARACTER*2 ICHAR(30)
20     CHARACTER*26 ILBL(3,2)
21     CHARACTER*1 ANS1,ANS2
22     CHARACTER*2 JLBL1
23     CHARACTER*5 JLBL2
24     CHARACTER*5 JLBL3
25
26     DATA X1/3.0,2.5,5.5,5.5/
27     DATA X2/10.0,4.0,10.0,10.0/
28     DATA Y1/3.0,5.0,5.0,2.0/
29     DATA Y2/7.5,8.0,8.0,3.5/
30
31     DATA ICHAR/'01','02','03','04','05','06','07','08',
32     1      '09','10','11','12','13','14','15','16',
33     2      '17','18','19','20','21','22','23','24',
34     3      '25','26','27','28','29','30'/
35
36     SZ1(1)=.35
37     SZ1(2)=.35
38     SZ1(3)=.70
39     SZ2(1)=.40
40     SZ2(2)=.40
41     SZ2(3)=.80
42
43     ICNT(1,1)=12
44     ICNT(2,1)=10
45     ICNT(3,1)=26
46     ICNT(1,2)=14
47     ICNT(2,2)=14
48     ICNT(3,2)=12
49
50     ILBL(1,1)='CONC (ug/m3)'
51     ILBL(2,1)='TIME (LDT)'
52     ILBL(3,1)='CROSS-VALLEY DISTANCE (km)'
53     ILBL(1,2)='HEIGHT (m AGL)'

```

```

54      ILBL(2,2)='HEIGHT (m AGL)'
55      ILBL(3,2)='CONC (ug/m3)'
56
57      TIC(1,1)=1.0
58      TIC(1,2)=200.
59      TIC(2,1)=1.0
60      TIC(2,2)=200.
61      TIC(3,1)=1.0
62      TIC(3,2)=1.0
63
64      TIK(1,1)=0.5
65      TIK(1,2)=100.
66      TIK(2,1)=1.0
67      TIK(2,2)=100.
68      TIK(3,1)=0.5
69      TIK(3,2)=0.5
70
71      WRITE(6,100)
72      100 FORMAT(1H , 'WHAT IS THE NAME OF THE DATA FILE?')
73      READ(5, '(A20)') INFILE
74      OPEN(UNIT=3, FILE=INFILE, TYPE='OLD', FORM='FORMATTED')
75
76      C**** READ DATA IN FROM UNIT 3
77      READ(3,601) NSTEPS,NTSR,NINDX,NTOTI,NAS,ITIME
78      601 FORMAT(1H ,5I8,A3)
79      IF(ITIME.EQ.'LST') ILBL(2,1)='TIME (LST)'
80      READ(3,602) CLCONC,DELTAT,SUM1,SUM2,X,CHIOFF,
81      1SIGMAZ,SIGMAZ,THETA1,THETA2,WIDTH,HZERO,H
82      602 FORMAT(1H ,13F10.5)
83      SUM1=SUM1*100.
84      SUM2=SUM2*100.
85
86      DO 153 I=1,NTOTI
87      DO 153 IND=1,NAS+1
88      READ(3,610) II,MNN,TTIME(IND),CONC(IND,I)
89      610 FORMAT(1H ,I2,I5,F12.7,F12.7)
90      153 CONTINUE
91
92      DO 154 I=1,NSTEPS
93      READ(3,603) HC(I),HT(I)
94      603 FORMAT(1H ,6(2F9.3))
95      154 CONTINUE
96
97      C**** SPECIFY PLOTTING DEVICE
98      WRITE(6,102)
99      102 FORMAT(1H , 'OUTPUTMODE:1=RAM,2=TEK,3=HP ')
100      READ(5,*) IMODE
101
102      C**** SPECIFY WHAT YOU WANT TO PLOT
103      WRITE(6,500)
104      500 FORMAT(1H , 'DO YOU WANT THE FIRST PLOT OF CONCENTRATION
105      1 VERSUS TIME?')
106      READ(5,501) ANS2

```



```

107      501 FORMAT(A1)
108      IF(ANS2.NE.'Y') GO TO 502
109      WRITE(6,103)
110      103 FORMAT(1H,'THE FIRST PLOT IS CONCENTRATION VS TIME')
111      XMAX=TTIME(1)+NINDX*DELTAT/3600.
112      WRITE(6,104) NTSR,XMAX,CLCONC
113      104 FORMAT(1H,'MIN AND MAX VALUES ARE: TIME ',15,2X,
114      1F8.2,5X,'CONCENTRATION 0.0',2X,F4.2)
115      WRITE(6,105)
116      105 FORMAT(1H,'ENTER TMIN,TMAX,CONCMIN,CONCMAX')
117      READ(5,*) XMIN,XMAX,YMIN,YMAX
118      XBORD(1)=XMIN
119      XBORD(2)=XMAX
120      XBORD(3)=XMAX
121      XBORD(4)=XMIN
122      XBORD(5)=XMIN
123      YBORD(1)=YMIN
124      YBORD(2)=YMIN
125      YBORD(3)=YMAX
126      YBORD(4)=YMAX
127      YBORD(5)=YMIN
128      WRITE(6,106) NTOTI
129      106 FORMAT(1H,'THERE ARE ',I2,' GRID ELEMENTS')
130      WRITE (6,107)
131      107 FORMAT(1H,'HOW MANY CURVES DO YOU WANT TO PLOT?')
132      READ(5,*) NC
133      WRITE(6,108)
134      108 FORMAT(1H,'CURVES ARE TO BE DRAWN FOR WHICH GRID ELEMENT
135      1 NUMBERS? EX:3,6,9')
136      READ(5,*) (NBOX(N),N=1,NC)
137
138      C**** DRAW THE PLOTS
139      CALL KTERM(IMODE)
140      CALL KBEGIN
141      CALL KPAGE(X1(1),X2(1),Y1(1),Y2(1),0)
142      CALL KSCALE(XMIN,XMAX,0,YMIN,YMAX,0)
143      CALL KAXIS(XMIN,YMIN,XMAX,1.0,0.5,0,0.0,1,0.35,0.,
144      1ILBL(2,1),10,1,0.40,0.)
145      CALL KAXIS(XMIN,YMIN,YMAX,0.2,0.1,1,0.,1,0.35,0.,
146      1ILBL(3,2),12,1,0.40,0.)
147      CALL KCURVE(XBORD,YBORD,5)
148      XMAXI(N)=0.
149      YMAXI(N)=0.
150      DO 3 N=1,NC
151      DO 2 MN=1,NAS+1
152      CONCEN(MN)=CONC(MN,NBOX(N))
153      IF(MN.EQ.1) GO TO 14
154      IF(CONCEN(MN).GT.CONCEN(MN-1)) THEN
155      XMAXI(N)=TTIME(MN)
156      YMAXI(N)=CONCEN(MN)
157      ENDIF
158      14 CONTINUE
159      2 CONTINUE

```

```

160      WRITE(6,109) XMAXI(N),YMAXI(N)
161 109 FORMAT(1H,2F8.2)
162      CALL KLINE(N,0,0.,0.)
163      CALL KCURVE(TTIME,CONCEN,NAS+1)
164      3 CONTINUE
165      DO 4 N=1,NC
166      YMAXI(N)=YMAXI(N)+.10*(YMAX-YMIN)/(Y2(1)-Y1(1))
167      WRITE(6,110) YMAXI(N)
168 110 FORMAT(F8.2)
169      4 CONTINUE
170      DO 5 N=1,NC
171      I=NBOX(N)
172      WRITE(6,111) I,ICAR(I)
173 111 FORMAT(1H,13,A2)
174      CALL KUALFA(XMAXI(N),YMAXI(N),ICAR(I),
175      12,1,0.35,0.,0.)
176      5 CONTINUE
177      IX=X
178      XA=XMIN+.74
179      XB=XMIN+1.45
180      XC=XMIN+1.65
181      XPOS1=XMIN+0.4
182      YPOS1=.9*YMAX
183      YPOS2=.8*YMAX
184      YPOS3=.7*YMAX
185      HTL=0.4
186      WRITE(JLBL1,300) IX
187 300 FORMAT(I2)
188      WRITE(JLBL2,301) CLCONC
189 301 FORMAT(F5.2)
190      WRITE(JLBL3,302) SUM2
191 302 FORMAT(F5.1)
192      CALL KUALFA(XPOS1,YPOS1,'X= km',7,1,HTL,0.,0.)
193      CALL KUALFA(XPOS1,YPOS2,'CL CONC= ug/m3',19,
194      11,HTL,0.,0.)
195      CALL KUALFA(XPOS1,YPOS3,'% OUT TOP= %',16,
196      11,HTL,0.,0.)
197      CALL KUALFA(XA,YPOS1,JLBL1,2,1,HTL,0.,0.)
198      CALL KUALFA(XB,YPOS2,JLBL2,5,1,HTL,0.,0.)
199      CALL KUALFA(XC,YPOS3,JLBL3,5,1,HTL,0.,0.)
200
201 C*** SET UP AND DRAW THE SECOND PLOT
202
203      502 WRITE(6,*) 'DO YOU WANT THE SECOND SET OF PLOTS?'
204      READ (5,199) ANS1
205 199 FORMAT(A1)
206      IF(ANS1.NE.'Y') GO TO 13
207
208      CALL KCLEAR
209      DELTAY=.01
210 C*** SET UP TIME ARRAY
211      DO 6 MN=1,NINDX
212      IF(MN.EQ.1)THEN

```

```

213      TIME(MN)=TTIME(1)
214      ELSE IF(MN.EQ.2) THEN
215      TIME(MN)=TTIME(2)
216      ELSE
217      TIME(MN)=TTIME(2)+(MN-2)*DELTAT/3600.
218      ENDIF
219      6 CONTINUE
220
221      C      WRITE(6,700) NINDX
222      C 700 FORMAT(1H ,18)
223      C      DO 46 MN=1,NINDX
224      C      WRITE(6,701) TIME(MN)
225      C 701 FORMAT(1H ,F12.2)
226      C 46 CONTINUE
227
228      DIST=((WIDTH+2.*HZERO/TAN(THETA1))/2.)/1000.
229
230      C**** SPECIFY WHAT YOU WANT TO PLOT
231      WRITE(6,201) CLCONC,HT(1),DIST
232      201 FORMAT(1H , 'CENTERLINE CONC=',F6.2, ' INVERSION DEPTH=',
233      1F8.2, ' SIDEWALL DISTANCE=',F8.2)
234      WRITE(6,202)
235      202 FORMAT(1H , 'ENTER CONCMIN,CONCMAX,TMIN,TMAX,YMIN,YMAX,
236      1ZMIN,ZMAX')
237      READ(5,*) T(1,1),T(1,2),T(2,1),T(2,2),T(3,1),T(3,2),
238      1T(1,3),T(1,4)
239      T(2,3)=T(1,3)
240      T(2,4)=T(1,4)
241      T(3,3)=T(1,1)
242      T(3,4)=T(1,2)
243
244      DO 8 K=1,1000
245      Z(K)=K
246      IF(Z(K).GT.HT(1)) GO TO 9
247      CHIZ(K)=CHIOFF+CLCONC*EXP(-.5*(Z(K)-H)**2/
248      1(SIGMAZ**2))
249      8 CONTINUE
250      STOP 2
251
252      9 K=K-1
253      DO 10 J=1,1000
254      Q=J
255      Y(J)=-DIST+Q*DELTAY
256      IF(Y(J).GT.DIST) GO TO 11
257      QQ=Y(J)*1000.
258      CHIY(J)=CHIOFF+CLCONC*EXP(-.5*QQ**2/(SIGMAZ**2))
259      10 CONTINUE
260      STOP 3
261
262      11 J=J-1
263
264      C**** DRAW THE PLOTS
265      CALL KTERM(INODE)

```

```

266      CALL KBEGIN
267      DO 12 M=1,3
268      CALL KPAGE(X1(M+1),X2(M+1),Y1(M+1),Y2(M+1),0)
269      CALL KSCALE(T(M,1),T(M,2),0,T(M,3),T(M,4),0)
270      XBORD(1)=T(M,1)
271      XBORD(2)=T(M,2)
272      XBORD(3)=T(M,2)
273      XBORD(4)=T(M,1)
274      XBORD(5)=T(M,1)
275      YBORD(1)=T(M,3)
276      YBORD(2)=T(M,3)
277      YBORD(3)=T(M,4)
278      YBORD(4)=T(M,4)
279      YBORD(5)=T(M,3)
280      CALL KLINE(1,0,0.0,0.0)
281      CALL KCURVE(XBORD,YBORD,5)
282      CALL KAXIS(T(M,1),T(M,3),T(M,2),TIC(M,1),TIK(M,1),
283      * 0,0.0,1,SZ1(M),0.,ILBL(M,1),ICNT(M,1),1,SZ2(M),0.)
284      CALL KAXIS(T(M,1),T(M,3),T(M,4),TIC(M,2),TIK(M,2),
285      * 1,0.0,1,SZ1(M),0.,ILBL(M,2),ICNT(M,2),1,SZ2(M),0.)
286      IF(M.EQ.1) THEN
287          CALL KLINE(4,0,0.0,0.0)
288          CALL KCURVE(CHIZ,Z,K)
289      ELSE IF(M.EQ.2) THEN
290          CALL KLINE(4,0,0.0,0.0)
291          CALL KCURVE(TIME,HC,NSTEPS)
292          CALL KLINE(2,0,0.0,0.0)
293          CALL KCURVE(TIME,HT,NSTEPS)
294      ELSE IF(M.EQ.3) THEN
295          CALL KLINE(4,0,0.0,0.0)
296          CALL KCURVE(Y,CHIV,J)
297      ELSE
298          STOP 4
299      ENDIF
300      12 CONTINUE
301      13 CONTINUE
302      STOP 1
303      END

```

APPENDIX C

RESEARCH PAPER ENTITLED "BREAKUP OF TEMPERATURE
INVERSIONS IN DEEP MOUNTAIN VALLEYS:
PART II. THERMODYNAMIC MODEL"

Reprinted from JOURNAL OF APPLIED METEOROLOGY, Vol. 21, No. 3, March 1982
American Meteorological Society
Printed in U. S. A.

**Breakup of Temperature Inversions in Deep Mountain Valleys:
Part II. Thermodynamic Model**

C. DAVID WHITEMAN

THOMAS B. MCKEE

Breakup of Temperature Inversions in Deep Mountain Valleys: Part II. Thermodynamic Model

C. DAVID WHITEMAN

Pacific Northwest Laboratory, Richland, WA 99352

THOMAS B. MCKEE

Department of Atmospheric Science, Colorado State University, Fort Collins 80523

(Manuscript received 31 March 1981, in final form 7 December 1981)

ABSTRACT

A thermodynamic model is developed to simulate the evolution of vertical temperature structure during the breakup of nocturnal temperature inversions in mountain valleys. The primary inputs to the model are the valley floor width, sidewall inclination angles, characteristics of the valley inversion at sunrise, and an estimate of sensible heat flux obtained from solar radiation calculations. The outputs, obtained by a numerical integration of the model equations, are the time-dependent height of a convective boundary layer that grows upward from the valley floor after sunrise, the height of the inversion top, and vertical potential temperature profiles of the valley atmosphere. The model can simulate the three patterns of temperature structure evolution observed in deep valleys of western Colorado. The well-known inversion breakup over flat terrain is a special case of the model, for which valley floor width becomes infinite. The characteristics of the model equations are investigated for several limiting conditions using the topography of a reference valley and typical inversion and solar radiation characteristics. The model is applied to simulate observations of inversion breakup taken in Colorado's Eagle and Yampa Valleys in different seasons. Simulations are obtained by fitting two constants in the model, relating to the surface energy budget and energy partitioning, to the data. The model accurately simulates the evolution of vertical potential temperature profiles and predicts the time of inversion destruction.

1. Introduction

In Part I (Whiteman, 1982) observations of vertical temperature structure and wind evolution were summarized for 21 case studies of nocturnal temperature inversion breakup in deep Colorado mountain valleys. Breakup occurred following one of three patterns of vertical temperature structure evolution. A hypothesis was offered to explain the observations in which sensible heat flux was the driving force and one of the three patterns occurred, depending on whether the sensible heat flux was used primarily to cause convective boundary layers (CBLs) to grow over the valley floor and sidewalls (Pattern 1), to remove mass from the inversion in the upslope flows (Pattern 2), or to accomplish both (Pattern 3). In Part II, a bulk thermodynamic model of temperature inversion destruction is developed based on the hypothesis, using several simplifying assumptions.

2. Mathematical model of inversion destruction

a. General equations

Two approaches can be used to develop a mathematical model able to simulate temperature changes

in the valley atmosphere. In the first approach detailed mathematical equations can be developed for the individual components of the overall system, including the various boundary layers and stable core. However, the valley atmosphere consists of many interrelated layers, and the coupling of the equations for the different layers to simulate potential temperature changes in the valley atmosphere as a whole would be difficult due to geometrical considerations and lack of detailed information on physical characteristics of the various layers. Consequently, a second approach is taken in which a bulk thermodynamic model is developed for the valley inversion. As more is learned about the individual components of the system, the model can be refined to introduce greater detail into the simulation of the individual components.

The thermodynamic model of valley temperature structure evolution developed here is based on the hypothesis of Part I. Fig. 1 shows a unit thick cross section of a mountain valley having sidewalls of inclination α_1 and α_2 and valley floor width l . At sunrise (t_i) the valley is assumed to have an inversion of depth h_i and constant vertical potential temperature gradient γ . The variable width of the valley at the

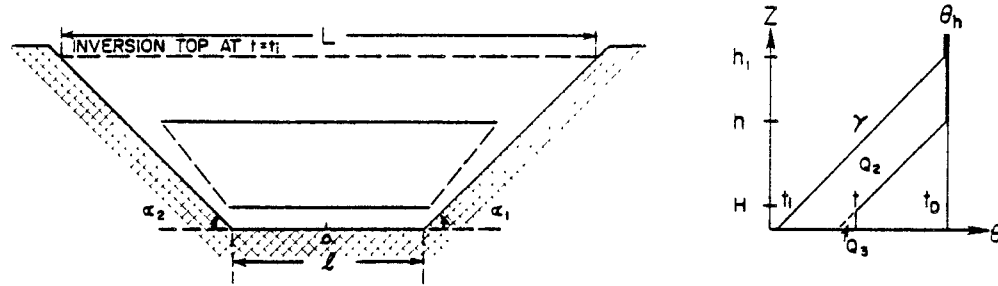


FIG. 1. Valley geometry and potential temperature profiles used to formulate a mathematical model of inversion destruction.

top of the inversion is designated by L , and the origin of a y - z coordinate system is placed at the center of the valley floor at point 0. After sunrise a typical Pattern 3 potential temperature evolution ensues, in which a CBL develops over the valley floor and sidewalls. Removal of mass from the valley in these CBLs allows the stable core to sink so that a sounding taken at an arbitrary later time t will show a lower inversion top height $h(t)$ and a shallow CBL of height $H(t)$ near the ground. A later sounding, taken at a time t_0 when the inversion has just been destroyed, will show a neutral atmosphere having a potential temperature $\theta = \theta_h$.

From the first law of thermodynamics, the increment of energy required to increase the potential temperature of a mass of air m by the potential temperature increment $\Delta\theta$ is

$$\Delta Q = mc_p \frac{T}{\theta} \Delta\theta = \rho V c_p \frac{T}{\theta} \Delta\theta, \quad (1)$$

where $T/\theta = (P/1000)^{R/c_p} \approx 1$, ρ is the density (assumed constant) and V is volume. Using (1), the energy required to change the valley potential temperature profile at time t_i to the profile at time t can be obtained by an integration over the valley volume below the height of the inversion top. The total energy requirement is composed of two parts: the energy increment Q_2 that removes mass from the valley and allows the top of the inversion to sink, and the energy increment Q_3 that causes a CBL to grow. These energies are represented by the areas designated in Fig. 1 and are given by

$$Q_2 = \rho c_p \frac{T}{\theta} \left[\int_0^{h_i} \int_{y_L}^{y_R} \int_0^l \Delta\theta_1 dx dy dz - \int_0^H \int_{y_L}^{y_R} \int_0^l \Delta\theta_2 dx dy dz \right], \quad (2)$$

$$= \rho c_p \frac{T}{\theta} \gamma \left[\frac{l}{2} (h_i^2 - h^2) + \frac{C}{6} (h_i^3 - h^3) \right], \quad (3)$$

where

$$\Delta\theta_1 = \gamma(h_i - z), \quad (4)$$

$$y_L = -\left(\frac{l}{2} + \frac{z}{\tan\alpha_2}\right), \quad (5)$$

$$y_R = \frac{l}{2} + \frac{z}{\tan\alpha_1}, \quad (6)$$

$$C = \frac{1}{\tan\alpha_1} + \frac{1}{\tan\alpha_2}, \quad (7)$$

$$\Delta\theta_1 = \gamma(h - z), \quad (8)$$

and

$$Q_3 = \rho c_p \frac{T}{\theta} \int_0^H \int_{y_L}^{y_R} \int_0^l \Delta\theta_2 dx dy dz, \quad (9)$$

$$= \rho c_p \frac{T}{\theta} \gamma \left[\frac{l}{2} H^2 + \frac{C}{6} H^3 \right], \quad (10)$$

where

$$\Delta\theta_2 = \gamma(H - z). \quad (11)$$

In order to simplify the integration, it was assumed that the valley temperature structure is horizontally homogeneous across the valley, that mass is removed from the valley in such a way that the potential temperature gradient in the inversion layer does not change with time, and that ρ and c_p are constant. By differentiating the individual energies Q_2 and Q_3 with respect to time, the rates of change of the height of the top of the inversion and the height of the CBL are obtained, such that

$$\frac{dQ_2}{dt} = \rho c_p \frac{T}{\theta} \gamma \left[-h \frac{dh}{dt} \left(l + \frac{hC}{2} \right) \right], \quad (12)$$

$$\frac{dQ_3}{dt} = \rho c_p \frac{T}{\theta} \gamma \left[H \frac{dH}{dt} \left(l + \frac{HC}{2} \right) \right]. \quad (13)$$

The total rate of energy input into the valley to accomplish these changes is the fraction A_0 of solar irradiance F coming across the area L of the top of the inversion that is converted to sensible heat. The solar irradiance may be approximated by a sine function having a certain amplitude A_1 and period τ , so that the total rate of energy input becomes

$$\frac{dQ_1}{dt} = A_0 L F = A_0 (l + hC) A_1 \sin \frac{\pi}{\tau} (t - t_i). \quad (14)$$

An energy balance for the valley inversion is obtained by equating (14) to the sum of (12) and (13). Alternatively, a fraction of the energy input is available to drive the growth of the CBL while the rest of the incoming energy is used to remove mass from the valley. The fraction of energy input used to drive the CBL growth is assumed to be of the form

$$k \left(\frac{l + HC}{l + hC} \right),$$

where k is a number between 0 and 1. This form is chosen in order to simplify later equations. Equating this fraction of the energy input to (12) and the remainder to (13) and solving for dH/dt and dh/dt results in the final model equations

$$\frac{dH}{dt} = \frac{\theta}{T} \frac{k}{\rho c_p} \left(\frac{l + HC}{l + \frac{1}{2}hC} \right) \times \frac{A_0 A_1}{\gamma H} \sin \left[\frac{\pi}{\tau} (t - t_i) \right], \quad (15)$$

$$\frac{dh}{dt} = - \frac{\theta}{T} \frac{1}{\rho c_p} \left[\frac{l + hC - k(l + HC)}{l + \frac{1}{2}hC} \right] \times \frac{A_0 A_1}{\gamma h} \sin \left[\frac{\pi}{\tau} (t - t_i) \right]. \quad (16)$$

These equations specify the dependence of the rate of ascent of the CBL and the rate of descent of the inversion top on inversion characteristics, incoming energy and valley topography. An integration of the coupled equations allows the simulation of the time-dependent behavior of the heights of the CBL and inversion top. If the potential temperature θ_h at the top of the inversion is known and is independent of time, and γ is constant, knowledge of the variation of h and H with time is sufficient to specify how vertical profiles of potential temperature change with time. When $k = 0$, the equations provide an approximate simulation of Pattern 2 inversion destruction in which destruction occurs solely due to the removal of mass from a valley in the slope flows, resulting in a descent of the inversion top. When $k = 1$, the equations provide a simulation of Pattern 1 inversion destruction, in which destruction occurs mainly due to the growth of a CBL over the valley floor. When $k = 1$ and the valley floor becomes very wide, the simulation approaches that of inversion destruction over the plains. When k is between 0 and 1, the equations provide a simulation of Pattern 3 inversion destruction in which the inversion is destroyed by the combined effect of a growing CBL and a descending inversion top. A more complete description of the characteristics of the model equations for Pattern 1, 2 and 3 temperature structure evolution follows.

b. Pattern 2 inversion destruction

The physical hypothesis of Pattern 2 inversion destruction requires a shallow CBL to form over the sidewalls so that additional energy can be used to cause mass to flow up them. Pattern 2 destruction may be approximated by assuming that all the energy available to destroy the inversion goes solely to move mass up the sidewalls, causing the top of the inversion to descend. This can be accomplished by setting k equal to zero in (15) and (16) resulting in the two equations

$$\frac{dH}{dt} = 0, \quad (17)$$

$$\frac{dh}{dt} = - \frac{\theta}{T} \left(\frac{l + hC}{l + \frac{1}{2}hC} \right) \frac{A_0 A_1}{\rho c_p \gamma h} \sin \left[\frac{\pi}{\tau} (t - t_i) \right]. \quad (18)$$

Following these equations, the CBL does not grow as a function of time, and the inversion is destroyed as the top of the inversion sinks. The rate of descent of the top of the inversion increases as the inversion descends. The descent rate is faster when more energy is available and when the potential temperature gradient of the inversion is weaker. The factor in large parentheses in (18) is a topographic factor that varies from 1 to 2 depending on the shape of the valley cross section. This accounts for the reduced volume of air within the mountain valley relative to that over the plains for the same energy flux on a horizontal surface. Since the valley has less volume to be heated by the same incoming energy, it warms more rapidly. By separating variables h and t and integrating from the initial conditions $h = h_i$ and $H = 0$ at $t = t_i$ to $h = h$ and $H = H$ at $t = t$, analytical expressions are obtained which describe how H and h vary with time, i.e.,

$$H = 0, \quad (19)$$

$$\begin{aligned} \frac{1}{4}(h^2 - h_i^2) + \frac{l}{2C}(h - h_i) + \frac{l^2}{2C^2} \ln \left(\frac{l + h_i C}{l + hC} \right) \\ = \frac{\theta}{T} \frac{A_0 A_1}{\rho c_p \gamma} \frac{\tau}{\pi} \left\{ \cos \left[\frac{\pi}{\tau} (t - t_i) \right] - 1 \right\}. \end{aligned} \quad (20)$$

Fig. 2 illustrates the shapes of the curves of h vs t for a reference simulation and for two cases where one parameter in the reference simulation is changed. The reference simulation uses representative values of valley parameters observed in western Colorado including $l = 1000$ m, $\alpha_1 = \alpha_2 = 15^\circ$, $h_i = 500$ m, $\gamma = 0.025$ K m $^{-1}$, $\tau = 12$ h = 43200 s, $T/\theta = 1$ and $\rho = 1$ kg m $^{-3}$. The reference inversion takes nearly $4\frac{1}{2}$ h to be destroyed when $A_0 A_1 / \rho c_p = 0.25$ K m s $^{-1}$. Fig. 2 was obtained by a numerical integration of (18) using a forward finite difference scheme and a time step of 10 min.

An analytical expression for the time required to

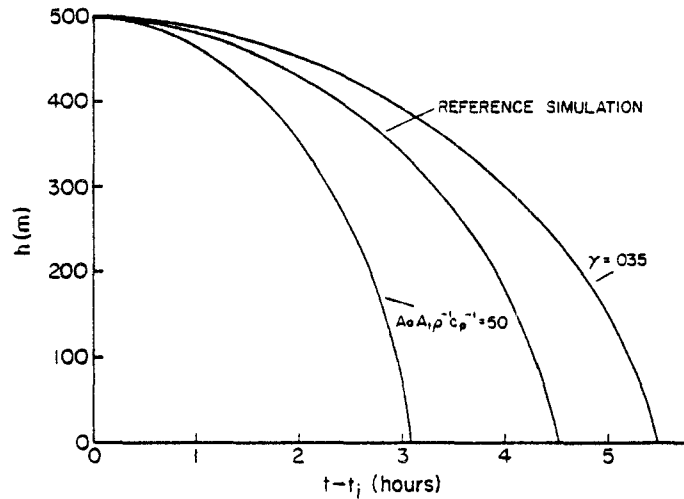


FIG. 2. Descent of inversion top as a function of time for the reference inversion simulation and for two simulations for which the single parameters indicated were changed. Pattern 2 destruction.

destroy an inversion can be obtained by integrating (18) from the initial conditions to the final conditions of $h = 0$ at $t = t_D$. This expression,

$$t_D - t_i = \frac{\tau}{\pi} \cos^{-1} 1 - \frac{T \rho C_p \gamma \pi}{\theta A_0 A_1 \tau} \times \left[\frac{h_i^2}{4} + \frac{l h_i}{2C} + \frac{l^2}{2C^2} \ln \left(\frac{l}{l + h_i C} \right) \right], \quad (21)$$

enumerates the factors affecting inversion breakup time. The sensitivity of inversion breakup time (measured from sunrise) to the various parameters is il-

lustrated in Fig. 3 using the reference simulation above. The reference inversion takes 4.4 h to break (vertical line in Fig. 3). The effect on the time required to destroy the reference inversion by varying the individual parameters is obtained by following the labeled curves. Thus, varying the initial height of the inversion from 400 to 600 m, other parameters being equal, changes the time required to destroy the inversion from 3.5 to 5.4 h. For the reference inversion, the most sensitive parameters affecting the time required to break an inversion are the available energy and the initial potential temperature gradient

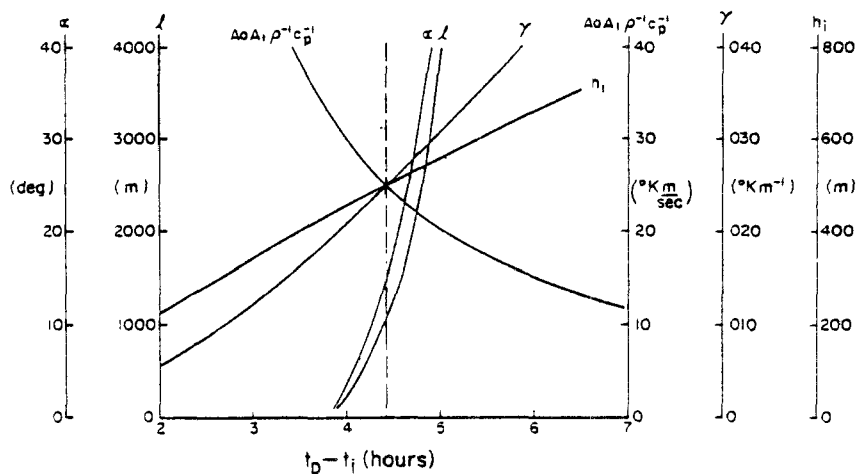


FIG. 3. Sensitivity of inversion destruction time to various model parameters for Pattern 2 destruction.

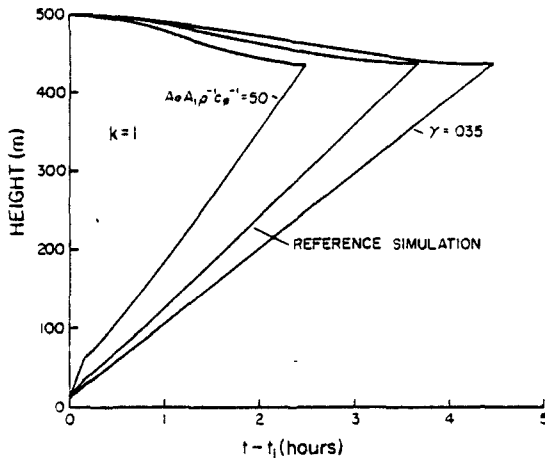


FIG. 4. Ascent of CBL and descent of inversion top as a function of time for Pattern 1 inversion destruction in a valley for the reference simulation and for two simulations in which single parameters were changed to the values indicated.

and inversion height. In the normally dry Colorado valleys the most important factors affecting the available energy are albedo (snow versus no snow) and latent heat flux. The effect of valley shape on the breakup time is relatively small for normal ranges of α and l encountered in valleys of western Colorado. Nevertheless, it is apparent that the valley width and sidewall angles may affect the mode of inversion destruction since they control, to a certain extent, the divergence of mass in the CBL's and thus determine whether inversion destruction more nearly follows Pattern 1 or Pattern 2. Overall, predictions of the time required to destroy inversions, given typical values of the parameters observed in field experiments, are consistent with the observed range of 3.5–5 h.

c. Pattern 1 inversion destruction—Valley case

A useful approximation to Pattern 1 inversion destruction can be obtained from the model equations by setting $k = 1$ in (15) and (16). The general equations then reduce to the two equations

$$\frac{dH}{dt} = \frac{\theta}{T} \left(\frac{l + HC}{l + \frac{1}{2}HC} \right) \frac{A_0 A_1}{\rho c_p \gamma H} \sin \left[\frac{\pi}{\tau} (t - t_i) \right], \quad (22)$$

$$\frac{dh}{dt} = - \frac{\theta}{T} \left[\frac{(h - H)C}{l + \frac{1}{2}HC} \right] \times \frac{A_0 A_1}{\rho c_p \gamma h} \sin \left[\frac{\pi}{\tau} (t - t_i) \right]. \quad (23)$$

Eq. (22) is formulated so that the entire fraction A_0 of the energy coming across the area $(l + HC)$ of the top of the CBL is used to cause the CBL to grow. The energy used to cause the top of the in-

version to descend is the fraction A_0 of the difference between the energy coming across the top of the inversion and the energy coming across the top of the CBL. The time-dependent behavior of the height of the CBL can be obtained by an integration of (22) from the initial condition of $H = 0$ at $t = t_i$ to the final condition of $H = H$ at $t = t$, such that

$$\begin{aligned} \frac{H^2}{4} + \frac{lH}{2C} + \frac{l^2}{2C^2} \ln \left(\frac{l}{l + HC} \right) \\ = \frac{\theta}{T} \frac{A_0 A_1}{\rho c_p \gamma} \frac{\tau}{\pi} \left\{ 1 - \cos \left[\frac{\pi}{\tau} (t - t_i) \right] \right\}. \quad (24) \end{aligned}$$

The integration of (22) and (23) can be accomplished numerically to determine how h and H change with time in a Pattern 1 inversion destruction in a mountain valley. This is done for the reference simulation and for two simulations in which a single parameter of the reference simulation is changed. The resulting plots are shown in Fig. 4. The characteristics of the plots include a near-linear growth of the CBL with time, a slow descent of the inversion top, and a more rapid breakup than for Pattern 2 destruction. Pattern 1 destruction takes 3.7 h versus the 4.4 h required for Pattern 2 breakup. The same total amount of energy is required to destroy the reference inversion, whether it is destroyed following Pattern 1 or Pattern 2. However, since the energy available to destroy the inversion comes across the area of the top of the inversion, and this area is larger when the inversion top sinks more slowly, the total amount of energy required to destroy the inversion is attained earlier in the day, resulting in an earlier inversion breakup.

d. Pattern 1 inversion destruction—Flat plains case

Application of (22) and (23) to a valley that is very wide or approaches a plain ($l \rightarrow \infty$) results in the equations

$$\frac{dH}{dt} = \frac{\theta}{T} \frac{A_0 A_1}{\rho c_p \gamma H} \sin \left[\frac{\pi}{\tau} (t - t_i) \right], \quad (25)$$

$$\frac{dh}{dt} = 0. \quad (26)$$

Thus, over flat terrain where no topographically induced mass divergence occurs from the CBL, the inversion is destroyed solely by the growth of a CBL. Performing integrations on (25) as described in the previous section results in the analytical expression

$$H(t) = \left\{ 2 \frac{\theta}{T} \frac{\tau}{\pi} \frac{A_0 A_1}{\rho c_p \gamma} \left[1 - \cos \frac{\pi}{\tau} (t - t_i) \right] \right\}^{1/2}, \quad (27)$$

and an expression for the breakup time,

$$t_D - t_i = \frac{\tau}{\pi} \cos^{-1} \left(1 - \frac{T}{\theta} \frac{\rho c_p \gamma}{A_0 A_1} \frac{\pi}{\tau} \frac{h_i^2}{2} \right). \quad (28)$$

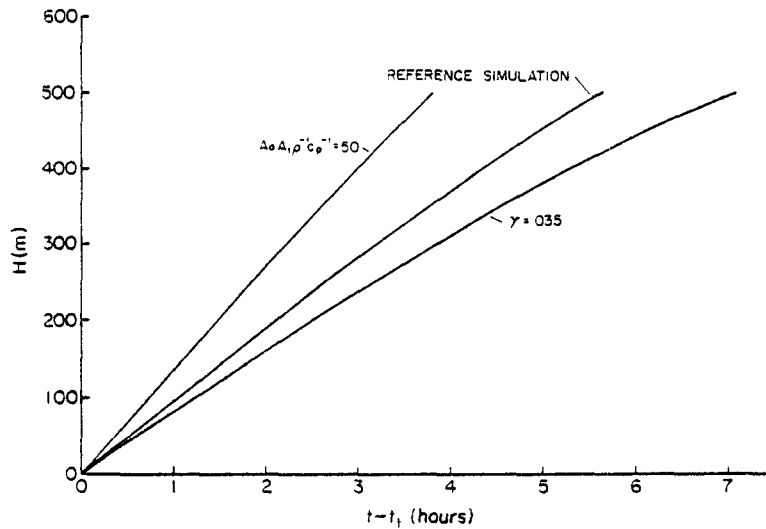


FIG. 5. Growth of CBL over flat terrain as a function of time for the modified reference inversion ($\alpha = 0$, $l \rightarrow \infty$) and for two simulations in which single parameters were changed to the values indicated. Pattern 1 destruction.

Eq. (27) is nearly identical to an equation for CBL growth over homogeneous terrain as derived by Leahey and Friend (1971). Following (27), Fig. 5 presents plots of H vs time for the reference simulation and for two cases where one parameter in the reference simulation has been changed. The reference inversion is destroyed in 5.65 h by a near-linear increase in the depth of the CBL. If the incoming energy is doubled, the inversion takes 3.8 h to break, and if the potential temperature gradient is increased to 0.035 K m^{-1} , the inversion is broken in $\sim 7.1 \text{ h}$. Fig. 6 indicates the sensitivity of the time required

to break an inversion on the different parameters of (28). The effect on the breakup time of changing individual parameters in the reference simulation is obtained by following the individual curves.

e. Pattern 3 inversion destruction

A simulation of Pattern 3 inversion destruction uses the general model [Eqs. (15) and (16)], in which a partitioning of energy is required to allow both CBL growth and inversion top descent. In order to use the general model equations, the fraction of sen-

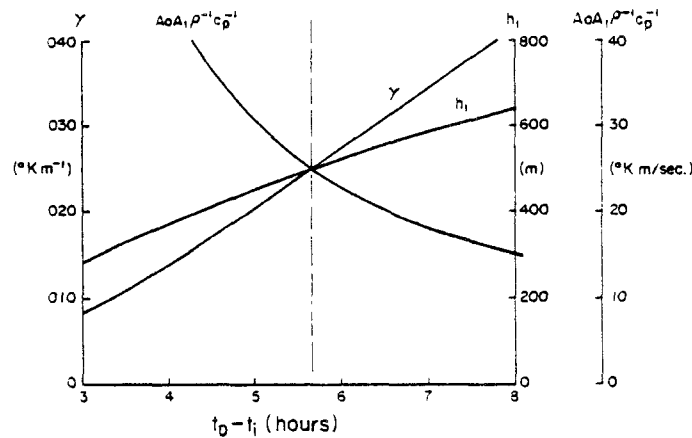


FIG. 6. Sensitivity of inversion destruction time to various model parameters for Pattern 1 inversion destruction over flat terrain.

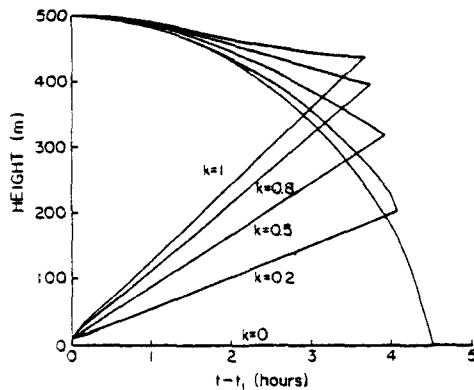


FIG. 7. Ascent of CBL and descent of inversion top as a function of time for Pattern 3 destruction of the reference inversion for different values of k .

sible heat flux $K = k[(l + HC)/(l + hc)]$ that drives the growth of the CBL must be determined. It is apparent that the fraction K is a function of time, since the initial energy input must be used primarily to develop the CBL's before appreciable mass can be carried up them. Factor K also depends on the topographic characteristics of the valley, since K must approach 1 as the valley width approaches infinity. It seems probable that K may also be a function of sensible heat flux. Since the functional dependencies of K are not yet known, it is assumed that k is a constant and, by comparing model simulations to actual data, the constant value of k that results in the best fit to data is determined. This approach allows an investigation of the effect of k on the simulation. Further research is necessary to determine the actual functional form of K , so that a better understanding of the energy partitioning phenomenon can be obtained, resulting in more accurate simulations.

The equations used to simulate Pattern 3 destruction are thus

$$\frac{dH}{dt} = \frac{\theta}{T} \frac{k}{\rho c_p} \left(\frac{l + HC}{l + \frac{1}{2}HC} \right) \frac{A_0 A_1}{\gamma H} \times \sin \left[\frac{\pi}{\tau} (t - t_i) \right], \quad (29)$$

$$\frac{dh}{dt} = - \frac{\theta}{T} \frac{l}{\rho c_p} \left[\frac{l + hc - k(l + HC)}{l + \frac{1}{2}hc} \right] \frac{A_0 A_1}{\gamma h} \times \sin \left[\frac{\pi}{\tau} (t - t_i) \right], \quad (30)$$

where

$$0 \leq (k = \text{constant}) \leq 1. \quad (31)$$

These equations can be integrated numerically to determine how H and h vary with time from a given

initial state. Fig. 7 shows several numerical integrations using this method, time steps of 10 min, the reference simulation, and several values of k . Replotted on the same figure are some of the limiting cases of the general equations for destruction of the reference inversion discussed earlier. The time required to break the reference inversion decreases from 4.4 to 3.7 h as the value of k is increased from 0 to 1. For all values of k the growth of the CBL is nearly linear.

Fig. 8 shows the effect of varying individual parameters in the reference simulation with k fixed. The inversion is destroyed when the ascending CBL and the descending inversion top meet at a height of $H_D = h_D = 205$ m. The fact that the fraction k uniquely determines the height at which the ascending CBL meets the descending inversion top at the time of inversion destruction, suggests a means of fitting the model results to actual data that will be used in a later section.

f. Model modification to account for warming of the neutral layer

Field observations show that the potential temperature θ_n at the top of the inversion usually increases slowly with time. The warming rate varies from valley to valley and from day to day with the average warming rate being about 0.4 K h^{-1} . From the physical hypothesis, this warming requires that more energy be spent to move mass up the sidewalls, since the parcels must be warmed to a higher temperature $\theta_n(t) = \theta_n(t_i) + (d\theta_n/dt)\delta t$ to be removed from the valley. The energy requirement can be cal-

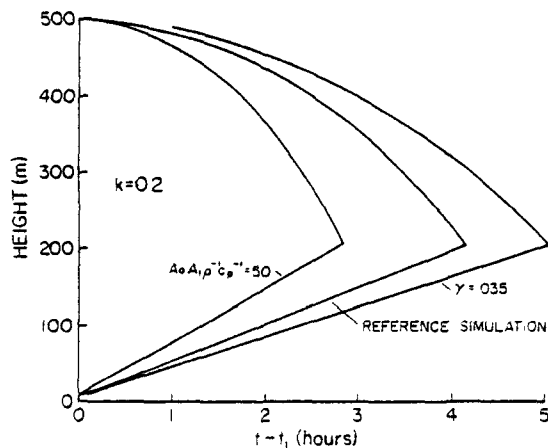


FIG. 8. Ascent of CBL and descent of inversion top for Pattern 3 destruction ($k = 0.2$) of the reference inversion, and for two simulations in which single parameters were changed to the values indicated.

culated by considering that the mass of air removed from the valley to allow the top of the inversion to sink from h_i to h is given by

$$\begin{aligned} \text{mass removed} &= \rho V \\ &= \rho(h_i - h)[l + \frac{1}{2}(h_i + h)C], \end{aligned} \quad (32)$$

and that the energy required to move this mass across a potential temperature jump at the top of the inversion, $\theta_h(t) - \theta_h(t_i)$ can be approximated by

$$Q_4 = \rho V c_p \frac{T}{\theta} \frac{1}{2} [\theta_h(t) - \theta_h(t_i)]. \quad (33)$$

If the warming in the neutral layer occurs linearly in time, the potential temperature jump is given by $\beta(t - t_i)$ where $\beta = \partial\theta_h/\partial t$ is the rate of warming. Then

$$\begin{aligned} Q_4 &= \rho c_p \frac{T}{\theta} \frac{\beta}{2} (h_i - h)(t - t_i) \\ &\quad \times [l + \frac{1}{2}(h_i + h)C], \end{aligned} \quad (34)$$

$$\frac{dh}{dt} = -\frac{\theta}{T} \frac{1}{\rho c_p} \times \left\{ \frac{[l + hC - k(l + HC)]A_0 A_1 \sin \frac{\pi}{\tau} (t - t_i) - \rho c_p \frac{T}{\theta} \frac{\beta}{2} (h_i - h)[l + \frac{1}{2}(h_i + h)C]}{h\gamma(l + \frac{1}{2}hC) + \frac{1}{2}\beta(t - t_i)(l + hC)} \right\}. \quad (39)$$

These equations can be used to simulate inversion breakup when significant warming occurs in the neutral layer above. Eq. (39) reduces to (30) when β is zero. It is important to note that (38) has the same form as before but, since more energy is required to move mass up the sidewalls, the partitioning of energy may be affected. If this actually occurs in nature, then the functional dependency of K is more complicated than previously discussed, since it will depend not only on time, energy input and valley width, but also on the rate of warming of the neutral layer above the inversion. As before, Eqs. (38) and (39) may be integrated numerically to simulate valley inversion breakup if $\theta_h(t)$ is known. If θ_h does not vary with time, Eqs. (29) and (30) can be used for the simulation.

3. Comparison of model results with data

In this section a finite difference form of the model equations (38) and (39) will be applied to simulate actual data collected in the valleys of western Colorado. The input parameters needed to solve the equations are given in Table 1 along with a summary of how they may be obtained. The output of the model is $h(t)$ and $H(t)$. From these outputs and the assumptions that γ is constant for altitudes between H and h , that potential temperature is independent

$$\begin{aligned} \frac{dQ_4}{dt} &= \rho c_p \frac{T}{\theta} \frac{\beta}{2} \left[(h_i - h)[l + \frac{1}{2}(h_i + h)C] \right. \\ &\quad \left. - (t - t_i) \frac{dh}{dt} (l + hC) \right]. \end{aligned} \quad (35)$$

The model equations are modified to account for this extra energy requirement by specifying that the fraction $k[(l + HC)/(l + hC)]$ of the inversion energy input dQ_1/dt drives the CBL growth, or

$$k \left(\frac{l + HC}{l + hC} \right) \frac{dQ_1}{dt} = \frac{dQ_2}{dt}, \quad (36)$$

while the remainder of the energy input drives the descent of the inversion and carries parcels across the potential temperature jump, such that

$$\left[1 - k \left(\frac{l + HC}{l + hC} \right) \right] \frac{dQ_1}{dt} = \frac{dQ_3}{dt} + \frac{dQ_4}{dt}. \quad (37)$$

Substituting Eqs. (12), (13), (14) and (35), the modified model equations are

$$\frac{dH}{dt} = \frac{\theta}{T} \frac{k}{\rho c_p} \left(\frac{l + HC}{l + \frac{1}{2}hC} \right) \frac{A_0 A_1}{\gamma H} \sin \left[\frac{\pi}{\tau} (t - t_i) \right], \quad (38)$$

of height in the CBL and neutral layer, and that $\theta_h(t_i)$ and $\partial\theta_h/\partial t$ are known, $\theta(t, z)$ for the CBL, stable core and neutral layer can be determined. Unfortunately, since two of the input parameters to the thermodynamic model (k and A_0) were not observed in the field programs, the equations cannot be applied directly. Instead, arbitrary values for k and A_0 are chosen until the best simulation of the data is obtained with the model. It is then determined whether the values of k and A_0 are reasonable for the situation at hand. Both k and A_0 are bounded, since they are fractions between 0 and 1. The value of k specifies the constant fraction of sensible heat flux that is used to cause the CBL to deepen. The model results are presented below for a winter Pattern 2 inversion destruction in the wide Yampa Valley and for a fall Pattern 3 inversion destruction in the Eagle Valley.

a. Pattern 2 simulation—Yampa Valley, 23 February 1978

The model input parameters required to simulate the Pattern 2 inversion destruction observed in the snow covered Yampa Valley on 23 February 1978 were obtained as follows. First, $\theta T^{-1} = 1.07$ and $\rho c_p = 1040 \text{ J m}^{-3} \text{ K}^{-1}$ were calculated using the ap-

TABLE 1. Model input parameters.

| Model input | | | Source |
|---|--------|--------------|---|
| Constants | (i) | θ/T | from average P and T of valley atmosphere |
| | (ii) | ρC_p | |
| Valley topography | (iii) | l | from topographic maps |
| | (iv) | C | |
| Initial inversion characteristics | (v) | γ | from sunrise sounding |
| | (vi) | h_i | |
| Solar irradiance | (vii) | A_1 | from extraterrestrial solar irradiance model or field notes for t_i |
| | (viii) | τ | |
| | (ix) | t_i | |
| External conditions (neutral layer warming) | (x) | β | from sequential soundings taken during observation of inversion breakup or from climatic data |
| Energy partition | (xi) | k | comparisons of theory and data |
| Surface energy balance | (xii) | A_0 | measurements, if available |
| Numerical | (xiii) | $H_i \neq 0$ | arbitrary |
| | (xiv) | Δt | |

proximate mean pressure (780 mb) of the early morning inversion and an average temperature of the valley atmosphere (-10°C) from the defining equation for potential temperature and from the equation of state, respectively. Second, the valley topographic parameters ($l = 2580$ m, $\alpha_1 = 9^\circ$, $\alpha_2 = 16^\circ$, $C = 9.80$) were obtained from topographic maps. Third, the initial inversion parameters ($h_i = 530$ m, $\gamma = 0.0345$ K m $^{-1}$) were estimated from a straight line fit to the top of the 0714 MST sounding on this date. The hyperbolic lower region of the sounding could not be adequately fit with a straight line, so it is ignored in the analysis. Fourth, a sinusoidal fit to the extraterrestrial solar flux curve obtained from a standard solar irradiance model (e.g., Sellers,

1965) provides solar irradiance parameters ($A_1 = 878$ W m $^{-2}$, $t_i = 0655$ MST, $\tau = 10.9$ h). The output of the solar irradiance model for the horizontal surface of interest is presented in Fig. 9. For reference, the solar fluxes on extraterrestrial surfaces with the same aspect and inclination angles as the valley sidewalls are indicated on the figure. The input required to run the solar irradiance model includes the date and the latitude and longitude of the Yampa Valley site. The remaining parameters necessary to run the inversion destruction model are fractions k and A_0 , and the neutral layer warming rate β . To simulate a Pattern 2 destruction, k must be zero. The neutral layer warmed only 1.1 K during the inversion destruction, for a warming rate β of 2.8×10^{-5} K

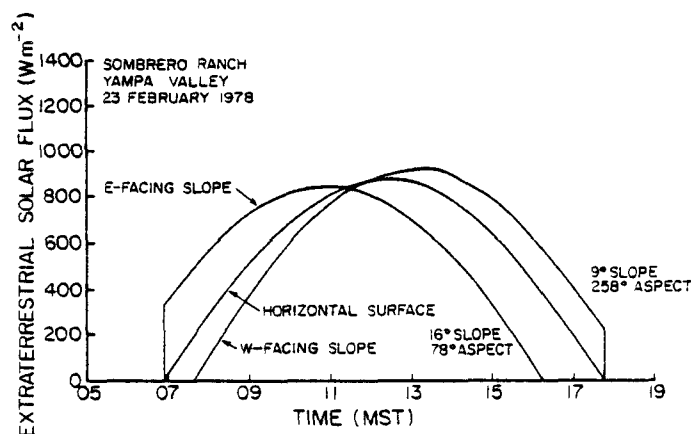


FIG. 9. Extraterrestrial solar flux calculated for valley floor and sidewall surfaces of the Yampa Valley, 23 February 1978.

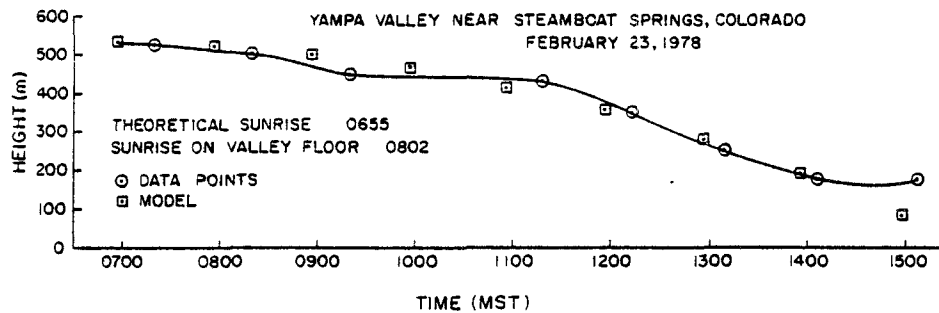


FIG. 10. Comparison of model simulation of $h(t)$ with actual data for the Yampa Valley, 23 February 1978.

s^{-1} . The best fit of the model output $h(t)$ to the inversion top data of Fig. 10 was obtained with $A_0 = 0.19$ by a trial-and-error procedure. Using this value, the simulation of the height of the top of the inversion agrees to within 25 m of the data over a 7 h period. In mid-afternoon, however, the simulation continues to call for the descent of the inversion top, when the actual data indicate that the descent stopped. This is probably due to afternoon shading of the valley by a mountain peak southwest of the site. The model, using a simple sine function to simulate solar flux, does not account for this shading. In Fig. 11 the potential temperature profile simulations are compared to actual sounding data. The sounding data consist of eight consecutive potential temperature soundings taken at ~ 1 h intervals throughout the day. The characteristics of the initial inversion were obtained from the 0714 MST sounding and are indicated by the straight line fit to the sounding in the figure. The slow neutral layer warming is also apparent in the figure. The excellent fit of the model simulations to the data in the stable core above the 50 m deep surface layer is shown for soundings 4 and 6. The value of A_0 required to obtain these results seems reasonable for the snow-covered valley with evergreen forests covering much of the valley sidewall above the observation site. It is particularly interesting that the model assumption of constant potential temperature gradient was satisfied well during the long period of inversion destruction in the complicated topography of the Yampa Valley. The case study is an excellent example of the effect of enhanced albedo due to snow cover in retarding the normal breakup of an inversion. Despite the fact that the temperature inversion was not destroyed on this clear day, the diurnal range of temperature at the ground was quite large.

b. Pattern 3 simulation—Eagle Valley, 16 October 1977

Pattern 3 inversion breakup in the Eagle Valley is remarkably consistent in all seasons when snow

cover is not present in the valley. To test the mathematical model, the Pattern 3 breakup on the clear day of 16 October 1977 is chosen for simulation. The input parameters to the model are obtained as for the Pattern 2 simulation above. Thus, values of the constants θT^{-1} (1.08) and ρc_p ($990 \text{ J m}^{-3} \text{ K}^{-1}$) are determined from the approximate mean pressure (768 mb) and temperature (0°C) of the valley inversion. The valley topographic parameters ($l = 1450$ m, $\alpha_1 = 21^\circ$, $\alpha_2 = 10^\circ$, $C = 8.28$) are determined from topographic maps. The initial values of the inversion parameters ($h_i = 650$ m and $\gamma = 0.0269 \text{ K m}^{-1}$) were taken from the 0650–0719 MST sounding since the pre-sunrise sounding was of insufficient height to determine h_i . A solar irradiance model was used to determine the parameters $A_1 = 906 \text{ W m}^{-2}$, $t_i = 0621$ MST and $\tau = 11$ h (Fig. 12). The value of β ($8.3 \times 10^{-5} \text{ K s}^{-1}$) was taken from valley temperature sounding data.

The fitting of the model output to the data on Fig. 13 was accomplished first by choosing the value of

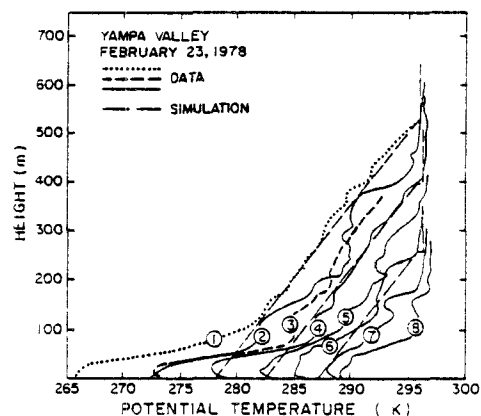


FIG. 11. Comparison of model simulation of potential temperature structure with data for the Yampa Valley, 23 February 1978. Upsoundings 1–8 were initiated at 0714, 0905, 0959, 1100, 1202, 1259, 1359 and 1508 MST, respectively.

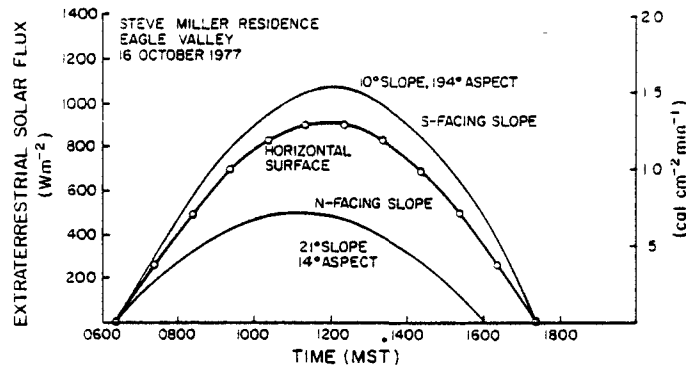


FIG. 12. Extraterrestrial solar flux calculated for valley floor and sidewall surfaces of Eagle Valley, 16 October 1977.

k so that the ascending CBL and descending inversion top met at the proper observed height at the time of inversion destruction. The value of A_0 was then varied until the model outputs $h(t)$ and $H(t)$ fit the data well. The fit in Fig. 13 was obtained with $k = 0.14$ and $A_0 = 0.45$. The value of A_0 seems realistic considering the dry nature of the valley surface on this date. The equations were integrated from the initial conditions of $h = 650$ m and $H = 10$ m at $t = 0705$ MST using a time step of 10 min. From Fig. 13 it is clear that a good fit to the data is obtained with the chosen values of the two parameters A_0 and k . The simulation of CBL height and inversion top height agrees with the data within 50 m over most of the period of inversion destruction. The CBL height was overpredicted early in the inversion period, due to the bulk nature of the model. Following sunrise, the CBL develops first over the illuminated sidewall or sidewalls, and somewhat later over the valley floor when it is sunlit. The bulk model, however, does not differentiate between CBL growth over the three different valley surfaces. All energy going into CBL growth is attributed, in the model, to growth of the valley floor CBL. Thus, the initial

overprediction of CBL growth over the valley floor is a characteristic feature of the model equations. The behavior of the simulation at mid-levels of the valley atmosphere near the time of inversion destruction should also be mentioned. The data typically show a more sudden inversion breakup is to be expected in nature since the final remnants of the stable core will break up in convective overturning, once the stable core becomes thin enough and the convective plumes rising from the valley floor become vigorous enough. Due to the chaotic nature of the breakup, actual soundings taken during this time will often show deformations in the vertical potential temperature profiles. Estimates of heights h and H from soundings are difficult to make during this time. A continued flux of energy into this region is nec-

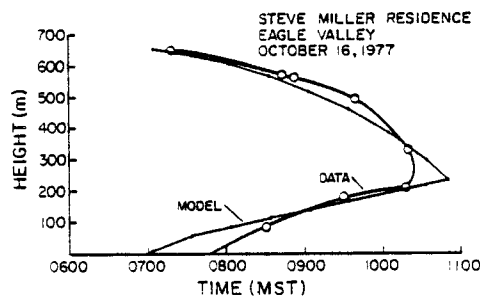


FIG. 13. Comparison of model simulation of $H(t)$ and $h(t)$ with actual data for the Eagle Valley, 16 October 1977.

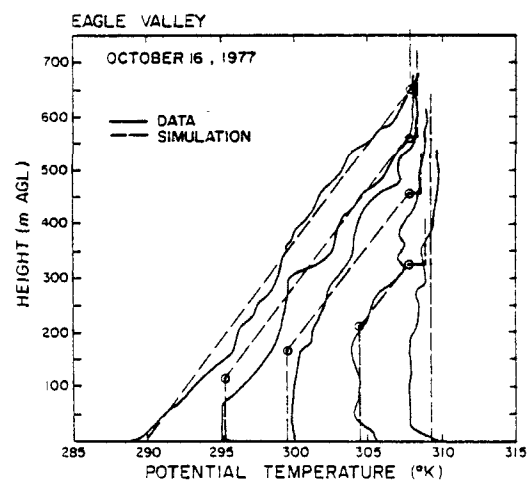


FIG. 14. Comparison of model simulation of potential temperature structure with data from the Eagle Valley, 16 October 1977.

essary before the deformations in the profiles are destroyed and well-organized convection through the entire depth of the valley results in smooth neutral profiles. When this occurs, the breakup can be considered as finished.

The potential temperature profiles corresponding to the data and simulation of Fig. 13 are presented in Fig. 14. The potential temperature data are from the tethersonde up-soundings taken at 0650-0719, 0829-0848, 0924-0948, 1013-1033 and 1106-1121 MST. The corresponding potential temperature simulations are plotted for the approximate midtimes of the tethersonde up-soundings at 0840, 0935, 1025 and 1115. Again, the model provides a good simulation of the actual data, reproducing the warming and growth of the CBL, the warming of the stable core, and the descent of the inversion top.

4. Summary and conclusions

A thermodynamic model of valley temperature structure evolution has been developed. By differentiating the first law of thermodynamics, the rate of energy input into the valley atmosphere is equated to the rate of descent of the inversion top and the rate of ascent of the CBL under the following assumptions:

- 1) The potential temperature gradient in the stable core is constant during the period of inversion breakup.
- 2) The temperature structure is horizontally homogeneous in the cross-valley direction.
- 3) The valley topography can be adequately represented by a horizontal valley floor of arbitrary width and two linear sidewalls of arbitrary slope.
- 4) The initial inversion at sunrise can be adequately represented by a constant potential temperature gradient layer of arbitrary depth.
- 5) Convective boundary layers can be adequately represented as constant potential temperature layers of arbitrary height.
- 6) The rate of energy input into the valley atmosphere is a constant fraction of the solar energy flux (assumed to be a sinusoidal function of time from sunrise to sunset) coming across the horizontal upper surface of the inversion.

To complete the model, the partitioning of the energy input into CBL growth and mass transport must be estimated. As a first approximation, it is assumed that a constant fraction of the energy input is used to cause the CBLs to grow. The remaining energy is used for mass transport in the upslope flows. Energy going into the growth of the CBL causes the CBL depth to increase with time. Energy causing air parcels to flow up the sidewall CBLs results in the descent of the top of the inversion. When most of the available energy drives the growth of the CBLs, a temperature structure evolves in which the inversion

is destroyed predominantly by the upward growth of a CBL from the ground. When most of the available energy drives mass up the sidewalls, a temperature structure evolves in which the inversion is destroyed by the descent of the inversion top.

The inputs to the model are 1) the initial inversion characteristics (depth and average potential temperature gradient); 2) valley topography (floor width and inclination angles of the two sidewalls); 3) the rate of energy input; and 4) the fraction of energy available to increase the depth of the CBL. The effect on inversion evolution of warm air advection above the inversion layer can be investigated by using a modified version of the model in which the warming rate is input.

The model simulates the changes with time of the height of the inversion top and the depth of the CBL during the inversion breakup period. From these simulations potential temperature profiles of the valley atmosphere can be constructed for any time during the period.

Sensitivity analyses were conducted for the limiting cases of the model. The results indicate that the time required to destroy an inversion depends primarily on the initial height of the inversion, on its potential temperature gradient, and on the amount of energy available to destroy it. Using a reference simulation in which model parameters were given values typical of valley inversions, inversion destruction took approximately $3\frac{1}{2}$ to $4\frac{1}{2}$ h after sunrise. These times correspond well with actual observations. Less time is required to destroy a valley inversion than an inversion of like dimensions over the plains, because the available energy is used to warm a smaller volume of air. For the dry valleys of western Colorado, the amount of energy available depends to a large extent on the presence or absence of snow cover or surface moisture in the valley. Valley inversions were destroyed sooner by the growth of a CBL than by the descent of the inversion top. Valley width and inclination angles of the sidewalls had only a limited effect on the time required to destroy an inversion. Increased valley width and steeper sidewalls both increased slightly the time required.

The thermodynamic model was used to simulate two specific sets of inversion breakup data for Pattern 2 and 3 temperature structure evolution in the topographically diverse Eagle and Yampa Valleys. Simulations were obtained by fitting two constants in the model (relating to the surface energy budget and energy partitioning) to the data. The model output fit the Pattern 2 inversion breakup in the snow-covered Yampa Valley very well using an energy input equal to 19% of the extraterrestrial solar flux on a horizontal surface, and assuming that all of this energy was used to drive the slope flows. A good fit to the Eagle Valley data was obtained using an energy input equal to 45% of the extraterrestrial solar

flux and assuming that 14% of this energy was used to cause the valley floor CBL to grow. The remaining energy was used to remove mass from the valley in the slope flows.

Results of the present study provide new insights into the evolution of valley temperature structure and quantify the influence of the various parameters affecting temperature inversion breakup. The model explains the importance of the initial sunrise inversion characteristics; the observed timing of the beginning of inversion destruction; the mean time required to destroy typical inversions in the deep valleys of western Colorado; the weak seasonal dependence of the time period required to destroy the inversions; the effects of snow cover and ground moisture and of valley topography; the patterns of warming observed in the various layers of the temperature structure; the typical observed inversion top descent rates of 40–150 m h⁻¹; and the retarded growth of the valley CBL's relative to the flat plains case. The thermodynamic model, while implicitly incorporating up-slope mass transport, is able to simulate tem-

perature structure evolution in a wide range of valley topography without taking account of along-valley wind systems.

Acknowledgments. The research was accomplished at the Department of Atmospheric Science, Colorado State University, under funding from Grant ATM76-84405, Atmospheric Sciences Section, National Science Foundation. The manuscript was prepared under funding from the Environmental Protection Agency through Interagency Agreement AD-89-F-0-097-0, with the U.S. Department of Energy.

REFERENCES

- Leahey, D. M., and J. P. Friend, 1971: A model for predicting the depth of the mixing layer over an urban heat island with applications to New York City. *J. Appl. Meteor.*, 10, 1162–1173.
- Sellers, W. D., 1965: *Physical Climatology*. University of Chicago Press, 272 pp.
- Whiteman, C. D., 1982: Breakup of temperature inversions in deep mountain valleys: Part I. Observations. *J. Appl. Meteor.*, 21, 270–289.

APPENDIX D
SUMMARY OF MODIFICATIONS TO VALMET

APPENDIX D

SUMMARY OF MODIFICATIONS TO VALMET

VERSION 1.0, DATED APRIL 30, 1983

Original version of VALMET.

VERSION 1.1, DATED DECEMBER 1, 1984

Major code changes:

1. Main Program

- The call to subroutine PRISE was fully incorporated into the code (it had been "commented out" in the original version).
- The code which corrects concentrations to standard conditions was moved from subroutine GAUSS to the main program.
- The call to subroutine GAUSS for the calculation of the plume centerline concentration was corrected to allow the plume to be offset from the valley centerline. Correction to standard conditions is now accomplished following the call to GAUSS.

2. Subroutine INPUT

- New code was developed to check the model parameter values that are input by the user. An error message is written when the user inputs values outside normal atmospheric ranges.
- Calculations of NBOX, NTOTI and AC were moved from the main program into the INPUT module to facilitate the new error checking code.
- A new error message scheme was developed for the INPUT module.

3. Subroutine PRISE
 - A new plume rise module was developed from the MPTER code to replace the old module derived from the CRSTER code.
 - A new code was developed in order to bypass the plume rise calculations when SRAD and/or SVEL are set to zero.
4. Subroutine GAUSS
 - The section of code that corrects concentrations to standard atmospheric conditions was removed and placed in the main program.
5. Subroutine INGRAT
 - A statement was added to this subroutine.
6. Subroutine BRKUP
 - A new exponential decay algorithm was added to handle variable time step lengths.

| TECHNICAL REPORT DATA | | |
|--|--|---|
| (Please read Instructions on the reverse before completing) | | |
| 1. REPORT NO. | 2. | 3. RECIPIENT'S ACCESSION NO. |
| 4. TITLE AND SUBTITLE GREEN RIVER AIR QUALITY MODEL DEVELOPMENT VALMET - A Valley Air Pollution Model | | 5. REPORT DATE |
| | | 6. PERFORMING ORGANIZATION CODE |
| 7. AUTHOR(S) C. D. Whiteman and K. J. Allwine | | 8. PERFORMING ORGANIZATION REPORT NO. PNL-4728 |
| 9. PERFORMING ORGANIZATION NAME AND ADDRESS Battelle, Pacific Northwest Laboratory Richland, Washington 99532 | | 10. PROGRAM ELEMENT NO. CDTAID/09-0726 (FY-85) |
| | | 11. CONTRACT/GRANT NO. IAG AD89F20970 |
| 12. SPONSORING AGENCY NAME AND ADDRESS Atmospheric Sciences Research Laboratory, RTP, NC Office of Research and Development Environmental Protection Agency Research Triangle Park, North Carolina 27711 | | 13. TYPE OF REPORT AND PERIOD COVERED Final FY-85 |
| | | 14. SPONSORING AGENCY CODE EPA/600/09 |
| 15. SUPPLEMENTARY NOTES | | |
| 16. ABSTRACT Following a thorough analysis of meteorological data obtained from deep valleys of western Colorado, a modular air pollution model has been developed to simulate the transport and diffusion of pollutants released from an elevated point source in a well-defined mountain valley during the nighttime and morning transition periods. This initial version of the model, named VALMET, operates on a valley cross section at an arbitrary distance down-valley from a continuous point source. The model has been constructed to include parameterizations of the major physical processes that act to disperse pollution during these time periods. The model has not been fully evaluated. Further testing, evaluations, and development of the model are needed. Priorities for further development and testing are provided. | | |
| 17. KEY WORDS AND DOCUMENT ANALYSIS | | |
| a. DESCRIPTORS | b. IDENTIFIERS/OPEN ENDED TERMS | c. COSATI Field/Group |
| | | |
| 18. DISTRIBUTION STATEMENT RELEASE TO PUBLIC | 19. SECURITY CLASS (This Report) UNCLASSIFIED 20. SECURITY CLASS (This page) UNCLASSIFIED | 21. NO. OF PAGES 22. PRICE |